Investigation of Syringe-Based Direct Write (DW) For Antenna Manufacture

Thesis submitted in accordance with the requirements of the University of Liverpool for the degree of Doctor in Philosophy

by

Rd. Khairilhijra KHIROTDIN

September 2012

To Fizza

Abstract

Miniature products and components are in great demand in the electronics industry and Direct Write (DW) has become the subject of interest due to its capability of printing small features and offering low manufacturing cost. DW technologies, a subset of rapid prototyping, have been applied to many applications in electronics, aeronautics, photonics and biomedical engineering. Among them, syringe deposition technology is a promising technique, providing precision deposition of materials with various viscosities, on-line design changes and ability to write on non-planar substrates. In addition, the low amount of material waste, low cost investment in production facilities and the versatility of the system make syringe-based DW technology ideal for low-cost electronics production especially for small batch production. Furthermore, the data-driven nature of digital printing manufacturing methods allows fast manufacturing runs and a short time cycle from design to manufacture which all translate into shorter delivery times in manufacturing.

Syringe-based DW technology is a new and promising technology and hence its capabilities have never been exploited comprehensively. The objective of this project was to investigate the possible use of a syringe-based DW technology by means of automatic syringe deposition system in conjunction with heating process to fabricate electronic components such as strain gauges, antenna and others. By doing this, the aim is to help improve the fundamental knowledge of syringe-based DW process behaviour and functional performance of components produced.

In this research, syringe-based DW was used together with laser and oven curing process to fabricate electronic devices particularly conductive tracks and antennas. The applied research focused on antenna manufacture where the technology development consisted of evaluating printed structures and the effects of controlling the printing processes parameters to the antenna electrical performance characteristics are investigated.

Using this hybrid electronic manufacturing technique, printed silver ink of radio frequency identification (RFID) tag and silver ink dipole antenna were successfully fabricated on plastic; polyethylene terephthalate (PET). The achievements are important since the advantages of this technique are plentiful including elimination of photolithography and etching steps, vacuum processing, masks, and material waste during manufacturing process, overall reduction of process and product costs and provided adequate throughput especially for small batch production. In addition, the technique gives a new and exciting opportunities and novel materials for antenna manufacturing. Controlling the deposition parameters which resulting a variety of cross-sectional shape of the conductor track affecting the electrical antenna performance characteristics hence open up new prospects especially for application in higher frequency range and low-cost antenna manufacturing. Printing on challenging surfaces (curve and doubly-curve) could also be realized hence promoting the development of new ways of integrating antenna into other structures such as packaging and on curvy products. The results obtained showed that RFID tags and dipole antenna can be manufactured by direct write technology.

Acknowledgements

The author is extremely grateful and appreciative to all the contributions made and advices given that has made this work possible. In particular acknowledgements are given to the following people and organisations.

Firstly I would like to thank my supervisors, **Professor Ken Watkins** and **Dr Geoff Dearden**, for their invaluable supports, insight thoughts, encouragements and supervision throughout my studies.

I would also like to thank the Lairdside Laser Engineering Centre (LLEC) manager, **Dr Eamonn Fearon** and his research assistant, **Mr. Doug Eckhart** for the ideas and assistance in setting up of the experiments and in the preparation of samples, without them this work could not have occurred. Highly appreciation goes to Dr Eamonn Fearon for the guidance and for his valuable advices in conducting my experimental work. Despite being a very busy man, he has always found the time to answer all the questions that I asked him every time I went to his office, often without notice.

Thanks must also go to **Mr. Stephen Boyes (PhD student)** and **Professor Yi Huang** from Electrical and Electronic Engineering Department. Thanks for the teachings, assistance and ideas for all the help and advices in performing the antenna performance testing set-up and analysis throughout these studies.

My fellow researchers in the Laser Group, including **Li Wei, Olivier Allegre, Dr Zheng Kuang** and **Dr Dun Liu** for giving me an outlet for my frustration.

Special appreciation for my wife, **Mrs Nurhafizzah Hassan** and my family especially my parents who endured this long process with me, for constant support and unwavering faith throughout my PhD.

And finally, I would like to greatly acknowledge the support by the **Ministry of Higher Education of Malaysia (MOHE)** and the **University of Tun Hussein Onn Malaysia (UTHM).**

Contents

List of Figures

List of Tables

List of Symbols

ρ	Specific resistivity (Ωm)
ε_{eff}	Effective dielectric constant of the surrounding medium (unitless)
ε_r	Relative dielectric constant of the substrate (unitless)
$\frac{dP}{dl}$	Applied pressure gradient (N/m^3)
μ	Viscosity of the conductive ink (Pa.s)
A	Cross sectional area of deposited structure (m^2)
A_Δ	Differences in cross-sectional area between the wider line and narrow line (m^2)
A_a	Average cross-sectional area by ratio (m^2)
A_n	Cross-sectional area of the narrow line (m^2)
c	Speed of light in vacuum (m/s)
l	Length of the needle tip (mm)
d_s	Internal diameter of the tip of needle (mm)
f	Resonance frequency (Hz)
h	Height of the conductive track pattern/structures (μm)
h	Thickness of the substrate (μm)
l	Length of trace deposited (mm)
L_{total}	Total length of the antenna (mm)
L_w	Wider line length (mm)
P_{crit}	Critical pressure (Pa)
P_o	Applied pressure (Pa)
Q	Flow of conductive ink from the needle (m^3/s)
R	Electrical resistance of a uniform specimen of the material (Ω)

t	Time (s)
V	Volume of conductive ink deposited (m^3)
v	Actual propagation speed on the dipole length (m/s)
v_0	Velocity of the substrate with respect to the syringe (m/s)
w	Line width (mm)
w	Width of the track (mm)
λ	Wavelength (mm)

Chapter 1

Introduction

1.1 Overview of Direct Write Technology

The utilization of electronic systems such as 3G mobile phones, digital cameras, light emission diode (LED) televisions and many others has increased drastically in the last ten years. They are seen at many places and have become indispensable for most users simply because they are attractive, small, light and quite cheap. Why have these modern and sophisticated products become less expensive nowadays? One of the reasons as mentioned by Peng et al [1] is that most potential new customers come from smaller incomes. They press down the cost of products. This is arguably true since most manufacturers will not make over-priced products which then prohibit customers from buying; whereas, the best way to get the best profitable margin is to make them in reasonable price range thereby being affordable for everyone.

So how can we make such sophisticated products cheap? One way is to reduce the cost of manufacturing processes. This has become a hot topic and

essential to all manufacturing companies. Remarkable changes are required to manufacturing philosophies and processes in order to gain a desirable profit margin. Due to this fact, many electronics companies face a tremendous pressure to reduce their production costs. Furthermore, they also need to provide and deliver the products earlier to market.

1.2 Disadvantages of Conventional Method

One way to reduce the production cost is by miniaturization. It can be done by reducing mainly the size of printed circuit board (PCB) that makes up most of the product. As a result, PCB which comprises of many components including conductive lines (interconnects), resistors and inductors are reducing. New low cost manufacturing tools must be developed and introduced to fabricate these electronic assemblies since the current methods to fabricate PCB use selective masking (photolithography) and etching technologies to create regions of metallization on substrates. These are expensive and time consuming. Furthermore, the masked substrates used are placed into a chemical bath that etches the unwanted metal from the substrate surface whereby such practice not only wastes precious metal material, but also generates substantial amounts of chemical pollutants which are hazardous to the environment. In addition, this method also involves with several other process cycles and hence more expensive.

1.3 Motivation

Rapid prototyping (RP) techniques are often the solutions to eliminating multiple steps and time constraints by building parts on a layer by layer basis; however, unfortunately they do not work with electronic materials. Therefore, there is a need to introduce a new low cost manufacturing technique which leads to the technique best called Direct Write (DW). By definition DW is an additive technology to fabricate two-or three-dimensional functional structures

by directly depositing material onto flat or conformal surfaces [2]. DW allows electrical conductors and components to be directly printed on almost surfaces. It mainly involves two main steps of processes. The pre-deposited material is usually in the form of an ink, slurry or paste, which is printed onto substrates and later cured by (mostly) heating process to consolidate metallic contents. With the ability of DW to write or print in any surfaces, it allows for further miniaturization for electronic devices whereby it provides feature sizes down to less than 20 microns with a wide range of materials possibilities [3]. It is a fast process and since it was an additive process, all materials used are fully utilized. It is a cheap technique where there is no mask involved and it provides a wide variety of materials that can be used. For development of electronics device applications, DW techniques can draw upon the availability of inks containing conductive metallic or organo-metallic particles that would have otherwise been used for screen printing and thin film coating technology. In this way, devices based on conductive films and tracks (or even active electronics materials) are potentially achievable. Numerous applications are adopting DW such as in electronics especially flexible electronics, telecommunications particularly RFID tag antenna, displays, optics, aerospace and many others.

Among the entire group of DW processes, inkjet DW is the most established followed by laser DW in terms of industrial applications, but still they have faced a number of problem such as limited choices of material that can be used, deposition rate, cost and resolution. Wang et al [4] stated that the existing inkjet printing print head has its own limitation in terms of delivering smaller droplets. Discrete droplet systems rely upon low dilution (less 5% solids by volume), low viscosity inks (typically 2 mPa.s but can be up to 0.1 Pa.s) which will form consistent droplet sizes. A feature of these low viscosity inks is their propensity to spread on contact with substrates, forming tracks with a very low ratio of height to width. Likewise, according to Li et al [5-7], most of the laser direct writing techniques such as laser-induced chemical vapour deposition (LCVD), laser-induced electro-less plating (LIEP), laser-induced solid deposition (LISD), and matrix-assisted pulsed laser evaporation

direct write (MAPLE-DW) suffer from numerous problems especially in deposition rate, high production cost and resolution of conductive lines which restricts their applications in many situations.

On the contrary, new and emerging DW process such as syringe-based DW technique has huge potential to overcome the inability or at least comparable to ink-jet and laser direct write technique. This method can utilise inks with much higher concentrations of solute and higher visco-elastic properties, allowing the generation of high-aspect ratio of 3D structures. It is a promising new DW technology which none of the previous researchers has extensively explored the prospect particularly in DW of antenna. The system is well equipped with a robotic system which is integrated with CAM controller as well as syringe technique that can dispense materials with precise volume control from 1 mPa.s to 100,000 Pa.s in Figure 1.1. In addition, it is a maskless process which results in a very cost effective process and it conformably print very fine features usually in micron on any surfaces as well as extremely flexible with wide variety of materials choices.

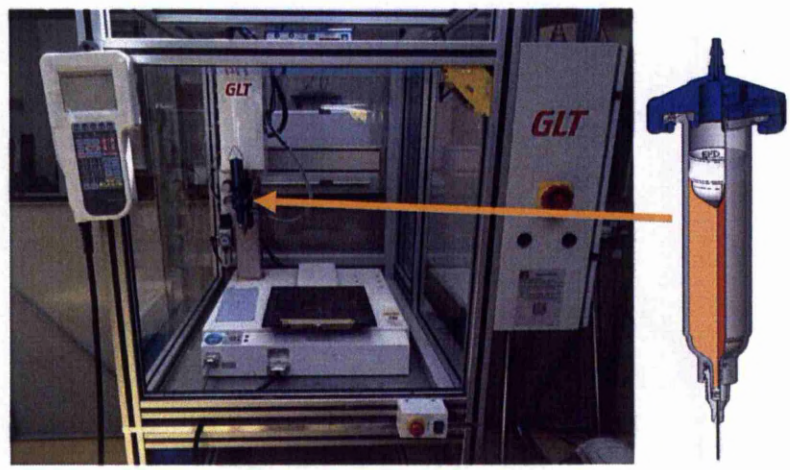

Figure 1.1: Automatic syringe deposition system

Despite the fact that syringe-based DW has several potential advantages, the fundamental knowledge of its process behaviour and the functional performance of components produced are still relatively unexplored. The required integration and optimisation of many factors, from the deposited material formulation to the process parameters, means there remains many research topics to be explored. The syringe-based DW technique must meet the criteria required. It consist of the ability to produce a quality conductive track in micro scale ranges, highly conductive, low in surface roughness especially for high frequency applications and it must well adhered onto the substrates.

1.4 Research Aim

One of the biggest limitations of DW, is the transfer and manipulation of materials to create the desired structure. The desired end material is often in a matrix with a carrier material that is removed before or after deposition. In this manner, the areas of potential for greatest progress in DW will come from improvements in transportation of material and new techniques in achieving material characteristics closer to bulk properties. In response to this challenge, investigations in this research project aim to determine the possible use of a syringe-based DW technology by means of automatic syringe deposition system in conjunction with heating process. The application is to fabricate electronic components such as strain gauges, antennas. The ability to print electronics will not only provide additional functionality and ultra-low cost electronics components. In addition, the ability to print an entire device on a single flexible substrate with a single material deposition technique is still far away from realization. The aim is to help improve the fundamental knowledge of syringe-based DW process behaviour and functional performance of components produced.

1.5 Scope of the Research

The scope of the research covers several key areas which are given as follows:

i. **Characterisation and evaluation of the capability of a syringe deposition system (syringe-based DW technology)**

The mechanism of dispensing method will be studied and its dispensing parameters will be identified and characterized including the stand-off distance, tip size, applied pressure and deposition speed. The capability of the method will be evaluated by fabricating simple and complicated lines as well as real electronics components such as antenna and strain gauges. The quality of the conductive lines produced will be assessed by analysing the resulting physical characteristics of the lines including its geometrical accuracy involving line width, height and spacing between lines with respect to the process parameters selected. The electrical characteristics of conducting lines especially its resistivity will also be evaluated accordingly.

ii. **Investigation of the effect of several direct write process parameters for process optimisation purposes**

Investigation will be done by varying the DW process parameters and the appropriate parameter ranges will be determined for process optimization. The relationship between the DW process parameters with the resulting physical and electrical characteristic of the conducting lines will also be established.

iii. **Investigation of the effect of different conductive material properties and substrate material on track morphology**

Investigation will also be done by using several inks and substrates where different properties of the inks used will generate different physical and electrical properties of the conductor lines. In addition, dispensing on several substrates will also result in different morphology of the conductor tracks.

iv. **Examination of the effect of controlling the DW process parameters on the functional performances of the pattern produced**

The performance of components will be tested and evaluated in terms of its physical, mechanical and electrical characteristics using direct measurement and it will be compared with results from simulation using specified simulation packages. The pattern performance parameters will be determined and analysed and the outcome will leads to the necessary improvements to improve the efficiency of the pattern produced as well as the understanding of the DW process behaviour

1.6 Organisation of the thesis

The thesis consists of six chapters describing all the work done in the research. These chapters are structured as follows:

The first chapter gives an overview of the research topic and the challenges it seeks to address. It also presents the background to the need to reduce manufacturing costs and alternative methods for printing circuitry in a cost effective manner. This chapter sets the work flows according to the aim and scope of the research.

Chapter 2 presents a literature review on the principle of traditional and current methods to produce circuitry and previous work on direct writing using other technologies. Methods of direct writing, conductive inks formulation, choices of substrates, theory of resistivity, measurement of physical and mechanical of conductive lines are reviewed in this chapter as they will then be used as part of the studies described in later chapters. In addition, a literature review on the direct write of antenna is also presented and discussed.

Chapter 3 presents the characterization of the syringe-based DW technology used in detail. The explanation of main components of the syringe-based DW process is described as well as the effect of its dispensing parameters to the pattern produced. A dispensing flow model applied to represent the deposition process is also expressed.

Chapter 4 describes the potential application of the syringe-based DW technology in manufacturing of radio frequency identification (RFID) tag antenna. The outcome of the comparative study between the etched copper (traditional method) and silver tracks fabricated by syringe-based DW technology was also presented and discussed.

Chapter 5 discuss the effects of controlling the deposition parameters on the structure of ink deposited. The influence factors of the cross-sectional shape of conductor tracks to the antenna electrical performance were also investigated. The steps on designing the planar dipole antenna, the software used for design and simulation, the structure of the designed antennas, and the measurement techniques are all explained.

Chapter 6 concludes by summarising the key findings of the research on the investigation of syringe-based DW technique for antenna manufacture. In addition, the contributions of the research are summarised and possible future research directions are proposed. The research is summarized to give general achievements so that future improvements can be made by other researchers.

Chapter 2

Literature Review

2.1 Introduction and Background of Direct Write

The employment of conventional DW technologies to printed electronics might be traced back to the 1980s, when metal conductors for solar cells were patterned with inkjet printing by Teng and Vest [8]. There are several definitions that best described Direct Writing (DW). Generally, DW is defined as a range of technologies to fabricate two or three dimensional functional structures, directly onto flat or conformal surfaces. Lewis and Gratson [9] have described direct-write as a fabrication method that employs a moveable pattern-generating device with computer-controlled translation stage to create materials with controlled architecture and composition. Likewise Pique and Chrisey [10] defined DW as any technique or process capable of dispensing or processing different types of materials over various surfaces following a pre-set pattern or layout. It is also described as a range of flexible multi-scale, CAD/CAM controlled fabrication technologies, which can be used

to produce 2D and/or 3D structures on pre-existing substrates with a wide range of materials. They can be used to form simple 2D components or complex 3D architectures on curved and doubly-curved surfaces.

2.2 Classification of Direct Write Technologies

Within all definitions of DW lie several techniques in which they can be broadly placed based on the mechanism of materials transfer. The several categories comprises of droplet-based, flow or filament-based, laser-based, tip-based and energy-beam based DW technologies as depicted in Figure 2.1. Within these categories are several sub-categories of technologies that can deposit materials from the nm scale to mm. Droplets-based group is sub-divided into liquids and aerosol where its techniques rely on the deposition of inks to create structures layer-by-layer. In contrast, laser-based group is categorized into four different types which is solid, gas, liquid and bio-material. Its writing technique is based on creating patterned materials through ablation or reactive chemical processes. Meanwhile, for the tip-based technique, it is represented by two processes; dip-pen nanolithography and nano fountain pen. Focused ion beam is the only technique under the energy beam-based dispensing technique. The newest ink-based DW technology is flow or filamentary-based DW where it is further separated into pump and extrusion type of dispensing techniques. For the pump technique, it requires high precision micro-dispensing technology via a precision pump as in nScrypt process according to Li et al [11].

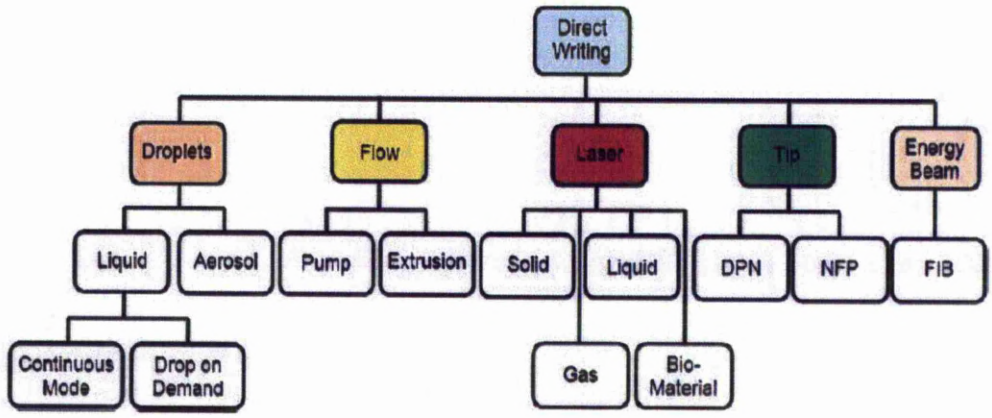

DPN : Dip-Penlithography

NFP : Nano-fountain pen

FIB : Focused Ion Beam

Figure 2.1: Classification of Direct Writing Methods (Hon et al [104])

2.3.1 Droplets-based Direct Write

Ink-jet printers have become very familiar over the past 30 years in the context of small office and home (SOHO) applications. The rapid development of this technology followed the earlier introduction of ink-jet printing in an industrial context for in-line date coding and marking of products, and is now being followed by the progressive use of similar technologies in the manufacturing of products themselves, both in the large-scale printing of text and graphics, and also in the controlled digital deposition of structural and functional materials. Ink-jet based direct writing involves the formation and deposition of a sequence of droplets of liquid material, often called an ink or fluid. After deposition this material usually becomes solid, by the evaporation of a solvent, chemical changes (e.g. through the cross-linking of a polymer) or through cooling (e.g. by crystallization or vitrification). Subsequent processing steps, such as curing and sintering, may also be involved. There are two different methods most commonly used to generate drops in ink-jet printing, termed continuous ink-jet (CIJ) and drop-on-demand (DOD).

2.3.1.1 Continuous ink-jet (CIJ) Printing

In continuous ink-jet (CIJ), a continuous stream of ink drops is generated from a nozzle by exciting the natural tendency of a continuous liquid jet to break up under surface tension forces. Each drop is then individually steered (deflected) to write spots on the substrate. Drops that are not selected in this way are fed into a gutter and recycled. Simple CIJ systems use single nozzles, but systems also exist with multiple nozzles. Figure 2.2 shows the break-up of a continuous ink-jet. A typical commercial CIJ printing system might have a jet diameter of 60 μm and a jet velocity of 20 m/s, giving drops about 120 μm in diameter and requiring a drive frequency of about 75 kHz. In a typical CIJ print head, shown schematically in Figure 2.2, the jet is generated by pumping the liquid into a chamber from which it emerges through a nozzle, and the modulating disturbance is provided by a piezoelectric transducer in contact with the ink or the nozzle.

An alternative method of stimulating the jet break-up is by the use of a small heating element very close to the nozzle outlet, fed with a periodic electric current. In most CIJ systems the drops are deflected electrostatically. The charging electrode surrounds the jet at the point at which it separates into drops, and the application of an electrical potential to this electrode induces an electrical charge on each drop as it leaves the stream. The liquid requires enough electrical conductivity for this charge to pass along the intact stream from the nozzle. By varying the potential of the charging electrode, the charge carried by each drop can be controlled and varied. The drops then pass through a region of steady electric field and are deflected sideways to an extent determined by the magnitude of their charge. Uncharged, and therefore undeflected, drops pass into a gutter from which they are recycled, while charged drops will be 'steered' to strike the substrate at a range of possible positions.

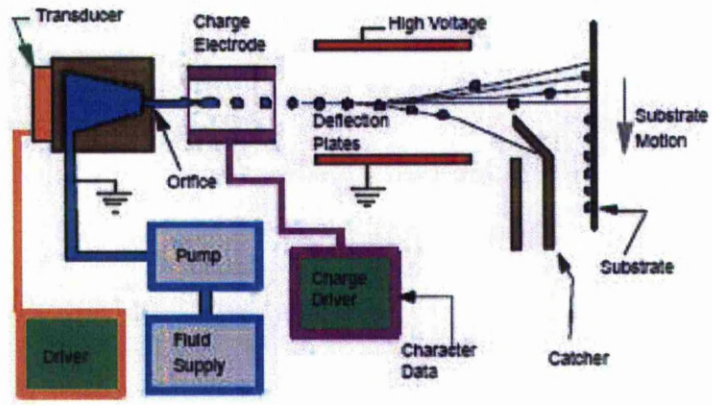

Figure 2.2: Schematic illustration of the principle of operation of a continuous ink-jet system (Shah et al [12])

By using a fluid with appropriate properties of which the most important are surface tension and viscosity, and optimising the frequency and amplitude of the modulation, it is possible to arrange that the satellite drops recombine with the main drops, which are present in a very regular and repeatable sequence. By deflecting the drops and moving the substrate appropriately, a pattern of droplets can be written on to the substrate. More complex CIJ systems can employ nozzles fed with different inks, for example to print four-colour graphics at high speeds, and commercial systems also exist which use linear arrays of many hundreds of nozzles.

2.3.1.2 Drop-On-Demand (DOD) Printing

In the DOD method, drops of ink are only ejected from the system when they are required to be printed, and there is therefore no need to recycle unused liquid. The liquid is ejected from an ink cavity in response to a trigger signal, as shown schematically in Figure 2.3, through the generation of a pressure pulse by an actuator. There are two common types of actuator. The thermal DOD (or bubble-jet) method is widely used in home and small-office printers; rapid transient heating of the ink by a small electrical heating element located in the ink cavity close to the nozzle creates a short-lived bubble of

vapour which drives a jet of ink out of the nozzle. The bubble then collapses, drawing ink from the reservoir to refill the cavity, and the process can be repeated. More common in industrial ink-jet systems is the use of a piezoelectric element which changes the internal volume of the cavity on the application of an electric field, and generates pressure waves which in turn eject ink from the nozzle and then refill the cavity. Since thermal DOD involves the vaporisation of a small volume of the ink, this places significant restrictions on the materials which can be jetted by this method; they must be relatively volatile, or at least have a volatile component. There are no such restrictions for the piezoelectric DOD method. Print heads for both methods of DOD typically contain tens, hundreds or even thousands of separate nozzles, fed by a single ink manifold but each individually addressable.

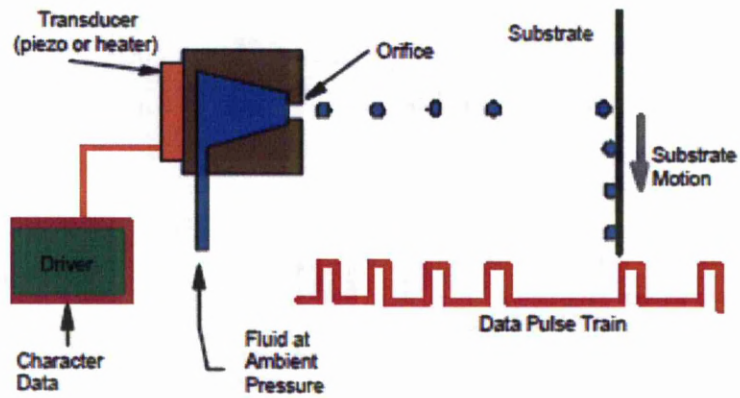

Figure 2.3: Schematic illustration of the principle of operation of a drop-on-demand print head (Shah et al [12])

2.3.2 Laser-based Direct Write

Laser direct writing (LDW) refers to the creation of 2D to 3D features by laser-induced deposition of metal, ceramics, semiconductors, polymer, composites and bio-materials without the use of masks or lithographic methods. LDW was introduced in the early 1980s with pioneering work from Lawrence Livermore National Laboratory and AT&T Bell Laboratories to

enable the fabrication of micro-electronic circuits with 2D features. The technology was further developed in the 1990's, e.g. with critical contributions from the Max Plank Institute in Germany and the US Naval Research Laboratory, to enable the creation of 3D features for wider applications including photonic crystals and micro-electro-mechanical system (MEMs). Since late 1990s LDW has become more mature and new applications, particularly in the biomedical sector, have been actively investigated by the wider scientific communities and industries. In this section, the basic characteristics of major laser direct writing techniques and the mechanisms of feature formation and material transfers are presented. Laser direct writing can be carried out in a number of ways including depositing from gaseous, liquid and solid precursors and material transfers. The techniques involve either laser-induced chemical/electrochemical or physical reactions that lead to the deposition of a material to the substrate

2.3.2.1 Matrix-assisted Pulsed Laser Evaporation (MAPLE) Direct Write

The matrix-assisted pulsed laser evaporation (MAPLE) DW technique utilizes all of the advantages associated with laser-induced forward transfer (LIFT) and MAPLE to produce a laser driven direct-write process capable of transferring materials such as metals, ceramics, and polymers onto polymeric, metallic, and ceramic substrates at room temperature. The overall write resolution for this technique is currently on the order of 10 μm. Since MAPLE DW uses a highly focused laser beam, it can easily be utilized for micromachining, drilling, and trimming applications, by simply removing the ribbon from the laser path. The flexible nature of MAPLE DW allows the fabrication of multilayered structures in combination with patterning. Thus, MAPLE DW is both an additive as well as subtractive direct-write process. MAPLE DW can also be adapted to operate with two lasers of different wavelengths where the wavelength from one laser has been optimized for the

transfer and micromachining operations (i.e. UV), whereas the second laser is used modify the surface and anneal either the substrate or any of the already deposited layers (i.e. IR or visible). In MAPLE DW, a laser-transparent substrate such as a quartz disc is coated on one side with a film a few microns thick. The film consists predominantly of a mixture or matrix of a powder of the material to be transferred and a photo-sensitive polymer or organic binder. The polymer assists in keeping the powders uniformly distributed and well adhered to the quartz disc. The coated disc is called the ribbon and is placed in close proximity (25 to 100 mm) and parallel to the acceptor substrate. As with LIFT, the laser is focused through the transparent substrate onto the matrix coating. When a laser pulse strikes the coating, a fraction of the polymer decomposes into volatile by products which propel the powders to the acceptor substrate. In MAPLE DW, the material to be transferred is not vaporized, because the laser required to decompose the photo-sensitive polymer are below the ablation threshold of the powders. By avoiding the vaporization of the material, complex compounds can be transferred without modifying their composition, phase, and functionality. Furthermore, there is no heating of the substrate on which the material is transferred. Both the acceptor substrate and the ribbon are mounted onto stages that can be moved by computer-controlled stepper motors. By appropriate control of the positions of both the ribbon and the substrate, complex patterns can be fabricated. By changing the type of ribbon, multi components structures can easily be produced. Furthermore, because the laser in the MAPLE DW system can also be focused onto the substrate, operations such as micromachining, drilling, trimming, and annealing can be performed by simply removing the coated ribbon from the laser path.

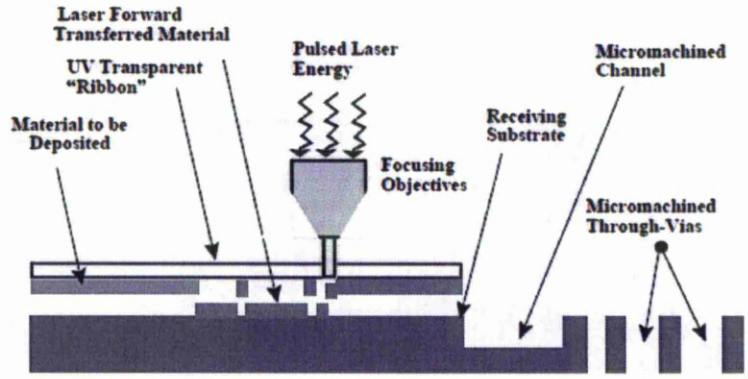

Figure 2.4: Schematic representation of the MAPLE DW process (Marinov et al [31])

2.3.2.2 Laser-induced Forward Transfer (LIFT)

Over the past decade, many direct-write techniques based on laser-induced processes have been developed to deposit materials for a variety of applications. Among these techniques, LIFT has shown the ability to direct write metals for interconnects and mask repair and also simple dielectric materials such as metal oxides. LIFT was first demonstrated with metals such as Cu and Ag over substrates such as silicon and fused silica by utilizing excimer or Nd: YAG lasers. LIFT is a relatively simple technique that employs laser radiation to transfer a thin film from an optically transparent support onto a substrate placed below and parallel to it. Patterning is achieved by moving the laser beam (or substrate) or S280 by pattern projection. The former is a method of direct writing patterns. LIFT has several experimental requirements that can have significant effects on the quality of the pattern or device fabrication. The laser should be adjusted so that the process is carried out near the energy threshold to transfer only the film material. Target films typically do not exceed a thickness of a few 100 nm. The distances between the target film and the substrate must be controlled, generally within 25 to 75 mm. Overall, LIFT has proven to be a simple and effective technique that can be used on a

wide variety of metals, and some simple oxides, but not with complex multi-component materials such as ferroelectrics.

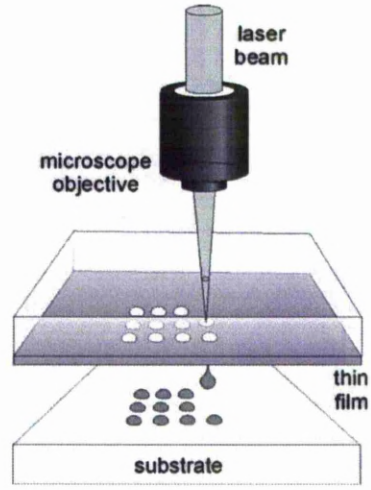

Figure 2.5: Schematic of the LIFT method of operation (Serra et al [82])

2.3.2.3 Laser Direct Write (LDW)

Laser direct-write (LDW) is a general term that encompasses modification, subtraction and addition processes that can create patterns of materials directly on substrates without the need for lithography or masks. The interaction of the laser with the substrate, or any other surface for that matter, results in material modification (melting, sintering, etc.) or material removal (laser micromachining). The later allows the generation of the trenches or pockets where the devices are to be embedded inside the substrate. Subtractive LDW can generate patterns by either moving the substrate or rastering the laser beam or a combination of both. In additive mode, the LDW technique behaves effectively as a "functional materials printer" as shown schematically in Figure 2.6. Simply stated, powders of the material to be deposited, i.e. Ag powders (to make metal patterns) are combined with a liquid carrier to form an ink. This ink is spread on a glass plate to form what is referred to as the ribbon. The ribbon is held above the substrate surface separated by a distance of 100 to 200 μm so it can move independent of the substrate. A pulsed UV laser irradiates

the ink from behind the glass plate to propel a mass of material forward to the substrate below. This laser printing process takes place by rastering either the beam or the substrate to produce a pattern of material. Different materials can be deposited by simply changing the composition of the ribbon. Details of the LDW process as applied to sensors, micro batteries and interconnects have been presented elsewhere [14].

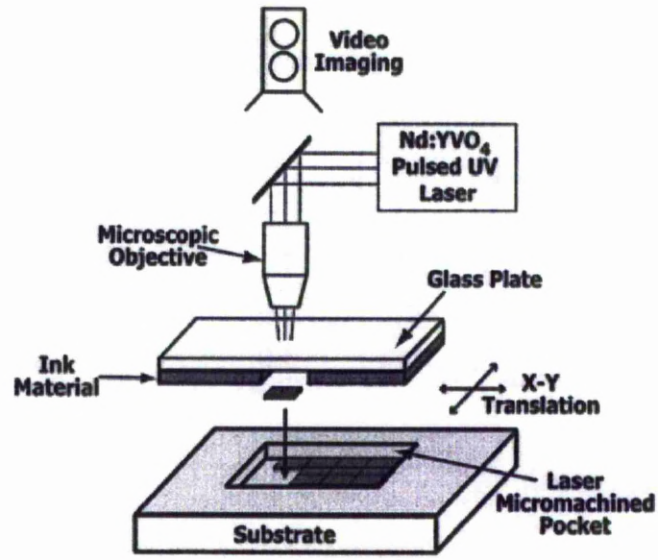

Figure 2.6: Schematic of Laser DW addition process showing deposition within the substrate (Wartina et al [14])

2.3.3 Tip-based DW

2.3.3.1 Dip Pen Nanolithography

Dip Pen Nanolithography is NanoInk's patented process for deposition of nanoscale materials onto a substrate. The DPN process uses a coated scanning probe tip to directly deposit a material with nanometer-scale precision onto a substrate. The vehicle for deposition can include pyramidal scanning probe microscope tips, hollow tips, and even tips on thermally actuated cantilevers. It is an amazingly robust and versatile technique, and can deposit a

variety of organic and inorganic molecules onto a variety of substrates under ambient conditions (Figure 2.7). Further, thermal DPN (tDPN) grants access to an even wider range of ink materials by enabling solid ink deposition via a heated tip.

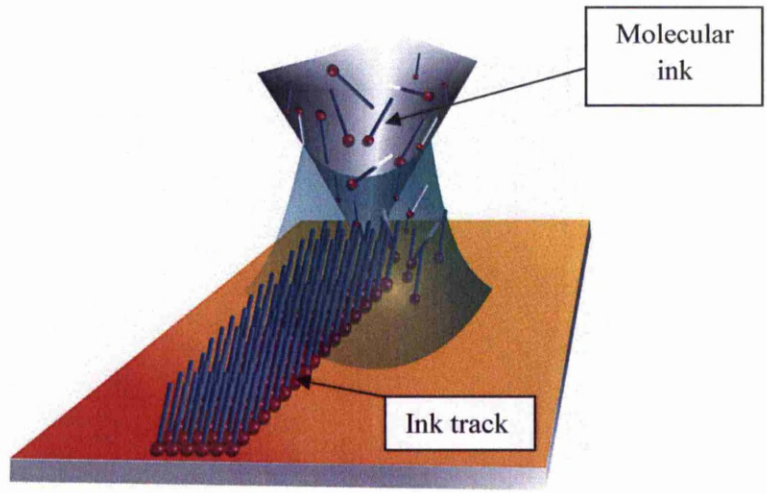

Figure 2.7: Schematic of the Dip Pen Nanolithography (DPN) process. A molecule coated AFM tip deposits ink via a water meniscus onto a substrate (Noy et al [15])

2.3.3.2 Nano Fountain Pen

In the fountain pen, a micro fluidic system consists of two micro channels and a high-capacity reservoir which contains ink. Ink from the reservoir is moved through micro channels by capillary action force; then ink is deposited at the tip. When the tip contacts the substrate, molecular inks makes a meniscus; after that if the tip is moved, a pattern will be made. The volume of meniscus can be controlled with time by varying pressure and velocity. If early meniscus is formed, because the tip is moved, in this time, line width is decided by spread after tip's transfer speed. In this case, the line width is formed by some effects, the velocity of tip, the diffusion of ink, the coefficient of diffusion, the concentration, the relative humidity, etc. Figure 2.8 depicts the

schematic of NFP. A tip is connected in channel. When the tip is attached to the substrate, then a pressure gradient is occurred, it makes the volume of channel change; so ink can flow out. It is possible that initial meniscus can be controlled.

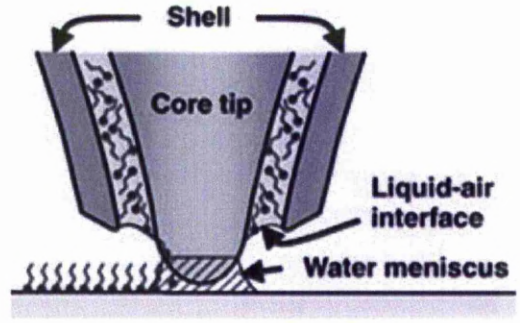

Figure 2.8: Schematic of the Nano fountain pen (Choi and Poulikakos [16])

2.3.4 Energy Beam-based

2.3.4.1 Focus Ion Beam (FIB)

In FIB (Figure 2.9), the ion beam is generated from a liquid gallium source. The ion beam energy is typically between 10 and 50 keV, with beam currents varying between 1 pA and 10 nA. When energetic ions hit a surface, four mechanisms can take place: sputtering of neutral and ionized substrate atoms, electron emission, displacement of atoms in the solid and emission of phonons. For the DW mode, the process requires the spraying on the substrate surface of a precursor gas. For the deposition of W, the organometallic precursor gas is $W(CO)_6$. Other precursor gases are available for the deposition of conductors such as Au, Al, Cu, Mo and Pt, and insulators such as TEOS, $TMCTS/O_2$, $PMCPS/O_2$. The principle of deposition is similar to LCVD except that FIB offers better resolution but lower deposition rate, typically 0.05 $\mu m^3/s$. The minimum feature that can be produced under the conditions used is 80 nm due to particle scattering and migration of the carbon from the near-surface atmosphere prior to deposition [14]. The minimum thickness is about 10 nm

and aspect ratios are between 5 and 10. FIB DW is a well-established tool for the repair of conventional and phase-shift masks to add missing absorber materials. As organo-metallic compounds are used for metal deposition, FIB deposits are not pure because of organic contaminants and Ga^+ ions. Due to rather large carbon contents, the resistivity of these deposits is generally about one to two orders of magnitude higher than those of pure metal [15]. FIB is a relatively slow process and its applications are restricted to low volume production, especially repair work. It is capable of conformal deposition and forming 3D micro-structures which can be used for hermetic encapsulation for micro-sensors.

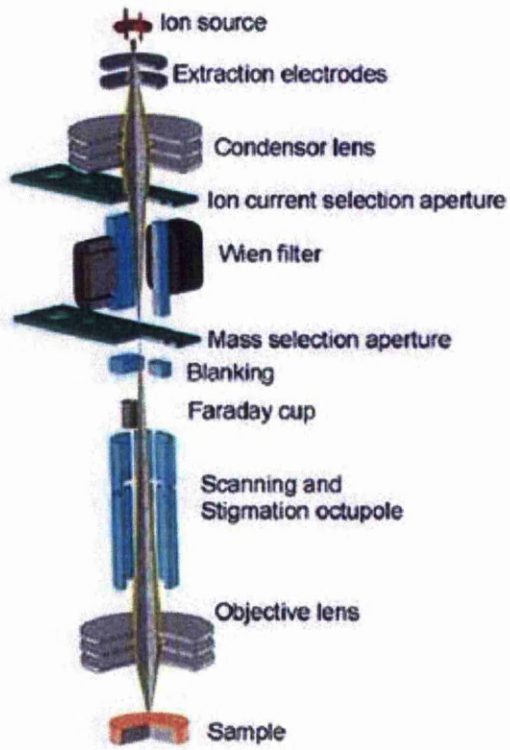

Figure 2.9: Schematic of the Focus Ion Beam (FIB) process (Hoey et al [98])

2.3.6 Filament-based Direct Write

The common property of processes grouped under flow-based DW is that they all require a positive mechanical pressure to achieve precision micro-dispensing through a positive displacement pump, air pressure or extrusion through a syringe. Unlike inkjet or aerosol jet DW where a line is formed from individual droplets, flow-based DW is characterized by a continuous flow of ink, paste or slurries on to the substrate. This group of methods differs from the Fused Deposition Method (FDM) in two main respects. Firstly, there is no heating of the material, and secondly, the volume of flow is much lower, in the order of nL/sec. The two most well-known and established methods are known as nScrypt and MicroPen, both of which are trademarks.

Generally, the filament-based DW technology is considered as the flow-based writing where the deposited material is continuously extruded through a fine cylindrical nozzle (or orifice) to create a filamentary element. According to Lewis et al [16], for the deposited material delivery, there are two types of material delivery systems for filament-based writing which is first, the constant-displacement and secondly, the constant-pressure extrusion. The filament diameter is determined by the nozzle diameter, the deposited material and printing speed. During constant-displacement printing, the deposited material filaments are extruded at a uniform volumetric flow rate. In constant-pressure writing, the deposited material filaments are extruded by applying a uniform pressure to the reservoir. This approach is less common as slight variations in rheological properties induce fluctuations in the volumetric flow rate.

The deposited material flows through the deposition nozzle when a pressure gradient ΔP is applied along the length and a radially varying shear stress (τ_r) develops;

$$\tau_r = \frac{r\Delta P}{2l} \tag{1}$$

where r is the radial position within the nozzle (i. e. r = 0 at the centre axis and r = R at the nozzle wall). Depending upon the velocity profile and the deposited material stability, plug or laminar flow may occur within the nozzle. In the molten state, this deposited material must possess both a low viscosity and a high solids loading to minimize component shrinkage during binder removal and sintering. They have also mentioned that filament-based printing faces at least three problems. First, when building solid objects, the ink delivery system must precisely deliver the proper volume of material to fill perfectly the space between adjacent tool-path lines. The tool-path lines represent the locus of points traced by the center line of the deposition nozzle, but the extruded filament has a finite diameter (assuming that the orifice is circular). The selection of which variables to fix is a matter of user preference and ink behaviour. As the extrusion nozzle is nearly always circular in cross section, the filament must deform upon extrusion to fill the space traced by the nozzle.

The second challenge faced is the inevitable need to stop the ink flow, reposition the nozzle on a new tool path, reinitiate the flow, and continue printing. For filament-based printing, it is desirable to minimize the number of start–stop events. Algorithms have been proposed to minimize either the number of start–stop events or the distance between the start and stop positions when changing tool-path lines. The third challenge of tool-path calculation involves consideration of the stacking of layers when spanning, cantilevered, or floating elements exist. Algorithms for calculating unsupported regions of the pattern are required along with a suitable fugitive material. In the case of printing colloidal fluids or gels, a suitable support should print, solidify, and be chemically compatible with the colloidal ink. These problems will only occur when dealing with fabrication of three dimensional structures. For fabricating two dimensional conductive lines, such problem will not be considered. The only important fact that matters is the filament diameter of the deposited material in which it was determined by the nozzle diameter, the deposited material and printing speed. In addition, during dispensing clogging may occur at the nozzle tip but make sure the deposited material possess a low viscosity

and a high solids loading to minimize component shrinkage during binder removal and sintering.

2.3.6.1 nSycrpt System

nScrypt system is a new and promising DW technology which provides a smart pumping technique that can dispense materials with precise volume control from 1 to 1 million centipoises as illustrated in Figure 2.10. It also has a unique suck-back system as illustrated in Figure 2.11 which cannot be found in other DW technology where the material will be sucked back into the dispensing nozzle after the dispensing stopped. It helps to prevent clogging at the dispensing tip as it removes the materials from sticking on the tip and create a fresh start for the next round of dispensing. In addition, it is a maskless process which results in a very cost effective process and it conformably print very fine features usually in micron on any surfaces as well as extremely flexible with wide variety of materials choices.

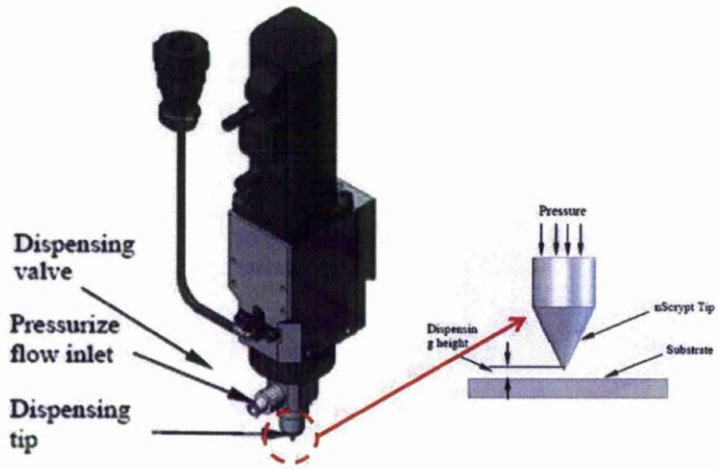

Figure 2.10: The smart pump (Li et al [11]

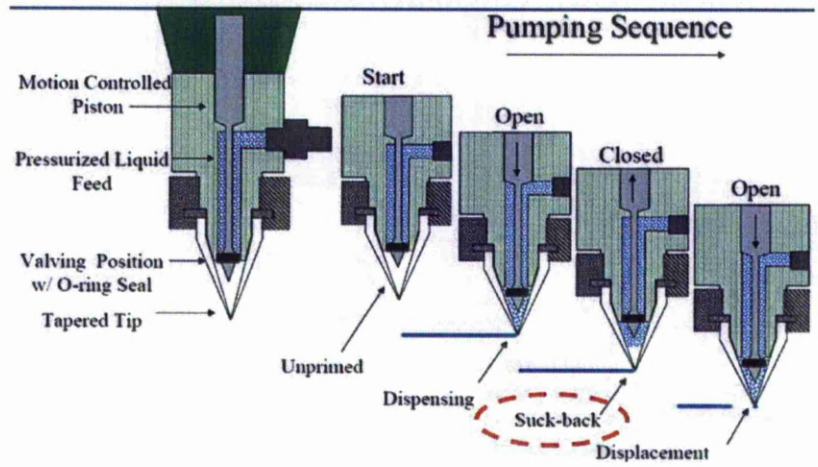

Figure 2.11: Valve operation with computer controlled piston actuation (nScrypt [3])

Moreover, nScrypt system has been implemented in numerous applications. nScrypt system has been used to produce scaffolds and other biomedical structures purposesly for tissue engineering with the aid of Computer Aided Biological (CAB) tool. The work is done by Li et al [11] where they used a direct write technique via nScrypt system since the conventional system suffered from lack of consistency and repeatabillity as well as not being fully controlled and unable to reproduce the previous work with accuracy. The aim of the research was to demonstrate the ability of nScrypt system associated with CAB tool to create porous scaffold with a controlled strut size and porosity. In this work, the scaffold was designed to replace or repair the damage tissue or organ by using a combination of PCL and glacial acetic acid solution. The results shows that the struts and pores within the generated 3D scaffolds were uniform and evely spaced by comparing with its expected dimension. It is found that the overall size and porosity is consistent with an overall deviation of ±3% in pore size and as little as ±1% in total porosity. Besides, these scaffolds were able to withstand 4 to 8 pounds before breaking. The ultimate strength is found to be varied from 24 to 40 MPa with an average of 29.62 Mpa. Hence, it clearly shows that the nScrypt sytem with the aid of CAB tool and its smart pump technology is capable of producing porous structure with a precise controlled 3D geometry.

Another research was conducted by Whites et al [17] in which the combination of nScrypt system and Maskless Mesoscale Material Deposition (M^3D) was used to directly print multilayered applique antennas on high impedance surfaces. The M^3D was employed to deposit the conducting lines while nScrypt system was utilized to dispense dielectric layers. The work started by fabricating a thick sheet of Rogers RO4003C laminate. Square metal rings were then printed onto the laminate in a two dimensional array. M^3D was used to deposit silver ink and a 75 microns thick layer of liquid polymide was deposited using nScrypt machinie. These three layers and the single-sided substrate form a high impedance surface (HIS) and the antenna was then tested to evaluate its performance. The results shows that the antenna has a usable bandwidth of 4.9 GHz to better than 6 Ghz, or greater than 20.2% relative bandwidth. The absolute gain is also measured in which the main lobe of the radiation pattern at 5.3 Ghz was found to be approximately 30^o off normal in the elevation plane. Thus, it was concluded that the multilayered applique antenna was succesfully printed on HIS and it was manufactured solely from direct-write methods.

Kirchesman et al [18] also utilized the direct-write technologies by means of incorporating the used of inkjet printer (FUJIFILM Diamtix DMP-2830) with nScrypt system (model 600 machine) to deposit silver conductive ink (Cima NanoTech) and liquid polymide. A dual frequency band stacked patch antenna was succesfully fabricated as an example of microwave frequency devices. In this work, two identically sized microstrip antenna were fabricated on top of each other and designed to operate at 5 GHz on 813 microns of thick Rogers RO4003C laminate. A 150 microns of dielectric (liquid polymide) was produced in between these two laminates and the antenna is tested later to determine its performance. The results shows that the measured match point and radiation pattern were in good agreement with simulation. From this work, it shows that the integration of multiple direct-write technologies widen the device prototype capabilities to include multilayer devices with reduced building time.

Likewise, another succesful implementation of integration of multiple direct-write technologies was found in the work to fabricate "Altshuler" antenna with discrete resistive loading accomplished by Montoya and Kirchesmann [19]. The conductive portion (traces) of the antenna were made by using a silver-based nano-inks on an Optomec M^3D system and commercial inks (Paralec) on an nScrypt system. Later, the antenna was measured by soldering it to SMA bulkhead connector on a 91.4 x 101.6 cm copper ground plane to determine its perfomance. The results shows that the simulated results were in good agreement in which the input resistance and reactance are relatively stable over a wide frequency range especially compared to a conductive monopole of the same overall length. This work clearly shows that the successful fabrication of an "Altshuler" type antenna via direct-write fabrication on a flexible polymide substrate which have great commercial potential due to its inherent flexibility and low cost.

2.3.6.2 Syringe and Extrusion Method

Another form of direct writing based on a micro-capillary tip is Micro-Pen which is the trademark of a DW system produced by OhmCraft Inc. In operation, a flowable material which can be liquid or particulate slurry is loaded into a syringe that is then connected to the writing head of the MicroPen. A pneumatic ram compresses the plunger of the syringe and forces the material into the writing head known as the 'block'. The writing head consists of a metal double piston cylinder, an A-frame fluidic pathway and micro-capillary writing tip. Flowable material fed into the 'block' is pressurized up to 13.8 mPa and dispensed through the writing tip. The tip traverses perpendicularly on the surface of the substrate surface without direct contact. A schematic diagram of the MicroPen set-up is given in Figure 2.12 [20].

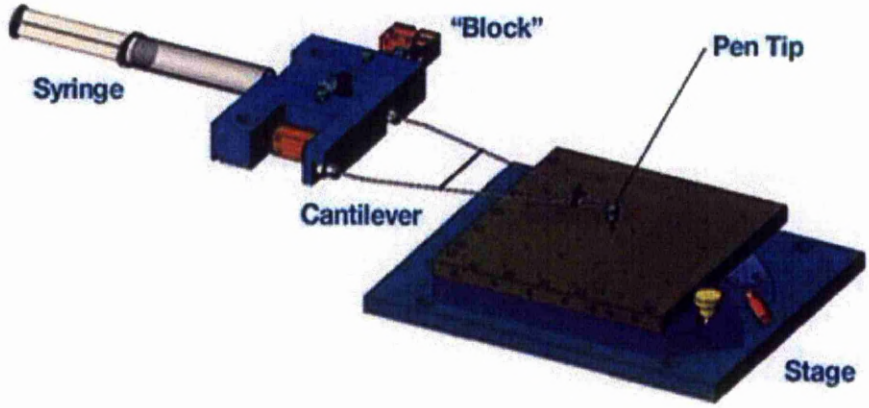

Figure 2.12: Schematic diagram of MicroPen (Cao et al [20])

The MicroPen uses an extrusional method for depositing material and there are unique writing parameters for each pen orifice size, writing speed and paste material. The pressure required must overcome the frictional stresses at the wall and the capillary force of the orifice. As the height of the pen tip is continuously sensed and its force can be controlled to tens of microNewtons levels, MicroPenning enables deposition on extremely soft surfaces with active topologies, including inflatables such as medical balloons. Any liquid material whose viscosity ranges between 5 to 500,000 mPa.s is a candidate for MicroPen deposition. The line widths are in the range of 50 μm to 2.5 mm with a height from 1.3 μm to 250 μm. The system can also dispense individual dots with a volume as small as 100 nL. For an orifice of 50 μm, a writing speed of 25.4 mm/sec has been used to write functional silanes.

2.4 Curing Process in DW

The type of laser used was a 532 nm Nd:YAG laser. The lasing medium in the Nd:YAG laser is solid state crystal of yttrium aluminium garnet (YAG), which has the composition of $Y_3Al_5O_{12}$ and to which has beo yttrium in the crystal lattice. Hence, the crystal is then referred to as Nd:YAG and this gives its name the laser type. The transitions that can be made to occur in the

neodymium ions in YAG when the crystal is pumped with optical energy. The main advantage of Nd:YAG lasers over CO_2 lasers are that the 1.06 μm radiation produced can be delivered by optical fibre. This type of laser has a maximum power output of 60W and it is a relatively high power laser to produce a green 532 nm beam. This laser machine is able to produce a laser beam near Gaussian beam where a Gaussian beam is a beam of electromagnetic radiation whose transverse electric field and intensity (irradiance) distributions are well approximated by Gaussian functions. Figure 2.13 below illustrates this laser.

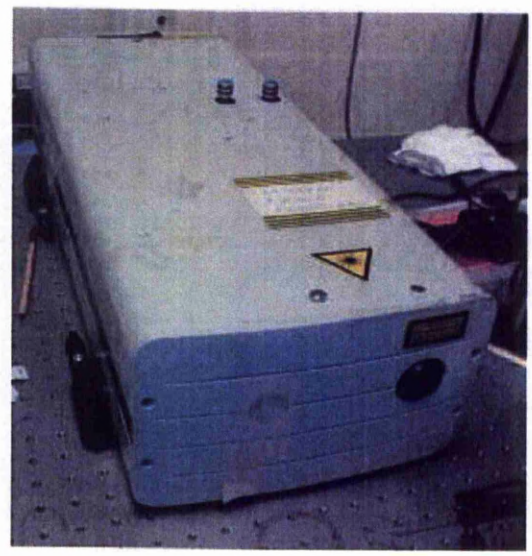

Figure 2.13: Nd:YAG (Green) Laser (Facilities in Lairdside Laser Center)

The laser system used is also consisted of a CNC control table (Figure 2.14) where it was equipped with two-axis of movement (x and y directions). All the movement and parameters setting were done and controlled by the CNC control machine as depicted in Figure 2.15.

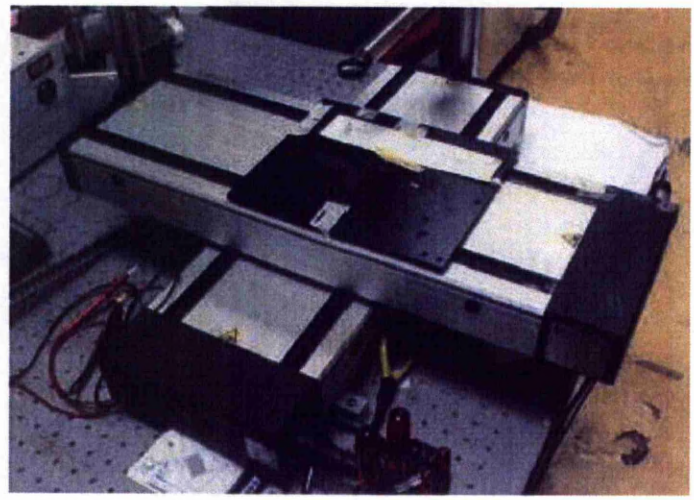

Figure 2.14: CNC control table (Facilities in Lairdside Laser Center)

Figure 2.15: CNC control machine (Facilities in Lairdside Laser Center)

Laser-based DW technology lately has been seen popular and widely engaged in curing conductive ink for numerous applications. Particulate silver inks are finding increasing use in the direct manufacture of electronic circuitry. Laser curing of these inks as opposed to traditional oven-curing methods is advantageous for reasons of speed and the protection of nearby heat-sensitive

components, and particularly for the construction of circuitry on conformal surfaces and 'on the fly' modification or production according to Sato et al [21]

To fully appreciate the benefits provided by using a laser based process, it is important that the final cured component has electrical and physical properties that are comparable to if not better than those that are produced using the conventional technique. Currently in some single pass techniques cavities are formed in the track due to rapid boiling off of solvents that leads to a higher resistivity than that of oven cured tracks. By going from a single pass curing process to a multiple pass process, it is possible to improve the track quality by allowing the gradual release of solvent vapour from the ink. This incremental process improves settling of the silver particulates leading to a resistance of the cured inks that is lower than that achievable through oven curing. This creates the possibility of fabricating a surface mounted antenna or embedded damage sensor without thermally affecting the substrate

According to Pique et al [10], there are generally two categories of the direct-write tool which are first those that can deposit functional materials during the deposition process and those that can deposit materials which have to be subsequently heat treated to induce controlled and reproducible functionality. For example, materials dispensed by nScrypt process was characterized under second category in which requires post-processing, typically sintering, in order to achieve their final properties and characteristics.

Table 2.1: Several curing techniques applied in direct write (X denoted as not available)

NO.	RESEARCHERS	YEAR	TECHNIQUE	SPECIFICATION		
				TIME	TEMPERATURE	TYPE
1	Chung and Grigoropoulos [23]	2004	Laser	X	X	X
2	Whites et al [17]	2007	Laser	X	100°C	Nd:YAG
3	Bieri et al [25-27]	2004	Laser	X	1063°C	Argon ion
4	Cai et al [29]	2009	Laser	X	X	Nd:YAG
5	Sato et al [21]	2009	Laser	X	X	CO_2
6	Marinov [32]	2007	Laser	X	X	Nd:YAG
7	Chung et al [24]	2005	Laser	X	200°C	Pulse
8	Kim et al [33]	1999	Laser	X	X	Argon ion
9	Khan et al [36]	2008	Laser	X	X	Nd:YAG
10	Atanasov et al [28]	2006	Hot plate	60 min.	220°C	X
11	Kim et al [34]	2006	Hot plate	30 min	100-300°C	X
12	Dockendorf et al [38]	2006	Hot plate	10 min	220°C	X
13	Fuller et al [39]	2002	Hot plate	10 min	100-300°C	X
14	Szczech et al [40]	2002	Preheated oven	15 min	300°C	X
15	Smith et al [41]	2006	Furnace	60 min	150°C	X

According to Chung et al [22-24], they found that printing and laser curing at the same temperature will benefit the processing speed/simplicity and feature size. They concluded that pulsed laser based curing of printed nanoink combined with moderate and controlled substrate heating was successfully produced conductive microlines having 4-5 times higher resistivity than the bulk value at low enough temperatures appropriate for polymeric substrates. In addition Whites et al [17] have used a Nd:YAG type of laser to sinter silver ink and Bieri et al [25-27] have used laser to cure a gold nanoparticle solution (NPS) in which they found that the total width of the line has increased with the increasing of laser power. In the meantime, Atanasov et al [28], had encountered the conventional oven and hot plate sintering may be incompatible with printed structures on a low-temperature polymer substrate. Cai et al [29] described laser sintering via continuous- wave Nd:YAG laser has been used to process thermal sensitive material (thick-film PTC thermistor paste) deposited by micro-pen direct-write technology. Laser sintering enabled finer thermistor

lines to overcome the resolution limitation of micro-pen deposition without the use of any high temperature post processing. The thermistors exhibited excellent electrical performance and resistance tolerance equivalent to traditional oven-fired electronic paste. The main advantages of this technique are no mask and no high temperature post processing involved. Marinov et al [30-32] presented experimental results for the microscale electrical resistance of two silver inks deposited by DW method and sintered with a continuous wave Nd:YAG laser. Result showed that higher laser powers reduce significantly the resistance of the silver inks. Chung et al [22-24] also studied pulsed laser based curing of a printed nanoink (nanoparticle ink) combined with moderate and controlled substrate heating was investigated to create micro conductors at low enough temperatures appropriate for polymeric substrates. Kim et al [33-35] have studied photocuring of acrylic resin by an argon ion laser for the development of an economic, automated, and computer-aided manufacturing process of screen for textile printing. Khan et al [36] presented nanoparticle inks deposited on low temperature polyimide substrates using Maskless Mesoscale Material Deposition (M^3D) technology were laser sintered using a continuous wave 1.06 micron Nd:YAG laser. It was shown that less than 0.05-$\mu J/\mu m^3$ started the sintering and 0.34-$\mu J/\mu m^3$ was enough for sintering the deposited samples regardless of initial resistance. Albert et al [37] had used the laser ablation of microparticle aerosol (LAMA) process to direct-write nanostructured, patterned films of silver with thicknesses in the range 20–200 μm at room temperature. LAMA-produced films were found to sinter to produce high strength, high conductivity films at temperatures 50–100°C lower than conventional processes that use organic additives.

Laser sintering involves localized fusion of particles spread over a thin section of the deposited material. The advantage of using laser assisted sintering was its ability to deliver significant heat in a very restricted depth area without damaging the underlying substrate material. This allows for much higher sintering temperatures on the surface of the deposited material than possible in the conventional oven processing.

Hot plate technique also have been used in numerous researches as mentioned by Atanasov et al [28] where they used the hot plate to sinter gold film and silver nanoparticles suspension. Kim et al [33-35] have also used hot plate to sinter silver nanoparticle whereby Dockendorf et al [38] have used hot plate to sinter gold nanoparticles (GNP). Fuller et al [39] have used hot plate to sinter gold and silver colloidal nanoparticle inks. Mainly hot plate has been used because of its simplistic reason.

Preheated oven also have been applied in several studies including Szczech et al [40] in which they have used preheated oven to sinter silver and gold nanoparticles fluids suspension whereas Smith et al [41] have used furnace to sinter silver organic compound.

As a conclusion, since the application of different types of sintering technique gives different surface morphology, the selection of sintering technique is vital in which it will give rise in different performances and surface morphology to the components produced by DW. There are several advantages discovered for different type of sintering technique applied.

Table 2.2: Several advantages of the sintering technique available

NO.	SINTERING TECHNIQUE	ADVANTAGES
1	Laser	a) Suitable for printed structures on a low-temperature polymer substrate b) Ability to deliver significant heat in a very restricted in depth area without damaging the underlying which allows for much higher sintering temperatures on the surface of the deposited material than possible in the conventional oven processing
2	Hot plate	a) Simple process b) Completely electrical and thus very environmentally Friendly c) Low cost d) Easily controlled
3	Oven/furnace	a) Environmental friendly b) Low cost c) Easily controlled
4	Photonic curing	a) Lack of aligning optics b) Ability to simultaneously cure complex patterns

2.5 Materials Requirement in Direct Write

In general, width and thickness (height) are material dependent while straightness is machine dependent. Thus, the suitable materials/material precursors for the conductive lines or components are critical to the design and fabrication of direct-write electronic components. The inks must contain the appropriate metal precursors and a carrier vehicle according to Bidoki et al [42]. Besides, Pique and Crisey [2] stressed that the material parameters that is needed to be considered during direct-write process are viscosity, mean particle size, particle size distribution, specific heat, density, solids loading, sintering rate parameter, melting temperature, surface tension/wetting properties, particle shape/geometry, thermal conductivity, emissivity, diffusivity, reflectivity, substrate material and porosity.

2.5.1 Mechanical Properties

Several literatures have been found addressing the importance of deposited material mechanical properties especially viscosity, surface tension and melting point to the performance of components produced by DW as illustrated in Table 2.3. Viscosity is a measure of the resistance of a fluid which is being deformed by either shear stress or extensional stress or it can be described as a fluid's internal resistance to flow or a measure of fluid friction. It is commonly perceived as "thickness", or resistance to flow. The study of viscosity is known as rheology. Meanwhile, surface tension is a property of the surface of a liquid that causes it to behave as an elastic sheet. It allows small objects to float on the surface of water, and it is the cause of capillary action. On the other hand, melting point of a solid is the temperature range at which it changes state from solid to liquid.

Table 2.3: Several researches addressing the influence factor of material mechanical properties on printed pattern

No.	Researcher	Year	Mechanical Properties	Pattern Studied
1	Dockendorf et al [38]	2006	Melting point	Multilayer chip with gold pattern track
2	Goghari and Chandra [43]	2007	Viscosity	Pure water and glycerine mixtures
3	Kim et al [34]	2006	Viscosity, surface tension	Silver (Ag) nanoparticles synthesized by polyol method
4	Morissette et al [44]	2001	Viscosity, shear thinning	Capacitor
5	Park et al [45]	2007	Melting point, viscosity, surface tension	Copper conductive ink
6	Periard et al [46]	2007	Viscosity	Flashlights, functional, electronics circuit in 2D and 3D, child's toy with embedded circuitry
7	Szczech et al [40]	2002	Viscosity, surface tension	Interconnect
8	Wang et al [4]	2004	Viscosity, surface surface tension	Gold (Au) nanoparticles suspended in solvent (water and propylbenzene)

According to Dockendorf et al, [38] the success of their research was primarily depended on gold nanoinks particles (GNP) as the deposited material in which due to its low melting temperatures, the GNP could be applied to a variety of substrates including flexible polymeric ones and suitable for new applications in electronics. The conductor lines and thickness generated were satisfactory according to the specification. Park et al [45] as well agreed with the use of low melting temperature of depositing material where they used copper conductive inks to fabricate conductive lines. Apart from its low melting temperature, copper also is inexpensive, highly conductive and air stable. In their research, copper nanoparticles used had been synthesized with sufficient anti-oxidation stability to develop a copper based conductive ink in order to produce highly conductive lines at low temperature. The conductive ink obtained monodisperse spherical particles with a size of 45±8 nm. As the particle size decreased to nanoscale, the melting point of particles decreased dramatically because specific surface area increased with particle size decreased. The use of smaller particles allowed the development of highly conductive films at lower annealing temperature. The melting point of gold nanoparticles decreases dramatically with decreasing size according to Dockendorf et al [38]. The lower melting point is a result of comparatively high surface-area-to-volume ratio in nanoparticles, which allows bonds to readily form between neighboring particles. Nanoparticles can be made into a colloid that can be printed like ink described by Fuller et al [39].

In addition, viscosity and surface tension also play a major part in characterizing the performance behaviour of components produced by DW. Goghari and Chandra [43] discovered that in their research, small droplets could not be generated when the deposited material viscosity used was too low or too high. They concluded that using more viscous mixtures material, smaller droplets could be produced. A high pressure is required to force the material through the nozzle if the material viscosity is high. In the mean time, Kim et al [34] also encountered that deposited material compositions should be well controlled in terms of their viscosity and surface tension characteristics in order to produce well defined patterns. The addition of a high boiling point solvent

with lower surface tension improved the quality of the components produced as well as the conductance. Szczech et al [40] also consent that both viscosity and surface tension were the critical properties of the deposited material in order to create stable deposition resulting in well-defined pattern in DW. The recorded line width and thickness were well expected and the conductivity was satisfactory. The low viscosity of metallic nanoparticles fluid suspensions (NPFS) is a promising alternative to standard PWB fabrication technology for rapid and low-cost application. Wang et al [4] found that if the surface tension and viscosity coefficients are both in low values, the more easily a droplet can be formed. Pique and Chrisey [2] had mentioned that micro-deposition systems are sensitive to material rheology formulation since the fine features were obtained from small gauge dispensing tips. In addition, the optimal linear velocity depends on the properties of the material that is being deposited. Dispensing studies have shown that viscosity, surface tension, needle gauge and length, and flow rate are critical for dispensing uniform structures. According to Park et al [45], the well-dispersed stable Cu ink with a low viscosity produces a continuous and smooth line. Likewise, Pique and Chrisey [2] had mentioned that in his book, the rheology of the conductor paste or ink will determine which method can be used to dispense the material and what feature sizes can be obtained.

On the contrary, Morissette et al [44] had different point of view in which they found that high viscosity at low shear will create high definition patterns and low viscosity will make low definition traces with smooth surface topographies. Clearly, low shear rheological behaviour of deposited material dictate setting behaviour and influences the line resolution and surface topographies. In addition, Park et al [45] in their study had confirmed that direct writing with high viscosity and high tension deposited material produced smaller size dot or line pattern. Based on the findings, investigation has to be done to examine the effect of both viscosity and surface tension to improve the knowledge of direct write process characteristics.

The higher viscous suspension, which was produced by suspending silver nanoparticles with a diameter of 10 nm in deionised water to which polyvinyl

alcohol (PVA) was added, had a higher onset voltage but thinner pattern width than the lower viscous suspension, due to the longer jet length induced by the higher viscosity according to Yu et al [47].

On the other hand, particle-size-distribution and particle shape also have a significant impact on the conductivity of a conductive line produced. The packing density is improved by using a bimodal distribution of particles instead of a monomodal distribution. The use of flaked particles gives better conductivity than the use of perfectly spherical particles due to the higher surface/contact area between the particles, but the flowability is decreased relative to the spherical particles. In contrast, spherical particles are highly desirable for controlled rheology and optimum solid loading. In addition, the conductivity of low temperature processed films can only be improved by the conversion of the metallic precursor. The higher the solid yield of the precursor and the connectivity between the individual particles, the better the final conductivity will be. According to Park et al [45], as the particle size decreases to nanoscale, the melting point of particles decrease dramatically because specific surface area increase with the particle size decrease. The use of smaller particles could allow developing highly conductive films at lower annealing temperature. However, too small particles may undergo significant volumetric shrinkage during sintering, causing poor adhesion to the substrate. As a general rule, smaller solid particles allow for better resolution control. Depending on the application, shear thinning, bleeding of the liquid vehicle after deposition, and other post deposition deformation and compositional changes need to be considered. Thickeners and surfactants can be added but can have a negative impact on the conductivity of the finished product when low-temperature processing is required.

Not only viscosity, surface tension and melting point are important, there are other properties that are needed to be thought about such as particle size, shear thinning, bleeding of the liquid vehicle after deposition, and other post deposition deformation and compositional changes. Thus, it clearly shows that there is a need to investigate systematically the characteristics of the

aforementioned critical mechanical properties in order to understand their effect to the resulting properties of the components produced.

Besides, a low melting temperature of the deposited material is recommended so that it could be applied to a variety of substrates. Likewise for the viscosity and surface tension, it has been suggested that the used of low value for both viscosity and surface tension is important and helps to improve the quality of printed components as well as the conductance.

2.5.2 Suitability of the material

Syringe-based DW system can be categorized as micro-dispensers with positive displacement piston. For novel linear positive displacement piston pump, studies have suggested that highly thixotropic materials perform best for continuous line dispensing. Thixotropy is the property of some non-Newtonian pseudoplastic fluids to show a time-dependent change in viscosity in which the longer the fluid undergoes shear stress, the lower its viscosity. A thixotropic fluid is a fluid which takes a finite amount of time to attain equilibrium viscosity when introduced to a step change in shear rate. Many gels and colloids are thixotropic materials, exhibiting a stable form at rest but becoming fluid when agitated.

Table 2.4 shows the materials and tools to fabricate various microelectronic devices and components. It can be seen that the direct-write materials recommended to be used for fabrication of conductors are consist of metallic nano-materials, conductive polymers and metalo-organic materials.

Table 2.4: Potential components fabricated by DW Technologies and materials (Pique and Chrisey [2])

No.	Components	DW materials	DW technology	Final processing
1	Capacitors	Metalo-organic materials	Micro-dispensing, jetting	Thermal
		Filled polymer thick films	Micro-dispensing, electrostatic	Thermal, UV, microwave
		Polymer-based dielectric materials	Micro-dispensing, jetting, electrostatic	Thermal, UV
		Ceramic dispersed in an organic binder	Micro-dispensing, jetting	Thermal, microwave, laser
		Ceramic dielectric nanomaterials	Laser-assisted transfer	Thermal, laser
		Donor material films	Laser-assisted transfer	Laser
2	Resistors	Filled polymer thick films	Micro-dispensing	Thermal
		Metalo-organic materials	Micro-dispensing, jetting	Thermal
		Donor material films	Laser-assisted transfer	Laser
3	Inductors	High μ materials	Micro-dispensing	Thermal, laser
		Donor material films	Laser-assisted transfer	Laser
		Metalo-organic materials	Micro-dispensing, jetting	Thermal, laser
4	Batteries	Metalo-organic materials	Micro-dispensing, jetting	Thermal, laser
		Electrolyte materials	Micro-dispensing, jetting	Thermal, laser
5	Antennas	Metallic nanomaterials	Laser-assisted transfer	Thermal, laser
		Metalo-organic materials	Micro-dispensing, jetting	Thermal, laser
		Conductive polymers	Micro-dispensing, jetting	Thermal, laser
6	Conductors	Metallic nanomaterials	Micro-dispensing, jetting	Thermal, laser
		Donor material films	Laser-assisted transfer	Laser
		Conductive polymers	Micro-dispensing, jetting	Thermal, microwave, laser
		Metalo-organic materials	Micro-dispensing, jetting	Thermal

According to Pique and Crisey [2], they found that the metallo-organic precursor has become an attractive solution for conformal write applications and a wide variety of low-temperature substrate such as smart cards where the precursor will decompose during heating process to form a metallic phase and 'weld' the metallic particles together. They had also mentioned that in order to obtain good conductivity, the particles need to be phase pure. The best conductors are the group of IB metals (Cu-Copper, Ag-Silver, Au-Gold). Pd and Pt are also good conductors and alloys are often formed to enhance overall performance or improve the compositional stability.

Several literatures have found researching the suitable material for direct write application including molten metals, conductive polymers, organo-metallic compounds and metallic nanoparticle suspensions as illustrated in Table 2.5.

Table 2.5: Numerous materials being researched for direct write application

NO.	RESEARCHERS	YEAR	TYPE	MATERIAL
1	Liu and Orme [48]	2001	Molten Metals	Solder
2	Orme et al [49]	2000	Molten Metals	Aluminum alloys (AA2024)
3	Kawase et al [50]	2000	Conductive Polymers	PEDOT/PSS poly (3,4-ethylenedioxythiophene)
				doped with polystyrene sulfonic acid
4	Cuk et al [51]	2000	Organo-metallic compounds	Copper hexanoate with R in isopropanol or chloroform
5	Smith et al [41]	2006	Organo-metallic compounds	Silver organic compound dissolved in toluene
6	Bieri et al [26]	2004	Metallic nanoparticle suspensions	A suspension of gold nanoparticles in toulene
7	Dockendorf et al [38]	2005	Metallic nanoparticle suspensions	Gold nano-particles suspension in a toluene solvent
8	Fuller et al [39]	2002	Metallic nanoparticle suspensions	Gold and silver colloidal nanoparticle inks
9	Wang et al [4]	2004	Metallic nanoparticle suspensions	Gold (Au) nano particles suspended in solvents
				such as water and propylbenzene
10	Szczech et al [40]	2002	Metallic nanoparticle suspensions	Silver and gold NPFS
11	Kim et al [34]	2006	Metallic nanoparticle suspensions	Silver (Ag) nano-particles synthesized by the polyol method
12	Sears et al [52]	2007	Metallic nanoparticle suspensions	Silver nanoparticle inks a) AG-IJ-G-100-S1 (Cabot –Superior Micropowders) b) Silver-copper P102 (Cima NanoTech™) c) an ink comprised of dimethyl acetimide (DMA) d) Ag-25-ST2 powder from Nanotechnologies, Inc. (NTI).
13	Park et al [45]	2007	Metallic nanoparticle suspensions	Copper conductive ink

As mentioned by Park et al [45], molten metal operating temperature was too high and they found that the conductivity of the components produced by conductive polymers is relatively low. In the mean time, organo-metallic compounds and metal precursors require additional heat treatment for reduction to metallic species and contain large amount of organic residues

which affect the conductivity. They observed that the metallic nanoparticle suspensions are the promising materials compare to others since the goal is to achieve high conductivity conductive lines. Recent studies normally use novel metal such as gold and silver nanoparticles because of their high conductivity and anti-oxidation properties but they were too expensive in large quantity. So, an alternative is needed in which the perfect candidate is copper because of it is inexpensive, highly conductive and air stable.

In addition, according to Calvert [53], printing patterns of conducting polymers which is relies on rapid evaporation of solvent is intrinsically difficult to maintain. He also added that the advantages of using particulate suspensions include the greater chemical stability of crystal over solutions, the higher concentration of active species for most partially soluble compounds, and the greater ease of immobilizing species within a printed layer. Calvert [53] also agreed with Park et al [45] where molten metal operating temperature was too high since solder as an example needed a further treatment to achieve low contact resistance.

2.6 Substrates in DW

As for substrate material, there are a wide variety of substrate materials that have been used in DW and recently many researchers have used polyimide, glass and polymers in their research as shown in Table 2.6. Polyimide was mostly chosen by them as its common use in flexible electronics according to Atanasov et al [28].

The material and substrate interaction also plays an important part to induce a quality printed components as mentioned by Scott [54]. When a high velocity spherical droplet collides with the substrate surface, the droplet becomes deformed resulting in a lamella that spreads radially out from the point of impact producing a shock front rim that expands to a maximum diameter. At this maximum the rim may continue to expand at a reduced rate in the case of complete wetting or to retract or stay at rest depending on the

wetting and impact conditions involved. The difference between the substrate surface energy and the fluid surface tension coupled with the geometry and momentum of the droplet affects the energy loss dynamics. Thus, spreading or wetting relates to the physical and chemical interaction of the liquid with the substrate.

2.7 Photolithography and Etching Process

Photolithography is the process of transferring patterns of geometric shapes via a mask to a thin-layer of radiation sensitive material normally called resist covering the surface of a semi-conductor wafer. The resist patterns defined by the photolithographic process are not permanent elements of the final device but only replicas of circuit features. To produce circuit features, these resist patterns must be transferred once more into the underlying layers comprising the device. The pattern transfer is accomplished by an etching process that selectively removes unmasked portions of the layer.

The pattern transfer process is accomplished by using a photolithographic exposure tool. There are basically two optical exposure methods: shadow printing and projection printing. Shadow printing may have the mask and wafer in direct contact with one another as in contact printing, or in close proximity as in the case of proximity printing. Figure 2.16 shows a basic setup for contact printing, where a resist-coated wafer is brought into physical contact with a mask and the resist is exposed by a nearly collimated beam of ultraviolet light projected through the back of the mask for a fixed time.

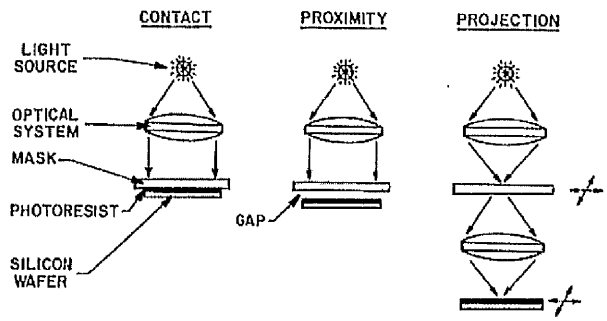

Figure 2.16: Schematic of the optical shadow printing technique (Pique and Crisey [2])

Masked used for IC manufacturing are usually reduction reticles. The first step in mask making is to use a computer-aided design (CAD) system in which designers can completely describe the circuit patterns electrically. The digital data produced by the CAD systems then drives a pattern generator, which is an electron-beam lithographic system that transfers the patterns directly to electron-sensitized mask. The mask consists of a fused silica substrate covered with a chrominum layer. The circuit pattern is first transferred to the electron-sensitized layer (electron resist), which is transferred once more into the underlying chrominum layer for the finished mask.

The photoresist is a radiation-activated compound. Photoresists can be classified as positive and negative, depending on how they respond to radiation. For positive resists, the exposed regions become more soluble and thus more easily removed in the development process. The net result is that the patterns formed (also called images) in the positive resists are the same as those on the mask. For negative resists, the exposed regions become less soluble, and the patterns formed in the negative resist are the reverse of the mask patterns.

Figure 2.17 illustrates the steps to transfer IC patterns from a mask to a silicon wafer that has an insulating SiO_2 layer formed on its surface. The wafer is placed in clean room which typically is illuminated with yellow light, since

photoresist are not sensitive to wavelengths greater than 0.5 μm. To ensure satisfactory adhesion of the resist the surface must be changed from hydrophilic to hydrophobic. After the application of this adhesion layer, the wafer is held on a vacuum spindle and 2-3 cc of liquidous resist is applied to the centre of wafer. The wafer is then rapidly accelerated up to a constant rotational speed which is maintained for about 30 seconds. The thickness of photoresist is co-related with its viscosity. After the spinning step the wafer is given a soft bake typically 90-120°C for 60-1200 seconds to remove the solvent from the photoresist film and to increase resists adhesion to the wafer. The wafer is aligned with respect to the mask in an optical lithography system and the resist is exposed to UV light as shown in Figure 2.17.

If a positive photoresist is used, the exposed resist is dissolved in the developer as shown in the right side of Figure 2.17. The photoresist development is usually done by flooding the wafer with the developer solution. The wafer is then rinsed and dried. After development the post-baking at 100°-180°C may be required to increase the adhesion of the resist to the substrate. The wafer is then put in an ambient that etches the exposed insulation layer but does not attack the resist. Finally, the resist is stripped (e.g. using solvent or plasma oxidation), leaving behind an insulator image (or pattern) that is the same as the opaque image on the mask (right side of Figure 2.17). For the negative photoresist, the procedures described are also applicable, except that the unexposed areas are removed. The final insulator image (left side of Figure 2.17) is the reverse of the opaque image on the mask. The insulator image can be used as a mask for subsequent processing. The dopant pattern is a duplicate of the design pattern on the photomask for a negative photoresist or is its complimentary pattern for a positive photoresist. The complete circuit is fabricated by aligning the next mask in the sequence to the previous pattern and repeating the lithographic transfer process.

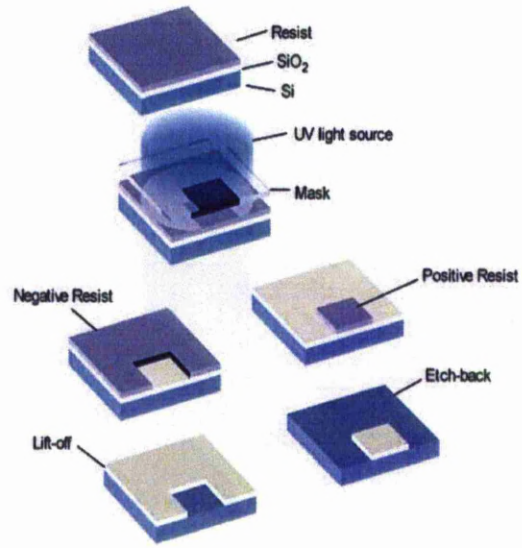

Figure 2.17: Details of the photolithographic pattern transfer process (Pique and Crisey [2]))

By looking at this highly complex photolithography process, several drawbacks could be identified. Its main advantages are that it requires a flat substrate to start with, it is not very effective at treating shapes that are not flat, and it can require extremely clean operating conditions as well as ideal temperature conditions. In addition, it could not do small print runs so people who want to print in small numbers cannot. The materials involved in the process are complex to use. The other disadvantages are in terms of the time over which the electron beam must be scanned across patterned areas pixel by pixel. Exposures can therefore take many hours to complete. Masks and photoresist processing are inevitable, which complicates the whole process and increases the processing time and the total cost. For the fabrication part, conventional fabrication techniques such as metal lift-off and etching can become difficult at sub-micron length scales. Cost and maintenance wise, the systems are generally expensive and highly complex machines which require substantial maintenance. Furthermore, the masked substrates used are placed into a chemical bath that etches the unwanted metal from the substrate surface. Such practice not only wastes precious metal material, but also generates

substantial amounts of chemical pollutants which are hazardous to the environment.

2.8 Reviews on the Alternative Processes

Screen printing (Figure 2.18) presents a more cost-effective ways of depositing a wide variety of films on planar substrates than does integrated circuit technology especially when fabricating devices at relatively low production volume. The technique constitutes one of several thick film or hybrid technologies used for selective coating of flat surfaces (e.g. ceramic substrate). The technology was originally developed for the production of miniature, robust, and cheap electronics. The up-front investment in a thick film facility is low compared with that of integrated circuit manufacturing. For disposable chemical sensors, recent industrial experience indicates that screen printing thick films is a viable alternative to Si thin film technologies. A paste or ink is pressed onto a substrate through openings in the emulsion on a stainless steel screen. The paste consists of a mixture of the material of interest an organic binder and a solvent. The organic vehicle determines the flow properties (rheology) of the paste. The bonding agent provides adhesion of particles to one another and to the substrate. The active particles make the ink a conductor, a resistor or an insulator. The lithographic pattern in the screen emulsion is transferred onto a substrate by forcing the paste through the mask opening with a squeegee. In a first step, paste is put down on the screen then the squeegee lowers and pushes the screen onto the substrate forcing the paste through openings in the screen during its horizontal motion. During the last step, the screen snaps back, the thick film paste which adheres between the screening frame and the substrate shears and the printed pattern is formed on the substrate. The resolution of the process depends on the openings in the screen and the nature of the pastes. With a 325 mesh screen, and a typical paste a lateral resolution of 100 μm can be obtained. After printing, the wet films are allowed to settle for 15 min to flatten the surface while drying. This removes

the solvents from the paste. Subsequent firing burns off the organic binder, metallic particles are reduced or oxidized and glass particles are sintered.

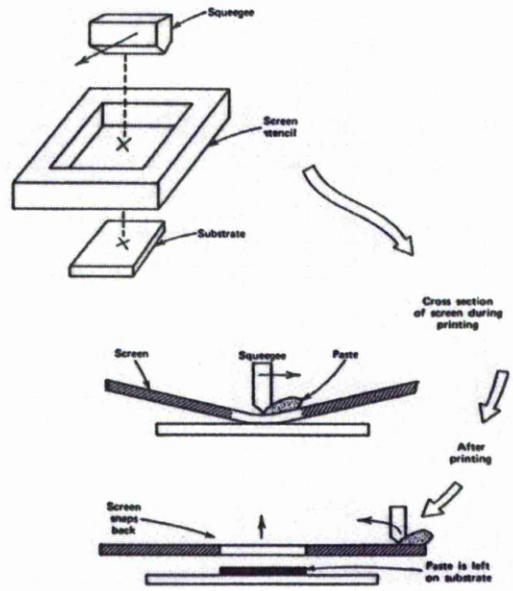

Figure 2.18: Schematic of screen printing process (Kim et al [33])

Several researches have used screen printing to print conductive lines and electronic components such as antenna. Leung et al [55-57] had used screen printing to fabricate conductive polymeric coil antennas with different line thicknesses and designs onto flexible substrates for use with 13.56MHz RFID tags. This study was done to investigate the effects of bending on RFID performance on curved surfaces. Besides, Chen et al [58] had studied the manufacture of RFID antenna tags (RFIDs) using silk-screen printing technology with conductive silver paste to reduce the cost of RFIDs. Merilampi et al [59] had used screen printing to print ultra-high-frequency (UHF) radio-frequency identification (RFID) tag antennas for the investigation of the effect of the conductive ink layer thickness on the performance of printed ultra-high-frequency (UHF) radio-frequency identification (RFID) tag antennas. When printing is used to produce conductive patterns, the ink layer is not uniform. Thickness variations occur even if the substrate material is smooth and the

edges of the conductor may become ragged. In addition, Bjorninen et al [60] had studied the performance of silver ink microstrip lines (MSLs) printed using screen printing. The results showed that despite the lower conductivity of the silver ink compared to copper, the screen-printed lines that authors studied are still applicable to microwave applications. Shin et al [61] discussed the selection of ink and printing process to fabricate RFID antennas. The radiation performances of various screen printed RFID antennas with silver nanopaste were found comparable to those of copper etched ones. Merilampi et al [62] had characterized the conductive silver ink patterns printed using screen printing technique on flexible substrates. The results of the tensile and electrical tests showed that with the screen printing method it is possible to produce highly stretchable electrically conductive patterns for practical applications. Although screen printing are seen employed quite widely in fabricating conducting lines/track, the ink layer suffers from thickness variation and also screen printing could not demonstrate fine pattern resolution capabilities for small and ultra small consistent line width, high quality surface finish and edge acuity definition according to Atanasov et al [28].

Ink jet also been used extensively as alternative to photolithography and etching process to fabricate antenna especially RFID tags due to the purpose of reducing the production cost to manufacture the antenna. As mentioned by Rida et al [63], ink jet was used to fabricate UHF antenna on paper substrate for RFID and Sensing Applications due to its simpler and faster method, it could provide development of a novel inkjet printing approach for the ultra-low cost fabrication of antennas on paper substrate over the UHF frequency range. Tentzeris et al [64] share the same opinion where he successfully employed inkjet-printed to fabricate antennas on paper substrates. This method was introduced as a system-level solution for ultra-low-cost mass production of UHF Radio Frequency Identification (RFID) Tags and Wireless Sensor Nodes (WSN) in which this approach could be easily extended to other microwave and wireless applications and potentially could set the foundation for the development of low-cost light-weight autonomous nodes for cognitive intelligence applications and for wearable communication and bio-monitoring

systems. Likewise, Virtanen et al [65-66] where they have used ink jet to print tags using narrow conductors, which enables low cost and fast manufacturing rate. They have presented a novel inkjet-printable RFID tag antenna design using extremely narrow conductors and presented a new alternative way to lower the manufacturing costs of inkjet-printed RFID tags by using very few conductive materials. In addition, Molesa et al [67] demonstrated ink jetted nanoparticle-Au conductors on plastic with sheet resistances as low as 0.03 ohms per square as a means of achieving ultra-low-cost electronic circuits with uses in displays and disposable electronics applications such as RFID tags. Together, these represent an important step towards the realization of all-printed RFID. High-quality passive components are a crucial component technology required for the demonstration of low-cost all-printed RFID. Yang [135] demonstrated, inkjet-printed UHF and microwave circuits fabricated on paper substrates are investigated for the first time as an approach that aims for a system-level solution for fast and ultra-low-cost mass production. A UHF RFID tag module is then developed with the inkjet-printing technology, proving this approach could function as an enabling technology for much simpler and faster fabrication on/in paper. The use of the inkjet-printing process in the development of multilayer paper-on-paper structures has also been demonstrated, verifying that paper-based inkjet-printing topologies offer a very low-cost eco-friendly solution to system-level packaging for UHF, wireless, and microwave applications. Redinger [69] described an all ink-jet-deposited process capable of creating high-quality passive devices suitable for an RFID front-end. Gold nanocrystals are printed to create conductive lines with sheet resistance as low as 23 meter per square. A low-cost method of fabricating passive devices on plastic substrates has been developed. This paper represents a first step in developing a low-cost all-printed RFID system.

Ink jet was also played a major part in fabricating conductive lines or track for electronic components including antenna. According to Sidén and Nilsson [70], they have concluded that electrical conductors based upon flexographic- screen- and inkjet printing are well able to serve as antennas for passive RFID tags. The experiments show that inkjet provides traces with very

high conductivity and excellent resolution, but also provide a thickness of less than a micrometer which can still lead to low antenna efficiency due to the conductors' small cross section. Likewise Kang and Oh [71], they used ink jet to study the effect of droplet/substrate interactions on the geometrical characteristics such as shape and morphology of as-printed conductive lines of nano silver suspensions. The effect of the surface energy, substrate temperature and droplet spacing on the geometrical characteristics such as shape and morphology of as-printed conductive lines of nanosilver suspensions was investigated in this study. The as-printed silver lines can be used in various printed electronics applications such as radiofrequency identification, flexible printed circuit boards, and solar cells.

Jung et al [72] studied the feasibility of employing inkjet technology for the creation of conductive pathways on printed circuit boards. Prediction of the width, length, and thickness of printed lines as a function of the dot diameter, resolution, and volume fraction of the particles in the ink is presented. Surface treatment of the substrate to promote desirable adhesion and wetting properties as well as the adjustment of the curing process to reduce the surface roughness of the printed traces were studied. Smith et al [41] used a drop-on-demand ink-jet printer in the production of conductive silver tracks onto glass, polyimide, polytetrafluoroethylene, carbon and glass fibre reinforced epoxy substrates. The influence of printing parameters and substrate surface properties on line quality is discussed. A silver-containing organometallic ink has been printed onto a range of substrates at room temperature using a drop-on-demand ink-jet printer. Jeong et al [73] synthesized silver nanoparticles via chemical reduction method in aqueous medium and poly-acrylic acid-sodium salt, a kind of anionic polyelectrolyte, was used as a capping agent as well as a dispersant. They fabricated narrow conductive features onto the polyimide substrate using ink-jet printing method and demonstrated the influence of substrate temperature on the morphology of printed patterns. Perelaer et al [74] presented a one-step process to fabricate conductive features on flexible polymer substrates by inkjet printing an organometallic silver ink directly onto a substrate that is heated to 130 ◦C. The

combination of this ink and the simultaneous printing/sintering process opens up routes for the direct fabrication of conductive features on common polymer substrates that could be applied, for example, in roll-to-roll production of flexible microelectronic system. Thereby, conductive silver tracks can be prepared in a direct and fast way.

Bidoki et al [42] presented an ink-jet printing technique has been used for printing highly conductive metallic patterns on different substrates and textile fabrics. They developed a novel method of printing metallic electrical conductive patterns on different substrates by ink-jet printing of metal salt solutions and reducing agents. Ink-jet printing of separate aqueous solutions of the metal precursor salt and reducing agent produce a conductive pattern on substrate surface. Conductivity measurements and physical tests have shown the great potential of this technique for printing Printed Circuit Boards (PCBs) on different materials. This two step printing method, compared to conventional nanoparticles printing processes is much simpler and cheaper, environment and user friendly and capable of producing conductive patterns in ambient conditions. The developed ink-jet deposition of metals is one of the most convenient method of inserting conductive materials into the textile texture compare to other methods such as sewing, embroidery, weaving and knitting. It has been shown that the deposition of conducting film with satisfactory conductivities can be achieved using the novel two step ink-jet printing process described herein. Perelaer et al [74] the temperature stability of silver tracks, prepared by inkjet printing different colloidal silver suspensions, was investigated. They have prepared a silver nanoparticle ink that has a critical curing temperature as low as 80°C. This low temperature opens the possibility to produce electronic devices on polymeric foils that have a low glass transition temperature, for example PET. Furthermore, the temperature stability of inkjet-printed silver tracks was studied in detail. High temperature stable inkjet printed silver tracks can be used for applications, where high processing temperatures are necessary, for example in plasma display production. Nur et al [75] had successfully used modified IBM piezoelectric DOD printer to deposit a jet printing developed ink containing 31

wt% an organic gold precursor (mercaptoproprionylglycine) for printing patterns and conductive tracks on a range of substrates including alumina plates, glazed tiles and glass slides. The ink provides a potential technology for industrial fabrication of electrical circuits or for decorative printing.

In the meantime ink jet was also employed to print high-frequency properties of printed electronics according to Mantysalo and Mansikkamaki [76] where they had designed and manufactured a transmission line and a patch antenna for 2.4 GHz ISM band. Their worked is to evaluate the suitability of printed electronics in high-frequency applications. From their result shows that printed electronics have a relatively good potential for many RF applications.

Among the entire group of DW processes, inkjet DW is the most established followed by laser DW in terms of industrial applications, but still they have faced a number of problem such as limited choices of material that can be used, deposition rate, cost and resolution. Wang et al [4] stated that the existing inkjet printing print head has its own limitation in terms of delivering smaller droplets. Discrete droplet systems rely upon low dilution (<5% solids by volume), low viscosity inks (typically 2 cp but can be up to 100 cp) which will form consistent droplet sizes. A feature of these low viscosity inks is their propensity to spread on contact with substrates, forming tracks with a very low ratio of height to width. This view is shared by Li et al [5-6] in which although jetting (including ink jetting) is a noncontact technology, it is limited by the materials that can be jetted in terms of viscosity and particle separation. In the meantime, according to Goghari and Chandra [43] the simplest way of decreasing droplet size in ink jet is to use smaller nozzle diameter; but very fine nozzles are prone to blockage. In addition, the cost of print heads was also high which limits the applicability of this technology in low cost applications. Besides, the inkjet print heads should also have good chemical compatibility, to handle different materials, and good droplet generation stability, to achieve high printing quality. All of these impose a big challenge on the print heads design and fabrication process. Not only the print heads is the main concern, some direct-write approaches including ink jet and M^3D suffer from edge effects that would appear to limit applicability in devices operating in the

gigahertz range according Marinov et al [31]. In the mean time, according to Siden and Nilsson [70] they concluded that careful considerations should however be given to the line widths and the thickness of the printed traces as they can easily also introduce ohmic losses to the antennas. The experiments show that inkjet provides traces with very high conductivity and excellent resolution, but also provide a thickness of less than a micrometer which can still lead to low antenna efficiency due to the conductors' small cross section. Inkjet ink with its very fine silver particles can however be more expensive to fabricate than ink with the micrometer sized particles used for flexographic- and screen printing.

As another mature DW technology, Laser-based DW technology also has been seen widely occupied in fabricating antennas and conductive lines/tracks. According to Alemohammad et al [77] they have investigated the morphology and microstructure of silver micro-lines fabricated by laser-assisted maskless microdeposition (LAMM). In LAMM technology, suspensions of silver nano-particles are used for layer-by-layer deposition and laser post-sintering. The characterization of a recently developed laser-assisted maskless microdeposition technology for the direct writing of silver micro-layers was performed. Auyeung et al [78] demonstrated the fabrication of a GPS conformal antenna under ambient-temperature conditions using a combination of laser micromachining and/or laser direct-write processes. The electromagnetic behavior of the antennas is then characterized and the design of the antenna structures is further optimized. Pattern simulations and input impedance measurements of the antenna are presented that demonstrate the usefulness and success of the iterative process made possible with this fabrication technique.

In addition, Zeng et al [79] reported a laser direct-write method to fabricate conductive lines and electronic components on insulating boards by using laser microcladding electronic materials. A workstation for implementing this direct-write method was developed, which integrated material deposition (micropen) and laser processing on a single machine. With the computer-aided

design/computer-aided manufacturing (CAD/CAM) capability of the workstation, conductive lines, resistors, capacitors, inductors, and thick-film sensors with different patterns were fabricated successfully by this technique in air without mask and with high deposition rates. This technique provides a novel method to fabricate the conductive lines and electronic components with high precision and high speed. It is clear that these processes are well suited to rapid prototyping applications. They can shorten the period of designing, fabrication, and testing of a given component and reduce the package size of electronic devices. They have a great number of potential applications in other fields such as MEMS, biomedical engineering, and so on.

In the mean time, Pique et al [80] developed a novel laser-based process to fabricate pseudocapacitors and microbatteries with tailored capacities for small electronic devices having size and/or weight restrictions. This process, called MAPLE DW (for matrix-assisted pulsed-laser evaporation direct write) can deposit rugged mesoscale (1 μm to 10 mm) electronic components over any type of substrate. With MAPLE DW, customized mesoscale electronic components can be produced, eliminating the need for multiple fabrication techniques and surface mounted components. In the mean time, Pique and Chrisey [2], presented a laser-based direct write technique termed matrix-assisted pulsed-laser evaporation direct write (MAPLE DW). This technique utilizes a laser transparent fused silica disc coated on one side with a composite matrix consisting of the material to be deposited mixed with a laser absorbing polymer. Absorption of laser radiation results in the decomposition of the polymer, which aids in transferring the solute to an acceptor substrate placed parallel to the matrix surface. Using MAPLE DW, complex patterns consisting of metal powders, ceramic powders, and polymer composites were transferred onto the surfaces of various types of substrates with less than 10 μm resolution at room temperature and at atmospheric pressure without the use of masks. The laser transfer process is spatially highly selective, because the area covered with transferred material depends on the incident laser beam, which can be focussed or patterned. Various types of

device configurations such as capacitors, inductors, and chemoresistors were demonstrated using this technique.

Serra et al [81] demonstrated the viability of the LIFT technique through the preparation of functional biosensors showing similar performances and higher scales of integration than those prepared through more conventional techniques due to its focusing power of lasers make them adequate tools for patterning applications that require high levels of spatial resolution. The preparation through LIFT of a specific biosensor, a DNA microarray, has proofed the viability of the technique for such a purpose. The prepared microarray is capable, not only to sense a specific DNA strand with a signal level detectable with conventional means, but also to discriminate two different human genes, what makes it perfectly functional. In addition, the quantitative analysis of the signal provided by the microarray has demonstrated that the DNA concentration of the transferred material is equal to that of the liquid film, what proofs that there is no biomolecule damage during LIFT. Therefore, LIFT constitutes a viable alternative to more conventional techniques for biosensors preparation, with the additional advantages of presenting higher degrees of integration, and avoiding contamination and clogging problems due to its non-contact nozzle-free nature.

In addition, Chen et al [82] presented a direct-write technique for rapid prototyping and manufacturing of sensors onto structural and functional components for many diverse applications. The technique combines thermal spray (an additive process), which produces blanket depositions of films and coatings, with ultrafast laser micromachining (a subtractive process) to produce functional sensors. Microheaters and strain gauges have been successfully fabricated in this work to demonstrate the feasibility and advantages of the proposed technique. Besides, Auyeung et al [83] have presented the combination of nanoparticle inks with laser direct-write allows the laser printing of fine electrically-conductive patterns on substrates requiring extremely low processing temperatures (< 250 °C). These features are equivalent to those seen in typical vapor deposited and lithographically patterned thin films. A CW 532 nm laser was used to cure as deposited silver

lines with a resistivity similar to that achieved in oven-curing. This approach is ideally suited for the prototyping and short production runs of interconnects for flexible electronics, RFID antennas and OLED displays. This work will show how these nanoparticle inks are processed using laser direct-write. Laser direct-write combined with oven or laser curing has been used to print narrow conducting lines onto a temperature- sensitive substrate (polyimide). Its ability to print both a low and high viscosity ink demonstrates its versatility as a direct-write technique for flexible electronics. In addition, Henry et al [84] investigated the latest industrial designs of Q-switched diode pumped solid-state lasers that are enabling the uptake of this process as a viable manufacturing technique. They report on the design of the current and next generation of laser systems, the optical techniques employed to achieve direct write, and the versatility of the technique in application for thin layers as diverse as ITO, SnO^2 and Molybdenum. They concluded that the application of laser direct write of thin films now presents a viable alternative to conventional lithographic techniques for displays manufacture, and offers significant benefits in terms of flexibility, processing steps and cost.

Likewise, according to Li et al [85-87], most of the laser direct writing techniques such as laser-induced chemical vapour deposition (LCVD), laser-induced electro-less plating (LIEP), laser-induced solid deposition (LISD), and matrix-assisted pulsed laser evaporation direct write (MAPLE-DW) suffer from numerous problems especially in deposition rate, high production cost and resolution of conductive lines which restricted their applications in many situations. According to Hon et al, LCVD allows 3D structures to be built but very slowly, although it is much faster than conventional CVD which builds at a few μm per hour. In most cases, the morphology and electrical conductivity of the deposited features are inferior to the bulk material, or the adhesion of the layer to the substrate is poor and cannot be controlled. Gas phase deposition is limited by the availability of volatile metal-organic or inorganic materials, contamination of metal deposits and the need for specialised reaction chambers. A further drawback of the technique is the high cost, due to the use of a reaction chamber and associated vacuum equipment. It is difficult to

deposit alloys, composites and organic materials using this technique. In addition, laser deposition in a liquid environment has high deposition rates and excellent adhesion, but is limited to 2D structures only. It can deposit metals and ceramics, but is not suitable for organic materials. Laser backward transfer, although fast in depositing metal and metal oxides, is limited to materials that are transparent to the laser beam wavelength. It would be difficult to deposit 3D structures using this technique. LIFT and MAPLE DW allow the building of 3D structures with the widest range of materials on various substrates. A great advantage is its capability to deposit biomedical materials at low temperatures without damaging the cells. It has better thickness control and allows a near-monolayer coverage that conventional ink jet technique struggles to achieve. One limitation is the substrate geometry. In LIFT and MAPLE DW the substrate needs to be flat and placed parallel to the donor disk. Multi-photon polymerization and laser guidance are recent developments that are mainly suited to organic and biomedical materials. They offer great flexibility and highest accuracy in creating 3D structures. They can deliver and grow cells on a 3D object or substrate. Laser trapping and guided deposition in liquid is limited to low volume materials and is typically suited only to small particles and cells.

There were numbers of researches employed other printing technologies to fabricate conducting lines/tracks and electronic components as an alternative to conventional method. According to Sangoi et al [88], they investigated rotary letterpress and flexographic printing for their potential use in making electrically conductive structures. Antennas for radio frequency identification tags were printed using these techniques. The ink used in this study was a dispersion of silver flakes, and organosilver compounds in an organic vehicle. Using rotary letterpress, we were able to examine some of the process limitations and successfully print RFID antennas. We have not yet been able to achieve continuous traces by printing this ink using flexography and the only available anilox roller. Atanasov et al [28] had demonstrated an approach based on the Mesoscale Maskless Material Deposition (M^3D) direct write technology. The M^3D process has been modified and applied to print

high quality, high-performance interconnects with precisely defined geometry on polymer substrates using nanosized silver inks. The method is applied to print high-frequency transmission lines on polyimide substrates using a silver nanosized ink. The modified direct-write method provides a number of benefits for high-frequency printed electronic devices on flexible substrates including an improved line edge definition, line resolution in the mesoscale range, and a consistent, precise linewidth for a significant reduction and increased consistency of signal attenuation. In addition, Ng et al [89] presented a novel manufacturing process that aims to pattern metal tracks onto polyimide at atmospheric pressure and ambient environment. It is also demonstrates a high-value manufacturing technique that is mass manufacturable, low cost and suitable for use on 3D surfaces. The direct-write process on polyimide developed has shown promise for a much simplified metal patterning process for flexible circuits and interconnections without the use of pressurised chambers or any pre-manufactured metal inks which still represent a bottom-line cost for manufacturing. In the mean time, Felmet and Loo et al [90] described a method for patterning conductive copper over large areas by nanotransfer printing (nTP). This technique is purely additive and yields feature sizes in the 1–500 μm range. With minor adjustments to the procedure, nTP can be a valuable tool for patterning conductive copper in a purely additive manner. Lee et al [91] described a silver nanoparticle suspension was first deposited onto a Kapton® polyimide film by using an electro-hydrodynamic printing system, including a guide ring and pin (nozzle)-to-pin (ground) electrodes. With the electro-hydrodynamic printing method, a nozzle (inner diameter: 140 μm, outer diameter: 320 μm) much larger than an ink jet nozzle could be used. King et al [92] discussed how the novel Aerosol Jet process is being used to deposit a wide variety of material without conventional masks or thin-film equipment and outline its features, benefits, and some select application areas. The process is non-contact, enabling traces to be printed over steps or curved surfaces. Printed features can be less than 10 microns.

Pudas et al [93-95] have used A roller type of gravure offset printing has been used to evaluate the printing process and pad printing to print for Ag-filled polymer conductor ink on the non-planar substrates. Usage of this gravure offset method provides an environmentally friendly, economically viable method for large volume production of electrical fine-line conductors. Although there can be such problems a gravure groove blocking in production lines, in radar reflector applications such problems, shown by narrowed or even randomly broken conductor lines, do not disqualify the product. Meanwhile, Choi et al [96] proposed a roll-to-roll gravure-offset printing system for the manufacturing of printed ultra-high frequency radio frequency identification (RFID) tag antennas. In the identification range test using an RFID reader, compared to the conventional RFID tags with copper-etched antennas, which show the identification range of about 3.2mon average, the three-layer printed antennas with bonded tag chips exhibit the identification range of about 1.8m on average (i.e. the performance of about 60 per cent of conventional copper-etched antennas), which implies that the printed antennas could be applicable to real fields. In spite of the advantages of high throughput and a low manufacturing cost conferred by the gravure printing method, it has been shown that antennas printed using the gravure printing method do not offer satisfactory performance because of the limitations of the conductive materials used as ink

King et al [92] developed a direct-write approach for fabricating highly integrated, multilayer components using a Micropen to deposit slurries in precise patterns. This approach provides the ability to fabricate multifunctional, multimaterial integrated ceramic components (MMICCs) in an agile and rapid way. Commercial ceramic thick-®lm pastes can be used directly in the system, as can polymer thick-®lm pastes (PTF). Pastes with highly volatile solvents are inappropriate for the Micropen. Hoey et al [97] studied the performance of a commercial-off-the-shelf ultrahigh frequency (UHF) etched copper antenna was compared to printed silver antennas prepared by the following three direct-write techniques: maskless mesoscale materials deposition; matrix-assisted pulsed laser evaporation direct-write; and, collimated aerosol beam direct-

write. The performance of tags that utilized direct-write silver antennas was comparable to the copper-based commercial tag. This is the first demonstration where some of the direct-write rapid prototyping attributes (e.g., slight overspray, overlap of written lines, overall thickness less than 500 nm) are shown to not seriously impede RFID tag performance. These results demonstrate the utility of direct-write for rapid prototyping studies for UHF RFID antennas. Merilampi et al [98] investigated the possibility of pad printing in RFID tag antenna manufacturing. Passive UHF RFID tags were printed on flat and on convex surfaces with two different polymer thick-film silver inks. The effect of the ink and substrate material properties on tag antenna performance was examined. The results show that pad printing is suitable for tag manufacturing on flat and on convex surfaces. The curvature of the substrate did not significantly affect the tag performance. It was more important to take into consideration other substrate properties, ink characteristics, morphology, and printing parameters. The best practice is to take these matters into consideration in the initial tag design process to ensure proper tag performance at the desired frequency. Likewise, Zeng et al [99] had investigated the performance of silver ink printed microstrip patch antenna for passive RFID application where the conducting parts of the patch antenna are printed with silver ink utilizing the flexographic printing machine and the cardboard is adopted as the substrate. Their performance is evaluated by means of comparisons with the same antenna structures made of copper. Cao et al [100] propose a novel approach for depositing polyimide patterns by the micropen direct-write deposition technique which is CAD driven, maskless, rapid-prototyping and diverse materials integration. A micro air-bridge array is successfully fabricated which shows its potential applications in the area of MEMS device fabrication

2.9 Influence Factors on Performance of Components Produced by DW

Based on the numbers of previous researches that have been done, the influenced factors contributed to the performances of components produced had to be investigated first in order to improve the fundamental of direct write process as well as its printed components performance. The impact factors can be categorized in three different main topics which are the DW technology used, the deposited material mechanical properties used and the sintering technique applied. By acknowledging and understanding these impact factors, the characteristics and behaviour of the components generated may well be studied and evaluated so that a high quality fabricated components can be achieved accordingly.

2.9.1 Depositing Tool

Numbers of researches had highlighted the significance of depositing tool process parameters to the performance of components produced by DW as shown in Table 1. According to Dockendorf et al [38], they used the depositing tool equipped with a vertical translation stage. This allows for movement of the probe in z-direction to maintain a constant liquid film height thickness in which is important to produce a high conductivity conductive line. In addition, Kirschenmann et al [18], have used nScrypt machine in which the material is maintained from the tip down to the substrate so that the tip is never in direct contact with the substrate. In other words the dispensing height is kept constant in order to create a constant line thickness which is vital to achieved quality printed components. Li et al [11], revealed that the dispensing height is important to generate accurate dispensing. By incorporating a high precision z stage and a height sensor available in nScrypt system they developed, the dispensing height is accurately maintained even on highly conformed surfaces. Wang et al [4] concluded that in order to obtain high printing quality, the working distance of the print head from a substrate must be kept smaller than

the stopping distance to degrade the air resistance so that it will improve the droplet ballistic accuracy. As a result, the Au patterns as small as 8 μm have been formed on silicon substrates by printing with suspensions of Au nano-particles.

Table 2.6: Several researches addressing the influence factor of direct write printing parameters on printed components

No.	Researchers	Year	Major Factors	Pattern Studied
1	Dockendorf et al [38]	2006	Nozzle diameter, dispensing height	Multilayer chip with gold pattern track
2	Goghari and Chandra [43]	2007	Applied pressure, nozzle size	Pure water and glycerine mixtures
3	Kirschenmann et al [18]	2007	Dispensing height, tip size	Antenna
4	Li et al [11]	2007	Nozzle size, applied pressure, dispensing height	Lines, dots, 3D structure
5	Li et al [11]	2007	Nozzle size, applied pressure, dispensing height	Scaffolds
6	Park et al [45]	2007	Voltage, lasting time, head frequency, inter-spacing	Copper conductive ink
7	Wang et al [4]	2004	Nozzle diameter, applied pressure, dispensing height	Gold (Au) nanoparticles suspended in solvent (water and propylbenzene)

The nozzle diameter also gives a reasonable impact to the performance of material deposited. Dockendorf et al [38] used micropipettes in their experiment in which the pipette openings are very small, 20 μm and a syringe is connected to one end of the capillary tubes to deposit the conductive ink. As a result, the resulting line width and thickness was satisfactory and the conductivity was beyond expectation. The depositing tool used was highly flexible and can be used to manufacture electronic circuits. According to Goghari and Chandra [43], the easiest way of decreasing droplet size is to use smaller nozzle diameter, but very fine nozzles are prone to blockage. Droplets size depends largely on nozzle diameter. In their research, they have used three different size of nozzles where small droplets could not be produced using a very fine 51 μm nozzle due to liquid accumulation at the nozzle exit. For the largest nozzle 204 μm diameter, droplets with mean diameters approximately

60% of the nozzle were produced with 70–90 wt% glycerin mixtures for which Oh ranged from 0.21–1.73. With smaller nozzles (102 μm diameter), droplets of 10–60% glycerin were about the same diameter as the nozzle. Meanwhile, with a used of smaller depositing tool tip size, a thinner layer of material can be deposited according to Kirschenmann et al [18]. Li et al [11] added that an optimization of the dispensing tip size on their nScrypt system has helped to reduce the pressure drop hence capable of producing very small features. The tip (changeable) has a conical shape inside (internal orifice diameter down to 12 microns) and outside, thus the pressure needed to push the material through the nozzle is reduced which is essential when printing with highly viscous materials. Wang et al [4] had found that to increase the resolution of the inkjet print head, the form of inkjet devices must consists of small nozzle diameter and optimum nozzle design to achieve minimum flow resistance. The nozzle shape dramatically influences droplet formation. A thinner nozzle will have smaller flow resistance; therefore a lower actuation pressure is needed for droplet generation

Another important process parameter is the applied pressure. The pressure variation in the droplet generator used by Goghari and Chandra [43] in their research generating considerable result to the droplet produced. Likewise study by Li et al [11] where they found that by accurately controlled the air pressure, timing and valve opening to the smart pump available in their develop nScrypt system, it gave rise to generate accurate dispensing hence well define patterns can be created. Wang et al [4] also raised up the importance of applied pressure where in their study, a pressure pulse with higher magnitude or longer pulse width will result in larger droplet velocity, slight enlargement of the droplet dimension, and satellite droplet formation.

It is obviously important to investigate thoroughly the effect of several process parameters especially the dispensing height to maintain a constant height thickness in which is vital to produce a high conductivity conductive line. The distance between the dispensing needle orifice and substrate is believed to affect the pattern features in which too great of a distance will affect the straightness of the line. In fact, the nozzle diameter itself needs to be

small in order to achieve small features and the air pressure used needs to be well controlled to generate accurate dispensing hence a well defined patterns can be created. As for nScrypt system, the smart pump technique plays a major role to dispense the material. Several printing parameters have been identified which is crucial to be considered during the experimental works involving the use of air pressure in the pneumatically actuated pump, the valve opening in the smart pump, the deposition speed and the dispensing height. The nozzle tip which has a conical shape inside (internal orifice diameter down to 12 microns) and outside as well is vital to yield the desired physical properties of the components printed.

As mentioned earlier, for nScrypt system, the smart pump technique is vital as a medium to deposit the material. Several printing parameters which is imperative are the air pressure in the pneumatically actuated pump used, the valve opening in the smart pump, the deposition speed and the dispensing height so that an accurate dispensing could be generated. The nozzle tip which has a conical shape inside (internal orifice diameter down to 12 microns) and outside also vital to determine the desired physical properties of the material deposited. The relationship that is significant to be regarded in the experimental works is shown below in Table 2.7;

Table 2.7: Printing parameter relationship to the resultant of conductive line properties

NO.	PARAMETERS	RELATIONSHIP
1	Dispensing height	a) Too great of a distance between the nozzle and substrate will affect the straightness b) Kept constant to create a constant line thickness to produce a high conductivity line
2	Nozzle diameter	a) Preferably small in order to achieve small Features b) Control the filament diameter
3	Air pressure	Should be well controlled to generate accurate Dispensing
4	Valve opening	Should be well controlled to generate accurate Dispensing
5	Deposition speed	a) Faster to achieve more straightness b) Control the filament diameter

2.9.2 Material properties

As for depositing material mechanical properties, several researches have addressing the importance of mechanical properties including the melting point, particle size, particle distribution, viscosity, surface tension and solid loadings. The relationships between these properties to the resultant conductive line characteristics are illustrated in Table 2.8

Table 2.8: Mechanical characteristics effect to the resultant of conductive line properties

NO.	CHARACTERISTICS	EFFECT
1	Melting point	Preferably low so that it could be applied to a variety of substrates
2	Particle size	a) Small - development of highly conductive films - better resolution control b) Flake particle - gives better conductivity due to the higher surface/contact area between the the particles, but the flowability is decreased relative to the spherical particles
3	Particle size distribution	Use bimodal distribution because it improve the packing density
4	Viscosity	a) Cannot be too low or too high c) Preferably low; - to produce continuous and smooth lines - to minimize component shrinkage during binder removal and sintering
5	Surface tension	a) Additional high boiling point solvent will lower surface tension – improve quality of components produced as well as conductance b) Low - droplet can be easily formed
6	Solid loading	a) Preferably low; - to minimize component shrinkage during binder removal and sintering b) High for better conductivity

2.9 Benefits of Direct Write

Numerous advantages have been established for DW. It is a rapid and very cost-effective process for prototyping to achieve novel functionality which will result in low cost in the development of a product. It is also enable very small features in microns to be direct write and has many varieties of

material choices. Besides, DW provides flexibility in production process giving capability to modify output in real-time, or customise individual products. It simplifies the process chain by eliminating unnecessary process steps and offering massive freedom in design through its geometrical versatility in which it will give rise to a better product design and performance hence improved the inventory control, customer support and supply chain. Less material are used since material deposition is performed on demand basis, material wastage is minimal causing fewer hazards and less impact to the environment. In application, DW has a very wide application window from prototype evaluation to high-throughput production. New applications are being announced regularly as this is still an emerging technology area. Niche applications in microelectronics, microsystems packaging, and medical devices have already been identified. There are exciting developments in the automotive, pharmaceuticals and biotechnology industries. DW has the potential to revolutionise manufacturing processes including aerospace, ceramics, ICT, displays, stealth materials, packaging, electrical and electronics, microwave and optical components. It could be used either to repair an existing object as well as making additions to existing objects

2.10 Definition of Some Antenna Parameters

Quality Factor (Q Factor) is a dimensionless parameter that describes how under-damped an oscillator or resonator or equivalently, characterizes a resonator's bandwidth relative to its center frequency. Higher Q indicates a lower rate of energy loss relative to the stored energy of the oscillator; the oscillations die out more slowly. A pendulum suspended from a high-quality bearing, oscillating in air, has a high Q, while a pendulum immersed in oil has a low one. Oscillators with high quality factors have low damping so that they ring longer.

Resonant is the tendency of a system to oscillate at a greater amplitude at some frequencies than at others. These are known as the system's resonant frequencies (or resonance frequencies). At these frequencies, even small

periodic driving forces can produce large amplitude oscillations, because the system stores vibrational energy. Resonance occurs when a system is able to store and easily transfer energy between two or more different storage modes (such as kinetic energy and potential energy in the case of a pendulum). However, there are some losses from cycle to cycle, called damping. When damping is small, the resonant frequency is approximately equal to the natural frequency of the system, which is a frequency of unforced vibrations. Some systems have multiple, distinct, resonant frequencies.

S11 Return Loss (S Parameter) is the loss of signal power resulting from the reflection caused at a discontinuity in a transmission line or optical fiber. This discontinuity can be a mismatch with the terminating load or with a device inserted in the line. It is usually expressed as a ratio in decibels (dB);

$$RL(dB) = 10 \log_{10} \frac{P_i}{P_r}$$

where RL(dB) is the return loss in dB, P_i is the incident power and P_r is the reflected power. Return loss is related to both standing wave ratio (SWR) and reflection coefficient (Γ). Increasing return loss corresponds to lower SWR. Return loss is a measure of how well devices or lines are matched. A match is good if the return loss is high. A high return loss is desirable and results in a lower insertion loss. Return loss is used in modern practice in preference to SWR because it has better resolution for small values of reflected wave.

Bandwidth is the difference between the upper and lower frequencies in a contiguous set of frequencies. It is typically measured in hertz, and may sometimes refer to passband bandwidth, sometimes to baseband bandwidth, depending on context. In the field of antennas, two different methods of expressing relative bandwidth are used for narrowband and wideband antennas. For either, a set of criteria is established to define the extents of the bandwidth, such as input impedance, pattern, or polarization.

Impedance is the measure of the opposition that a circuit presents to the passage of a current when a voltage is applied. In quantitative terms, it is the complex ratio of the voltage to the current in an alternating current (AC) circuit

Input Impedance an electrical network is the equivalent impedance "seen" by a power source connected to that network. If the source provides known voltage and current, such impedance can be calculated using Ohm's Law. The input impedance is the Thévenin's equivalent circuit of the electrical network, modeled by an RL (resistor-inductor) or an RC (resistor-capacitor) combination, with equivalent values that would result in the same response as that of the network. It is also called Z11 in terms of Z-Parameters. Generally speaking, the exact definition depends on the particular field of study.

Skin Effect is the tendency of an alternating electric current (AC) to distribute itself within a conductor with the current density being largest near the surface of the conductor, decreasing at greater depths. The electric current flows mainly at the "skin" of the conductor, between the outer surface and a level called the skin depth. The skin effect causes the effective resistance of the conductor to increase at higher frequencies where the skin depth is smaller, thus reducing the effective cross-section of the conductor. The skin effect is due to opposing eddy currents induced by the changing magnetic field resulting from the alternating current.

Penetration Depth is a measure of how deep light or any electromagnetic radiation can penetrate into a material. It is defined as the depth at which the intensity of the radiation inside the material falls to 1/e (about 37%) of its original value at (or more properly, just beneath) the surface. When electromagnetic radiation is incident on the surface of a material, it may be (partly) reflected from that surface and there will be a field containing energy transmitted into the material. This electromagnetic field interacts with the atoms and electrons inside the material. Depending on the nature of the material, the electromagnetic field might travel very far into the material, or may die out very quickly. For a given material, penetration depth will generally be a function of wavelength

2.11 Chapter Summary

High quality components can thus be seen to be affected by a significant number of interacting parameters. Figure 2.19 shows some of the key parameters and the interactions between them. By carefully investigating and understanding the effect of these key parameters, direct write process characteristics can well be investigated and improved hence will resulting a high performance of quality printed component.

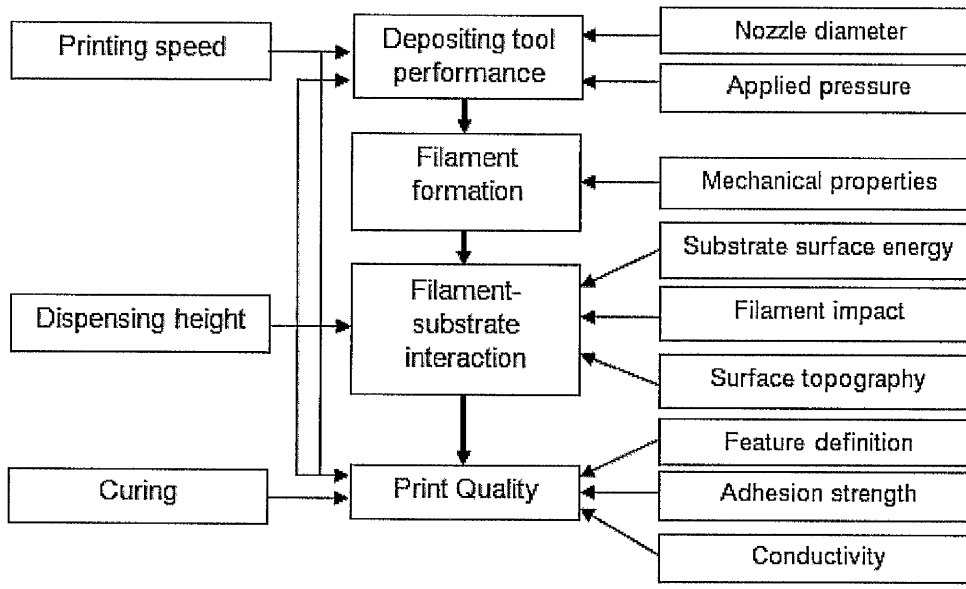

Figure 2.19: Interacting process components

For the widely-used versatile inkjet-based direct writing methods, there are many aspects which require further research and development. Improved models for jet and drop formation, drop impact and drying/curing would assist with process and material design. Some intrinsic limitations on fluid properties which result from the processes of jet formation and breakup are clear, but there is further scope to extend the range of fluids which can be printed, for example to achieve high concentrations of solid particles or polymer; better understanding of the printing of non-Newtonian fluids would be helpful.

Conductive inks with lower cost, which achieve high and stable conductivity deposits with long life times would find a ready market. There are wide opportunities for further development of functional optical, magnetic, optoelectronic and semi-conducting materials in forms amenable to inkjet printing, which is ideally suited to the precise deposition of very small volumes of special materials. With the development of new methods of droplet generation, e.g., electrostatic, and better awareness of the process and its capabilities, it is likely that the applications of inkjet printing in direct-write manufacturing will become much broader.

In the case of laser-based direct writing, further developments are necessary to overcome the limitations discussed earlier. Commercialization of the laser based direct writing techniques is slow due to the high cost of the systems, limitations in depositing materials and substrate dimensions. To speed up commercialization, faster deposition rates and reduction of the cost of the equipment would be desirable. Compared to electron beam and focused ion beam, the resolution of laser-based direct writing techniques is diffraction limited and therefore it would be difficult to achieve a dimensional resolution below 100 nm without major breakthroughs in the science and technology of lasers and optics

The syringe-based DW technology were not seen being extensively explored and applied especially in the fabrication of electronic components particularly antenna. This technology has huge potential in printed electronics not just because of it is simple and fast process allowing cost-effective manufacturing method but it can be used with wide variety of material choices and able to print on any surfaces either curve and doubly curve surface where others technologies could not and could easily be integrated with on-line curing system.

Chapter 3

Characterisation of Syringe-Based Direct Write Technique

3.1 Rationale of Syringe-based DW Technique

Syringe-based DW technology using laser has the potential to replicate and even overcome the limitation of other printing technologies such as ink-jet and screen printing. It is a new and promising DW technology which no previous researchers have used before for the writing of antenna. The process uses a syringe to dispense ink materials with precise volume control from 1 to 100,000 Pa.s. It is a maskless method which results in a very cost effective process. In addition, it conformably prints very fine features usually in micron on any 3D surface as well as being extremely flexible in adapting to a wide variety of materials types.

The selection of a suitable printing process for the fabrication of electronic components is an important consideration because it directly affects the requirements of the ink and the subsequent performance and productivity of the printed component itself. Some key requirements of the printing process are

that: (1) it is suitable for mass production, (2) it needs to be employable to produce various electronic components such as antenna, strain gauges and capacitor and is not constrained to one specific model, (3) job changes among components must be easy and quick, (4) printing as an additive process should consume less material than conventional etching techniques as a subtractive process to achieve low costs, (5) the infrastructure of the printing process must be well developed, (6) the cost of ownership needs to be considered, (7) it must be easy to use and maintain, (8) operators can solve problems on site, if possible, and (9) it must meet the rheological characteristics of the conductive ink.

Each DW technology involves different printing parameters and characteristics in terms of ink rheology, viscosity and printed layer thickness. Therefore, it is necessary to identify requirements of inks and the effect of the printing process on the fabrication of any components. Thus, the characterisation of this syringe deposition method is needed for the development of studies on several conductive inks and components.

3.2 Objectives

The following experiments mainly focus on characterisation of the dispensing/printing method which delivers the conductive ink, and on evaluating the influence of various process parameters (including post deposition steps) to achieve the required quality of conductive track specified by DW application in terms of its physical characteristics. In addition, it also serves to explore the capabilities of the dispensing/printing technique by fabricating simple lines and complicated lines such as strain gauges. The syringe deposition technique will be characterised based on its deposition parameters such as applied pressure, printing speed, tip size, stand-off distance and conductive ink viscosity. At the same time, the influence of these parameters on the topological structure of the ink tracks produced is also investigated. The experiments are aimed at identifying the optimum parameters from the device performance results. To assist with this, a fluid dynamic model

developed by Vozzi et al [101] is adopted and developed to allow an accurate prediction of the topological characteristics of the deposited ink track structures.

3.3 Description of Apparatus

3.3.1 Hardware

The syringe-base DW technology used is an automatic ink dispensing system with volumes. The system consists of a changeable plastic syringe which is available in several sizes; 3, 5, 10, 30 and 55 cubic capacity. It is equipped with a pressure control valve and a variety of metallic needle tips ranging from 50 μm to 1.5 mm internal diameter. The tip can be easily changed by unscrewing it from the bottom of the pressurized control valve. The tips available are in different shapes as shown in Figure 3.1, where the metallic tip with long and flat end is normally used in most of the work. The tip is connected to the control valve, where its purpose is to allow a better control over the fluid dispensed; whereas the syringe barrel is connected to the other end of the control valve. A solution of conductive ink is placed inside the syringe, then syringe piston is driven by filtered compressed air at a selectable pressure. The syringe is attached to the vertical z axis of a three-axis, stepper-motor drive micro-positioning system with a resolution of ±5 μm. The pressure gauge, pressure multiplier and associated control system allows the applied pressure to be controlled within the range of 0 to 200 psi, and the transverse velocity of the substrate with respect to the syringe can be varied between 0 and 100 mm/s. A planar substrate is fixed on the horizontal X and Y axes of the work table and is made to move under the syringe during deposition. A schematic illustration of the syringe-based DW technique arrangement for ink deposition is shown in Figure 3.2 (b).

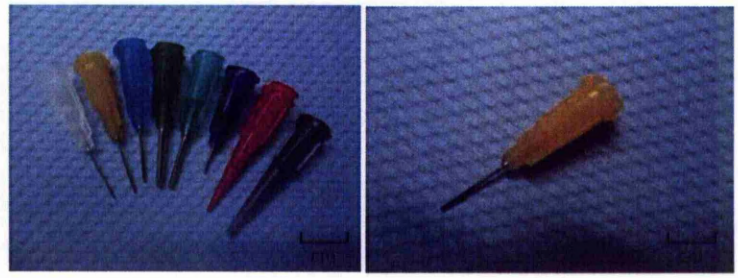

(a) (b)

Figure 3.1: (a) Syringe tips of various sizes used in DW experiments (b) Metallic tip with long and flat end

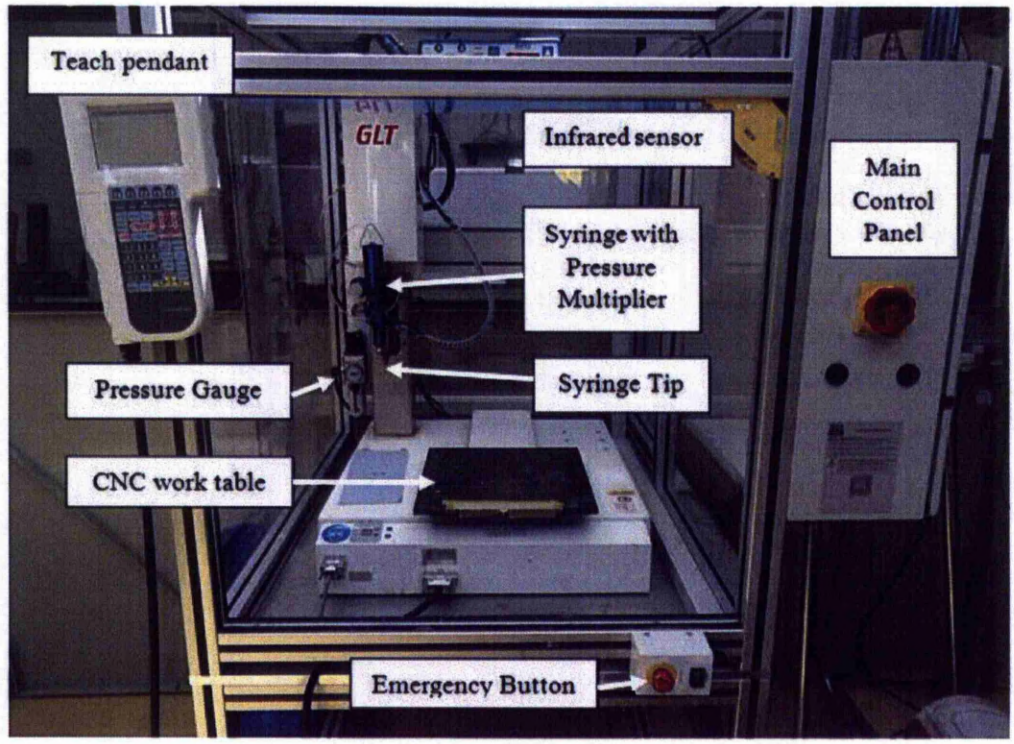

(a)

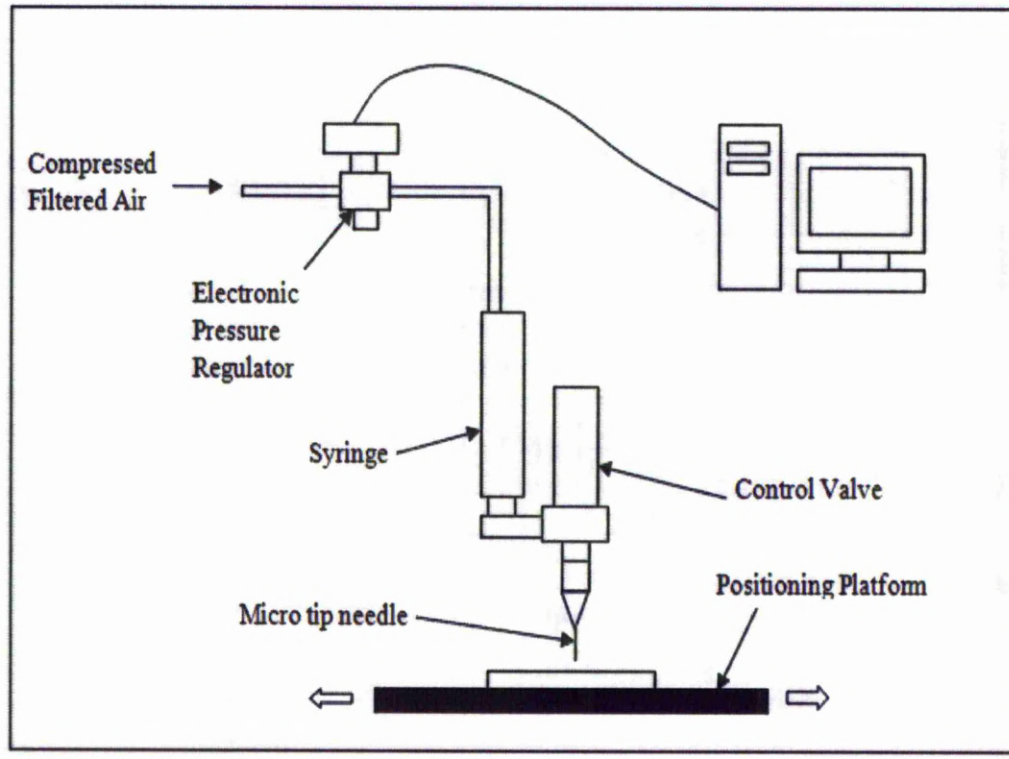

(b)

Figure 3.2: (a) Automatic syringe deposition system (b) Schematic illustration of the pressure-controlled deposition system

3.3.2 Software and Computer Interface

The entire system is interfaced and controlled by a personal computer through a GPIB (general programming interface bus) card. There were two CAD/CAM editor software programs that are integrated with the system. These are Visual Path Builder and JRC Dispensing

Visual Path Builder is a CAD/CAM editor software and visual programming environment for Janome TM Desktop and Scara Industrial Robots and can be used for automatic generation and reverse engineering of tool paths and waypoints for various applications like dispensing, tightening, soldering and etc. The software works like a 3D CAD application software with DXF, DWG, IGES, STL, OBJ, Gerber RS274D and Gerber RS274X vector and bitmap graphics import and export features and the ability to create

instant full functioning working robot programs. The software imports existing CAD models of your patterns into project files where tool paths and waypoints can be easily specified by using overlay features. Tool paths are constructed by using standard graphical elements like lines, multi-lines (with embedded arcs), arcs or circles. To create graphical elements, all well known software tools provided by the CAD applications are implemented. The order and direction of tool paths can be freely specified. Drawn paths and waypoints can be assigned to user defined task objects which can have free order. The integrated simulation feature allows testing programs without having a robot connected.

The JRC dispensing software was employed to drive the system to allow simple and intricate patterns such as lines, rectangular, hexagonal, triangular grids and spirals to be deposited. The software allows control of alignment between drawing and real world coordinates by using one or two reference points. The tool paths are automatically rotated and moved to appropriate positions if necessary. To edit the program data, a simple to use editor and optionally add point execution data are employed (like PointJob numbers, conditions, line speed). Programs can be exported in various millimetres and inches and transferred to the robot via RS-232 serial connection or external software application supplied by the robot vendor. Task objects will be automatically translated into robotic language of the type of robot used.

3.3.3 Manual and Automatic Operation

Two types of operation can be employed to control the dispensing operation of the robot; manual and automatic operation. In manual operation, the profiles of the pattern designed (normally represented by coordinates) are edited manually inside the robot programming using teach pendant. There were generally three coordinates involved; X, Y and Z. The X and Y coordinates are for movement in X and Y direction while Z coordinates is mainly corresponding to distance between the edge of the tip and the substrate. These coordinates need to be taught manually using teach pendant in order to be

recognized by the robot. All movements of the dispensing path will be executed using teach pendant.

For automatic operation, the existing CAD designs or models of the pattern are imported into Visual Path Builder into project files where paths and waypoints can be easily specified by using overlay features. Alternatively, manually drawn profiles could also be done in Visual Path Builder. Paths are constructed by using standard graphical elements like lines, multi-lines (with embedded arcs), arcs or circles. To create graphical elements all well known software tools provided by CAD applications are implemented. Drawn paths and waypoints can be assigned to user defined task objects which can have free order. Task objects will be automatically translated into robotic language of robot type. By specifying one or two reference points the system will compute offset-values and deviation angle in order to adjust the CAD coordinates with the machine coordinates. Within the plotted maximum procedure range in the 3D area paths, working points and waypoints are drawn visually. Alternatively, already existing outlines in a CAD design can be converted into tool paths fully automatically.

The finished project files are then sent to software provided via JRC dispensing to drive the robot for dispensing process. It will then convert the project files to language that recognized by the robot to execute the task. The flow of this process is shown below in Figure 3.5. This process not just allows intricate pattern to be printed but fast and provide a quick changeable lead time between productions.

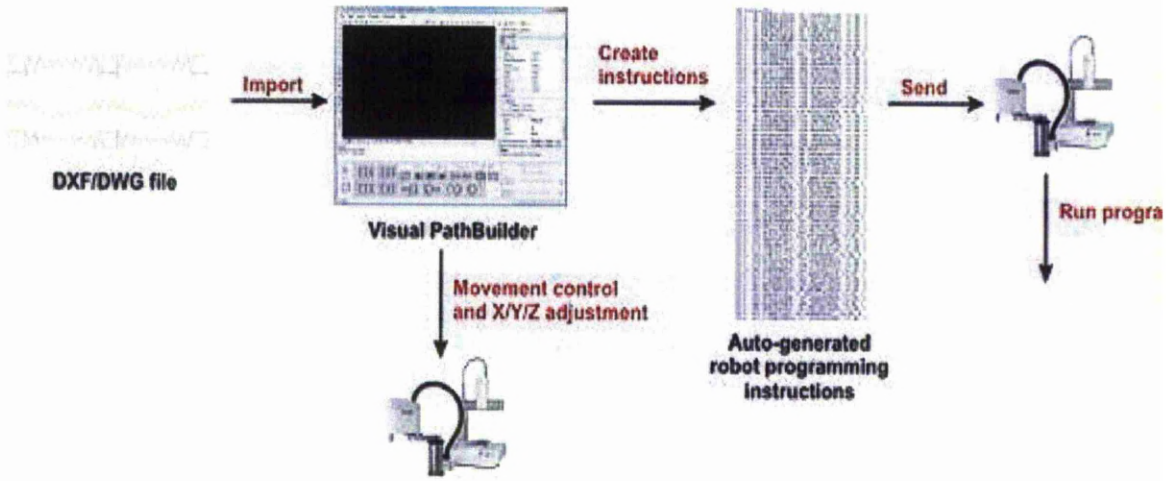

Figure 3.5: Process flow of transferring CAD files to the robot for dispensing (Source: EFD Product Catalogue)

3.3.4 Pressure and Meniscus Control

The automatic syringe system used is based on pressurised controlled deposition, in which filtered compressed air is the main medium to drive the piston in the syringe to deposit the ink. A pressure gauge is located beside the syringe and the pressure applied is controlled by manually turn the knob to its designated pressure range. The pressure gauge, pressure multiplier and associated control system allow the applied pressure to be controlled within the range of 0 to 200 psi when using pressure multiplier. Slightly lower pressure ranges could also be used without using pressure multiplier, but is then only suitable for less viscous material.

When pressure is applied to the syringe, tiny amounts via a filamentary bead of conductive ink dripped out through the tip. If the tip needle is too far from the surface, the ink solidifies on the tip, preventing further deposition. However, if the tip needle is drawn along the substrate, keeping it just high enough (around 50 μm distance between the tip and substrate) that it does not contact the substrate and break; fine lines of ink are outlined on the substrate (Figure 3.6). The cross-sectional shape of the ink bead is depended on the

selected pressure range which higher pressure will result in wider cross-sectional shape whereas lower pressure range producing narrow cross-sectional shape of ink beads.

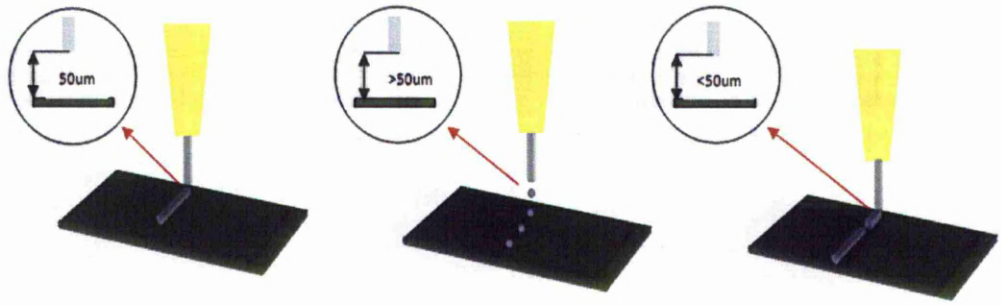

Figure 3.6: Effect of the stand-off distance

3.3.5 Speed Control

The cross-sectional shape of the ink bead also depends on the speed of the dispensing which increasing dispensing speed will result in narrower cross-sectional shape whereas reducing dispensing speed will cause wider cross-sectional shape of ink beads. The velocity of the substrate with respect to the syringe can be varied between 0 and 100 mm/s. It can be adjusted from the provided CAD/CAM software that is integrated to the system or from the teach pendant (manual operation).

There is also a limitation on the selection of speed used where too high speed causing non-continuous and distorted lines provided that the material used was thick. A reasonable speed should be considered when dispensing the material depending on the ink viscosity and substrate used.

3.3.6 Stand-off distance

Stand-off distance is a distance between the edge of the tip and the substrate and it can be properly set by manually measured the distance using a feeler gauge. Besides, the system (automatic deposition system via syringe) is well equipped with height sensor where constant stand-off distance could be controlled to ensure a consistent stand-off distance is adopted throughout the whole dispensing process.

According to Vozzi et al [101], they estimated the optimum distance would be on the order of the tip diameter but based on their experiments, if the needle is too far from the surface, the inks solidifies on the tip preventing further deposition. However, if the tip is drawn along the substrate, keeping it just high above the surface so that it does not contact the substrate and break, then fine lines or 'cracks' of inks are traced on the substrate.

3.4 Dispensing Flow Model

A dispensing flow model proposed by Vozzi et al [101] has been adopted and developed to allow the line width and height of the patterns deposited to be predicted. Adjustments to the model were carried out to adapt it to the case of the needle tip in this automatic syringe deposition technique. The dynamic wetting principle has been employed as a foundation to this model. The model uses the dynamic contact angle, which requires flow visualization techniques to be measured, to describe the equilibrium configuration of a liquid in a coating system.

As a first approximation, a simple fluid-dynamic model was developed that enables the prediction of the width and height of the patterns. The model is focused on the conditions at the tip of the needle, at the point where the polymer exits. It assumes a simple geometry for the tip and also that the conductive ink (which is normally a polymer and ink solution) does not change dimensions as the solvent evaporates. The forces involved at the tip where the

fluid is expelled as depicted in Figure 3.7 are the driving pressure, P_1 and the weight of the polymer in the syringe barrel. There is also an additional pressure, P_2 due to the vapour pressure of the solvent. There is a surface tension between conductive ink solution and substrate that is denoted as γ and dynamic friction between fluid and metal, which is a function of the viscosity, μ of the conductive ink solution.

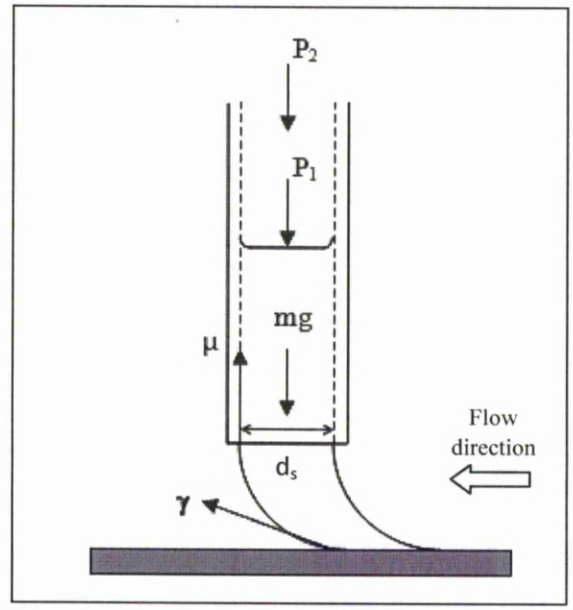

Figure 3.7: Forces involved during expulsion of the conductive ink from the syringe tip. d_s is the internal diameter of the tip.

If the balance of all forces and energies at the tip of the syringe is considered, a multivariable system of equations with an infinite number of solutions is obtained. To simplify the model, the driving pressure is assumed as the predominant force in this system and the other forces are negligible. The flow of conductive ink from the needle is:

$$Q = \frac{dV}{dt} \tag{3.1}$$

where V is the volume of conductive ink deposited and t is time. According to the optical profiler measurements via Wyko surface interferometer, the profiles of the tracks/lines can be approximated to an elliptical segment. Given the high aspect ratio (ratio of width to height), the product of width and height can be used to estimate the cross-sectional area of the deposited structures. Thus, the flow can be approximated as

$$Q = A\frac{dl}{dt} = wh\frac{dl}{dt} = whv_o \tag{3.2}$$

where A is the cross-sectional area of the deposited structure, w is the line width and h is the height of the conductive track pattern. l is the length of trace deposited in time t, and hence v_0 is the velocity of the substrate with respect to the syringe. If the flow is assumed to be a streamlined flow, and the conductive ink is to be a viscous Newtonian fluid, the flow inside the tip needle is given by Hagen-Poiseulle's equation. In fluid dynamics, the Hagen-Poiseuille equation is a physical law that gives the pressure drop in fluid flowing through a long cylindrical pipe. The assumptions made to the equation were the flow is laminar viscous and incompressible and the flow is through a constant circular cross-section that is significantly longer than its diameter.

$$Q = \frac{\pi d_S^4}{128\mu}\frac{dP}{dl} \tag{3.3}$$

where d_s is the internal diameter of the tip of needle, dP/dl is the applied pressure gradient, and μ is the viscosity of the conductive ink. Substituting equation (3.2) into equation (3.3), and rearranging the equation (3.3), an expression for the line width w can be obtained as

$$w = \frac{\pi d_S^4}{128\mu v_o h}\frac{dP}{dl} \tag{3.4}$$

Before the fluid exits the tip, a certain critical pressure, P_{crit}, proportional to the viscosity of the solution, must be applied. Below this critical threshold deposition cannot occur because the frictional forces are greater than the driving pressure. Thus, dP/dl has been approximated to $(P + P_{crit})/dl$, where $P + P_{crit}$ are the applied driving pressure and dl, is the length of the needle tip. Equation (3.4) can then be expressed as

$$W = \frac{\pi d_s^4}{128 \mu v_0 h} \frac{(P+P_{crit})}{dl} \tag{3.5}$$

The experimental pressure against line width data for conductive ink deposited were fitted to equation (3.5). The height of the conductive track structures, h was measured by averaging the optical surface profiler data. For a given profile aspect ratio, the model can be used to predict line width, w, as a function of applied pressure, $P + P_{crit}$, motor velocity v_0, and conductive ink viscosity, μ.

3.5 Experimental Arrangement

3.5.1 Pattern Design and Construction

Initial studies were done to investigate and analyse the relationship between the width and height profile of the conductive track pattern and the controllable experimental parameters (such as applied pressure, ink viscosity and speed) by printing simple parallel lines of silver conductive ink on two different substrates; plastic (PET) and alumina as illustrated in Figure 3.8. The morphology of the track, in particular the line width and height was measured using an optical profiler Wyko surface interferometer device. From this, a graph of line width and height as a function of varying pressure and speed were successfully plotted as shown in Figure 3.10 and 3.11. For both substrates, all lines were deposited at a constant printing speed of 5 mm/s with 250 μm tip and 50 μm stand-off distance, while the pressure was increased by 100 kPa for each successive line. The settings were prepared with the intention of

evaluating the effect of changing the pressure applied to the resulting line width and height of the conductive tracks. The mean width and height were found by averaging measured widths and height over each line deposited. At least six measurements of line width and height were made for each sample.

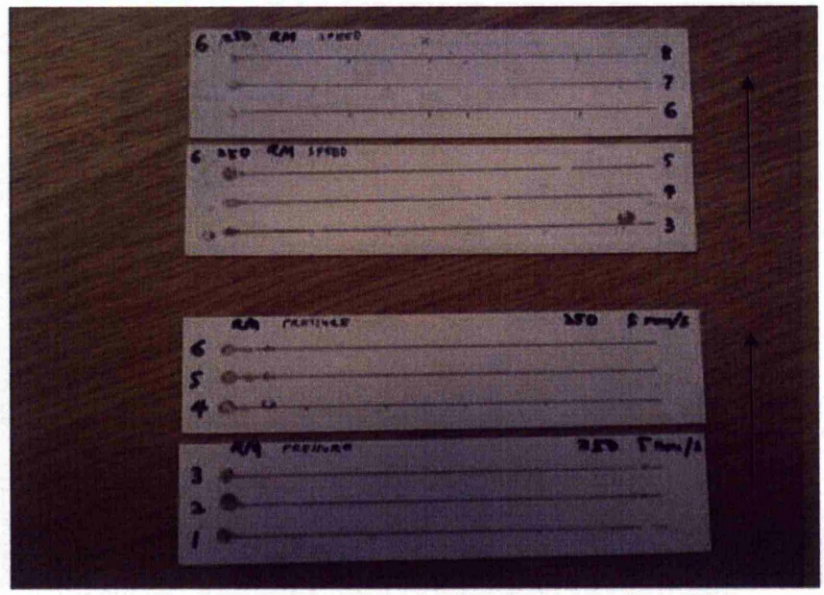

(a)

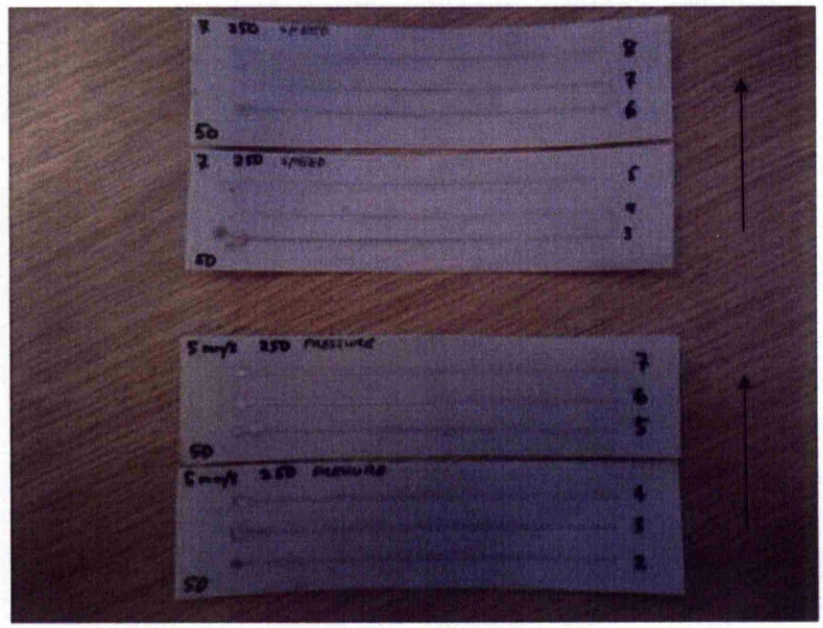

(b)

Figure 3.8: Simple parallel lines on two different substrates (a) Alumina (b) Plastic (PET). Increasing the applied pressure and speed (in the direction of the arrow) were applied during deposition

3.5.2 Material and Substrates

A Silver based polymer ink so called D58 from GEM Formulation was used due to it being both inexpensive compared to copper and printable in affordable way on thin substrates. The silver inks used consisted of 20 μm silver flakes dispersed in trixene, glycerol and butyl carbitol alcohol (Gwent Electronics Materials Ltd.). Polyethylene terephthalate (PET) film of 0.35 μm thickness and alumina of 0.50 μm thickness were used as the substrates for direct-write deposition process. The detail characteristics of the inks used is tabulated in Table 3.1.

Table 3.1: Characteristics of silver ink D58

Composition	Solid Content	Viscosity	Sheet Resistivity Per Square
Trixene BI 7953 Glycerol Butyl Carbitol	58.85 %	6 – 10 Pa-s	0.550 Ω

3.6 Results and Discussion

3.6.1 Effect of Applied Pressure

The ability to finely modulate line width by applying small variations in pressure is evident. Line width and height profiles obtained from optical profiler measurements are shown in Figure 3.9 (a), in which most were observed to have profiles approximating a squashed elliptical arc (plano-convex). Fine edges were also apparent as shown in Figure 3.9 (b).

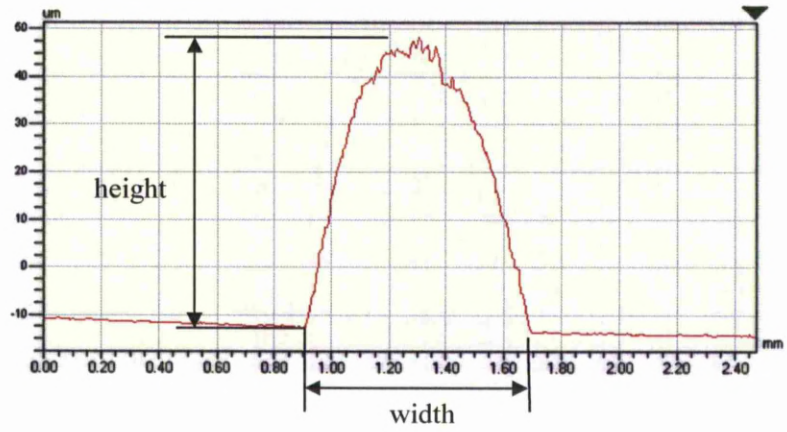

(a)

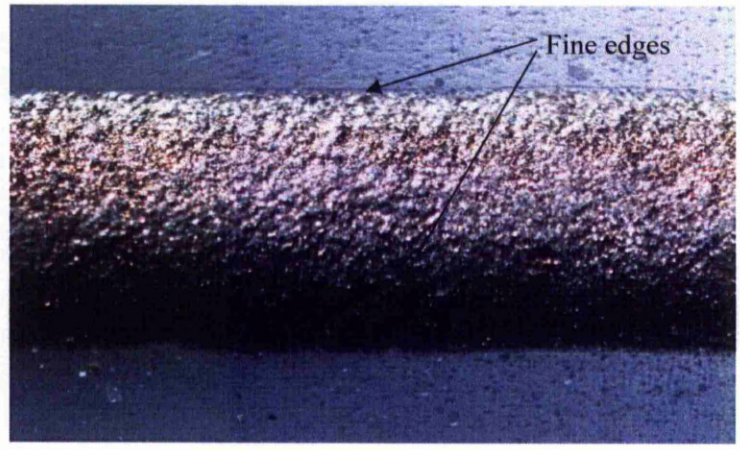

(b)

Figure 3.9: Profile of the lines/track (a) optical profiler (b) optical microscope

Figure 3.10 shows the measured line widths and height of conductive tracks, respectively, as a function of applied pressure. It was observed that as the pressure increased, the line width of the tracks on both substrates increased. When higher pressures were used, it drives more ink solution out from the tip and spread out on the substrates, hence causing the line width of the conductive tracks to increase significantly. It was also noticed that the amount of line width increment were greater for tracks on alumina rather than on plastic due to alumina has higher surface energy compared to PET. In the case of height measurements, only slight increase in height was observed for each of

conductive ink deposited using various pressures on both substrates. Although, larger volume of ink solution is deposited onto the substrates at higher pressure, the height of the track tends to be stable.

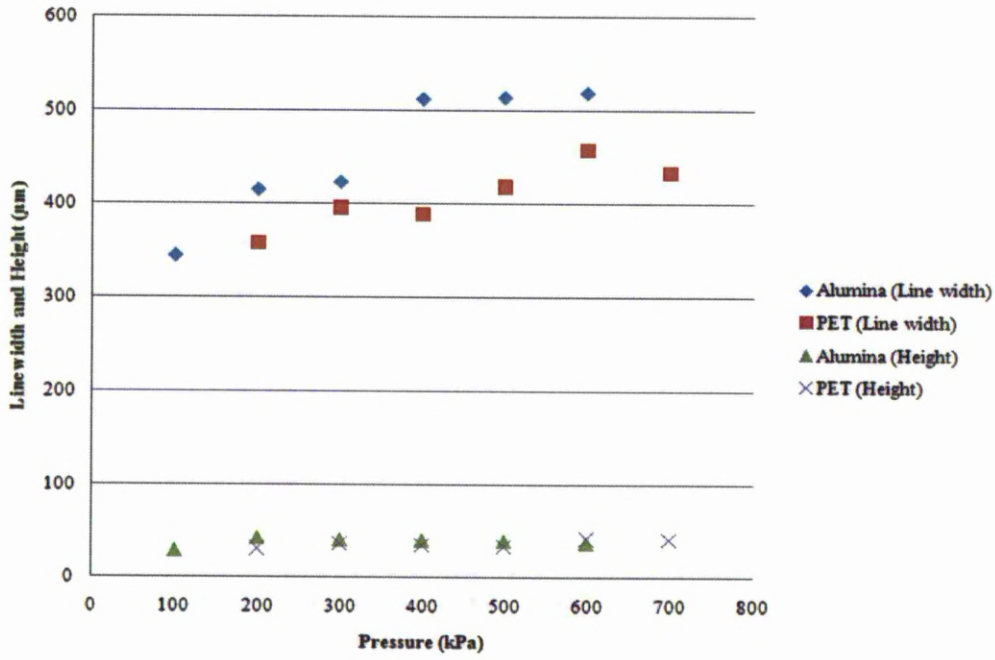

Figure 3.10: Line width and height of conductive inks deposited on both substrates at various pressures as measured with an optical profiler.

3.6.2 Effect of Speed

A further set of dispensing experiments were performed to evaluate the effect of changing the speed. All lines were deposited at a constant pressure of 700 kPa for PET and 600 kPa for alumina with the same 250 µm tip and 50 µm stand-off distances, while the printing speed was varied from 3 to 8 mm/s for each line. A graph of line widths and height as a function of printing speed are plotted in Figure 3.11. As predicted by the model, the line width is inversely proportional to printing speed. As the printing speed increased, both the line width and thickness of the tracks decreased exponentially. When higher speeds

were used, the inks did not have enough time to spread more on the substrates resulting in beads to form rather than spread out and also less material was dispensed and a reduced volume of inks deposited. The inks were stretched along the laying path as the printing speed increased causing the track line width and thickness to decrease. A similar trend as before occurred in which there was little reduction in conductive track height compared with line width for both substrates.

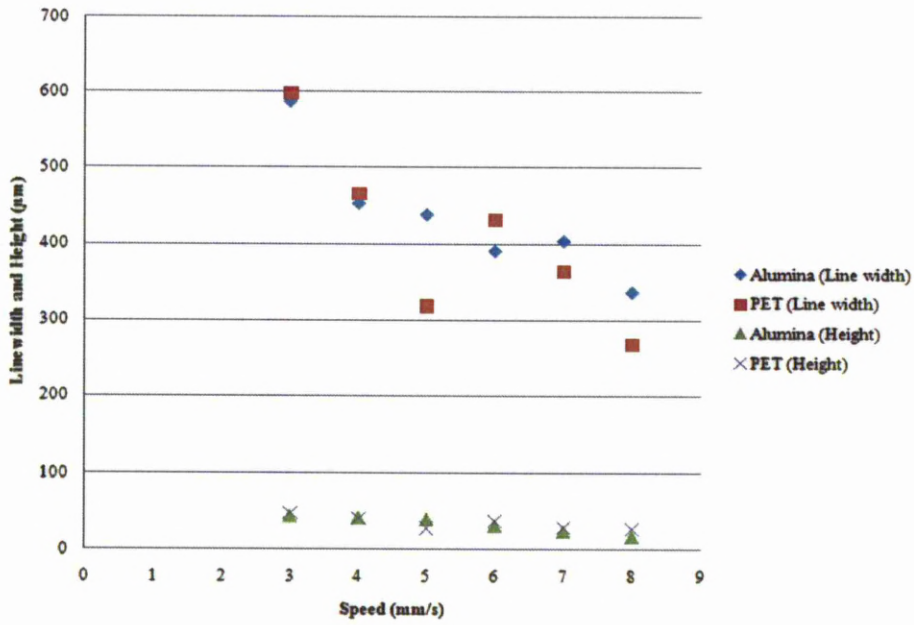

Figure 3.11: Line width and height of conductive inks deposited on both substrates at various speed as measured with an optical profiler.

3.6.3 Effect of Stand-off Distance

To evaluate the effect of stand-off distance, experiments were carried out on one substrate alone – that of PET. Simple parallel lines were printed by varying the stand-off distance from 50 - 90 µm for each line as illustrated in Figure 3.12. All lines were printed using a 250 µm tip with a pressure of 120 psi (1379 kPa) and 5 mm/s printing speed. A graph of line width and height as a function of various stand-off distances is depicted in Figure 3.13. It was

observed that the stand-off distance has a great effect on the track geometry which increasing the stand-off distance will reduce the width and simultaneously increase the height of the lines. Apart from the data at 85 μm stand-off distance, it is noted that both lines converge at the end of the curve, which shows that the stand-off distance will stop affecting the track geometry after a certain period.

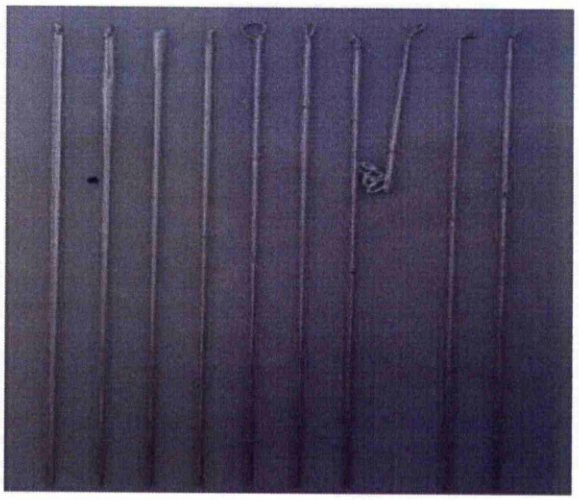

Figure 3.12: Simple parallel lines

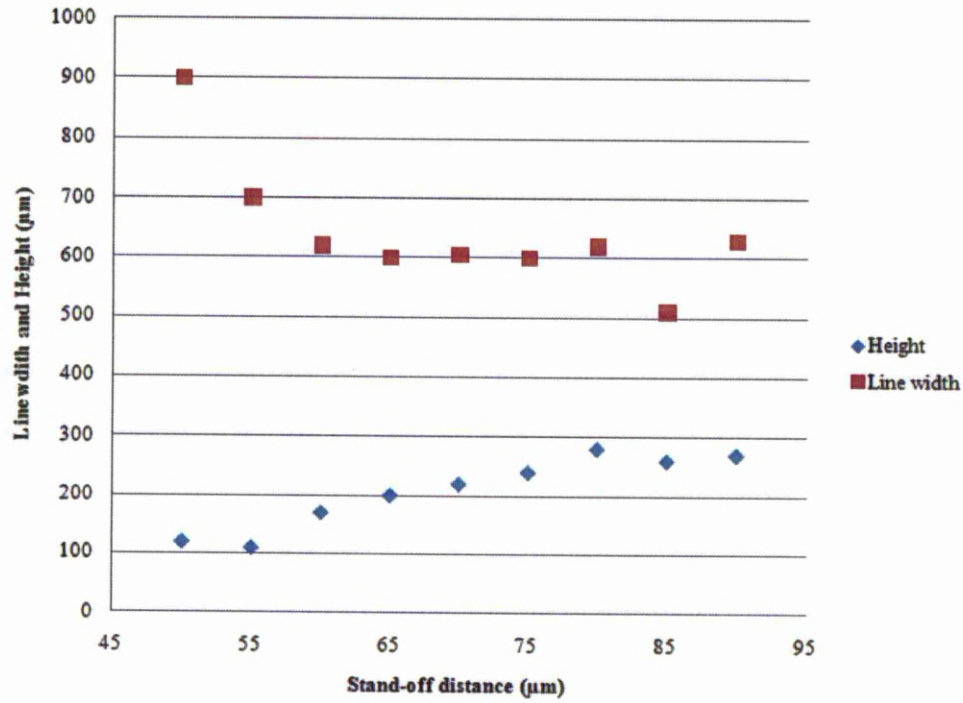

Figure 3.13: Line width and height of conductive inks as a function of various stand-off distances.

3.6.4 Effect of Substrate Type

Several simple lines were printed on two different substrates comprising of plastic (PET) and paper electronics in order to evaluate the effect of substrate on the morphology of the conductive tracks, since PET and paper electronics have different surface energy between one another (Table 3.2).

Table 3.2: Characteristics of substrates used in the experiment

Substrate	Thickness	Surface Energy (Ref)
Plastic (PET)	0.35 µm	44.6 mN/m^2
Paper Electronic	0.50 µm	35.0 mN/m^2

Initially the dispensing parameters were kept constant, with a 200 μm tip being used with a printing speed of 5 mm/s and about 50 μm stand-off distance. Variation of pressure ranges from 600 to 1300 kPa was adopted and silver based polymer type of ink (D8) was used as the material. The characteristic of the silver ink used is described in Table 3.3. The measured line width and height results were plotted as a function of various pressures applied (Figure 3.14) and it shows that both line width and height were increased with increasing of applied pressure as expected. The line width shows a significant amount of increment as to compare with height and it was noticed that the conductive inks were spreading more on PET rather than paper electronic due to PET has higher surface wettability than paper electronic. This observation can be seen from the resultant profiles of line width measured by optical profiler (Wyko surface interferometer) on both substrates (Figure 3.15). It was noticed that the ratio of line width against height were higher for tracks printed on PET compared to paper electronics. Lower surface energy of ink will spontaneously wet out thus causing the ink to spread more on higher surface energy of PET. The paper electronic however has a lower surface energy than the ink in which the ink beads up rather than wet out reducing its contact area with the paper electronic surface. Due to this, substrate type also played a major role as one of the factors affecting the morphology of ink structure.

Table 3.3: Characteristics of silver ink D8

Composition	Solid Content	Viscosity	Sheet Resistivity Per Square
Benzyl Alcohol (10-30%) Einecs	64.5-65.5 %	22 - 27 Pa-s	25 – 35 mΩ

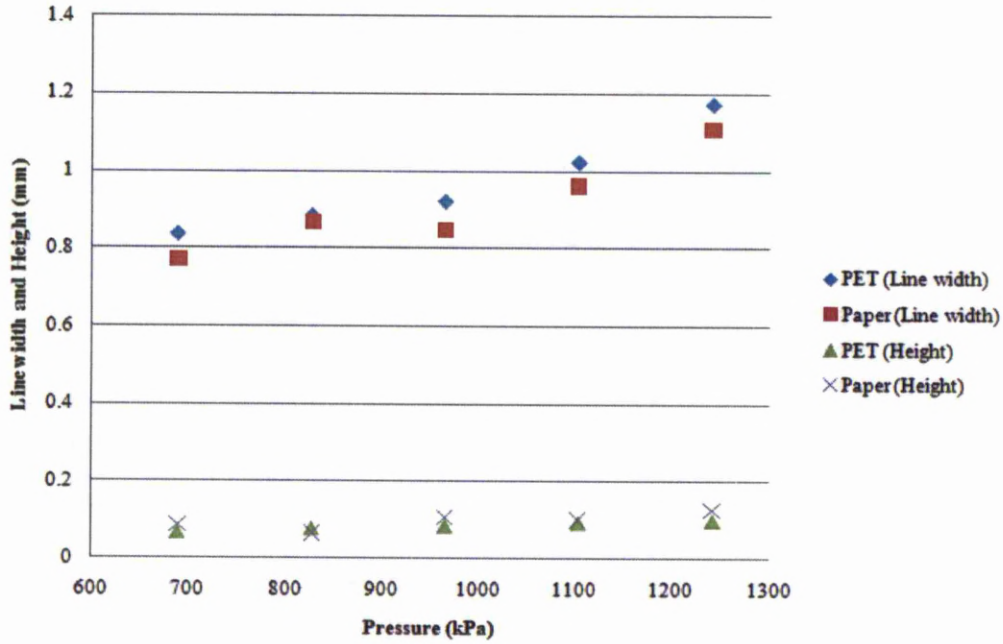

Figure 3.14: Graph of line width and height as a function of various pressures. Deviations are on the order of ± 50 μm

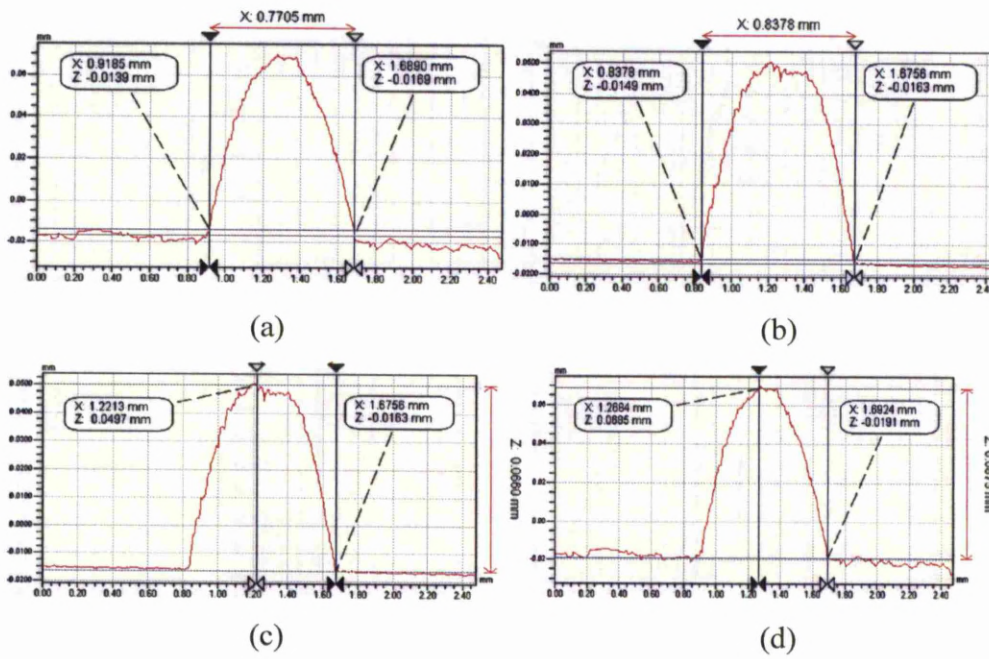

Figure 3.15: Profile of the lines/track printed on PET and paper electronic at 100 psi (a) Narrower track on paper electric (b) Wider track on PET (c) Lower track on PET (d) Higher track on paper electronic

A further set of experiments were carried out to examine the effect of varying the speed from 2 to 9 mm/s on the morphology of track, without changing other dispensing parameters. The results of the experiments are shown in Figure 3.16. It was observed that both line width and height were decreased with the increased of speed, as expected. A similar trend happened which the line width shows a significant amount of reduction as to compare with height and the inks were spreading more on PET rather than paper electronics. The ink beads up when printing on paper electronics since it has lower surface energy than the inks.

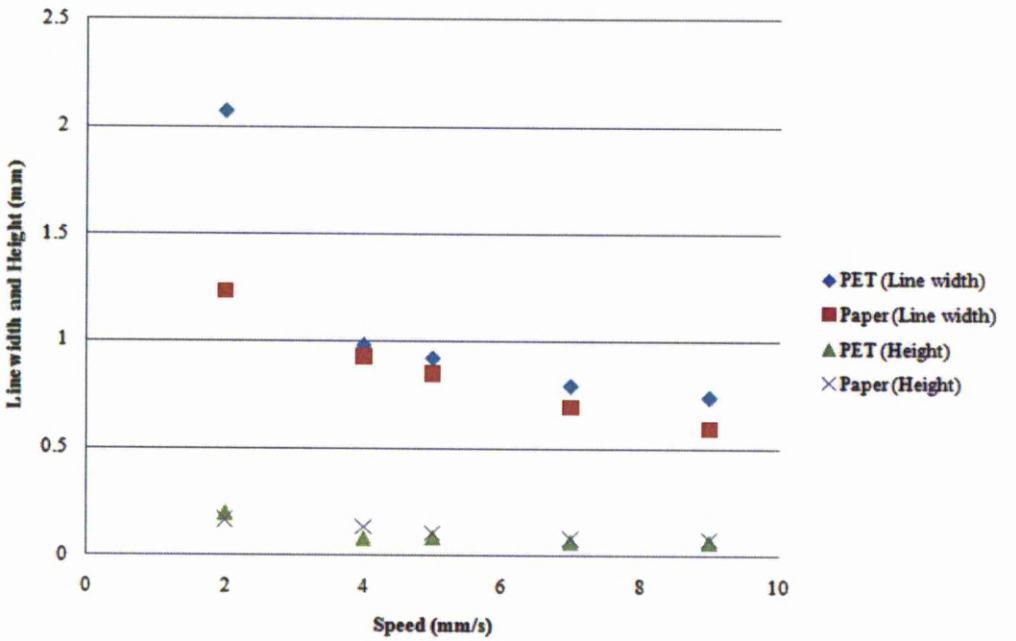

Figure 3.16: Graph of line width and height as a function of various speeds.

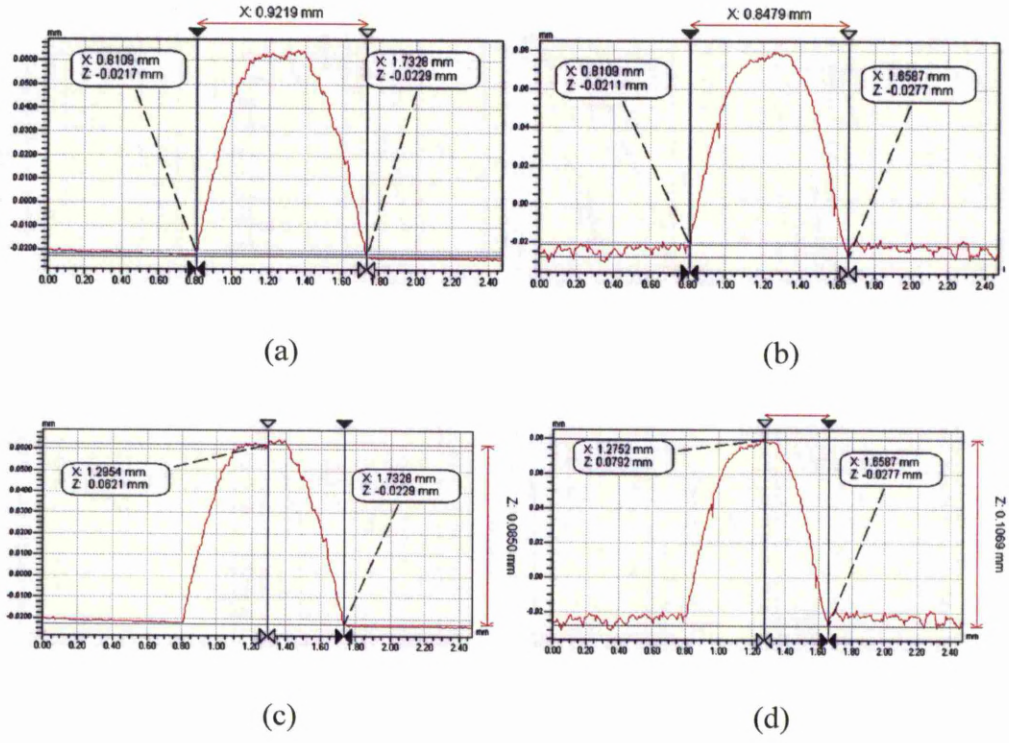

Figure 3.17: Profile of the lines/track printed on PET and A4 paper at 5 mm/s (a) Wide track on PET (b) Narrow track on paper electronic (c) Lower track on PET (d) Higher track on paper electronic

3.7 Chapter Summary

The characterization of a syringe-based DW technology for the direct writing of silver polymer ink paste was successfully performed. The characterization was basically focused on studying the effects of process parameters on the morphology of the fabricated samples.

As demonstrated by the graphs and photographs from Figure 3.8 to 3.17, the syringe-based deposition method described is capable of fabricating micro scale structures in the form of conductive tracks in a wide variety of patterns and geometries. This versatility is useful for the study of antenna construction to promote desired antenna performance. In addition, the operating system is user friendly and does not require special skills. Once the

geometry of the pattern has been chosen and fed into the computer, and the syringe is filled with a few millilitres of solution, several patterns can be micro fabricated in the space of several minutes (to make a series of parallel lines as shown in Figure 3.8 takes only about 1-2 min).

The syringe-based fabrication technique described here is based on a pressure-controlled deposition system. The main advantages of this technique over other direct-write fabrication methods are its simplicity and the possibility of modulating line widths and heights over a wide range by varying the polymer concentration (or viscosity), applied pressure, and deposition speed.

Other applications of this technique have been proposed in the field of scaffold manufacturing [101] and demonstrate the universality and flexibility of the technique. A simple fluid dynamic model has been developed to describe the physical dimensions of the fluid as it is expelled from the syringe tip. The model enables the prediction of essential topological parameters of the structures deposited.

Future investigations into the feasibility of this deposition technique for antenna manufacturing will be focused on the effect of its cross-sectional shape to the antenna performance characteristics.

Chapter 4

Study of Comparative Electrical Performance of Etched Copper and Silver Ink DW Conductor

4.1 Introduction

Radio frequency (RF) applications utilising printed electronics as a manufacturing method have recently become high profile technologies. Direct Write is an environmentally friendly process since the conductors are printed only on the areas that need to be conductive. This means that less chemicals are needed in the manufacturing process and less waste is produced. In addition, printing is possible on a wide variety of materials, which enables integration of printed electronics directly onto challenging non-planar surfaces, such as clothes or paper reels. Printing also allows mass production, and thus provides one possible manufacturing method for future printed circuit boards (PCB).

A variety of techniques are available for printing conductive patterns. Screen printing, gravure printing, lithography, flexography and inkjet printing

are examples of these techniques. They have been used to manufacture products such as radio frequency identification (RFID) transponder antennas [55-56], transmission lines [13] and patch antennas for microwave applications [99].

The above-mentioned printing technologies use conductive inks. In general these inks have lower conductivity than pure metals, such as copper or aluminium. The conductive inks consist mainly of inorganic particles (as conductive phase), binder material (insulator phase), solvents and additives. The composition and conductivity of the ink varies according to printing technique. Silver flakes, for example, are a commonly used filler material in screen printable inks. A typical conductivity value for this kind of ink is a few MS/m. In the inkjet technique, materials such as gold nanoparticles can be used as the filler.

In addition to the conductor material, the composition and the amount of ink have a crucial effect on the realised conductivity of the printed conductor. The particle properties (material, size, amount, shape, distribution and orientation) influence the electrical and mechanical properties of the printed conductors. Further, the viscosity of the ink affects the way it is transferred onto the substrate. In the case where the substrate surface is rough compared to the desired ink layer thickness, the current paths will elongate and variations in the deposited conductive layer thickness will occur, resulting in varying resistance. The curing temperature of the ink is also an important parameter [27]

4.2 Objective

The objective of this set of experiments is to evaluate the capabilities of using the syringe-based DW technique in conjunction with laser curing to fabricate real electronics component by depositing RFID tag antenna geometries and at the same time cure the silver ink. As such it presented two challenges in that it would need to be manufactured on PET using a computer-

controlled syringe deposition system and subsequently laser cured in a manner which limited or eliminated damage to the PET substrate and maintained its geometry after laser curing. In addition, the performance of the tag antenna will also be investigated and compared with the copper etched tag antenna.

4.3 Experimental Arrangement

4.3.1 RFID Tag Antenna Characteristics

The antenna is designed to be responsive at 13.56 MHz which is a common RFID frequency and it was modelled on a standard race track profile as shown in Figure 4.1. It was classified as a high frequency (HF) passive RFID tag and this frequency is accepted worldwide. This passive tag offers fair transmission in the presence of metals and liquids. The experiments were carried out in conjunction with an industrial sponsor, who generated the design of the antenna. This antenna design was produced as a means to attach to a flip chip possessing inputs which can accept signals from external sensor elements such as strain gauges that could also be manufactured by Direct Write techniques.

HF systems are widely used in library, mass transit and product authentication applications. A RFID antenna is normally applied to or incorporated into a product, animal or person for the purpose of identification and tracking using radio waves [60]. Some tags can be read from several meters away and beyond the line of sight of the reader. Figure 4.1 illustrates the 13.56 MHz RFID tag product sample. Traditionally the RFID tags were made from etching a copper layer on a FR4 dielectric substrate.

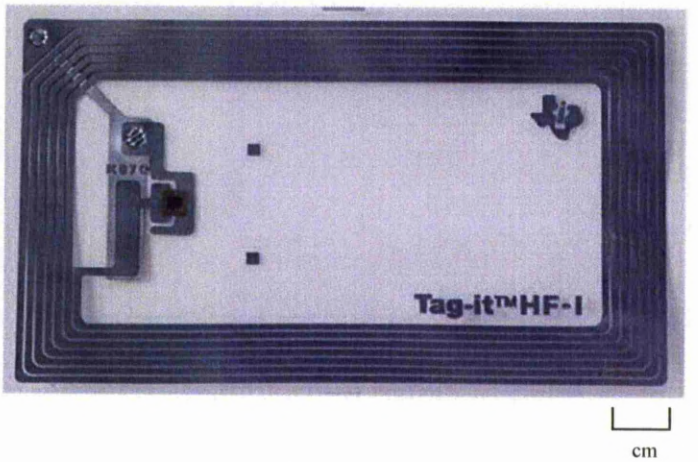

Figure 4.1: 13.56 MHz RFID antenna (Reference antenna)

To replicate the etched copper RFID tag, a reverse engineering approach was applied. The geometry of the silver tag design is shown in Figure 4.2 and the key dimensions are presented in Table 4.1. The overall dimension of the tag was 69.5 mm length x 46.0 mm width. The conductor width was set to be of 1 mm width and the height for traditional etched lines was generally very thin, about 19-20 μm (Figure 4.3). Thus this value was used as a target value for the height of the tag antenna.

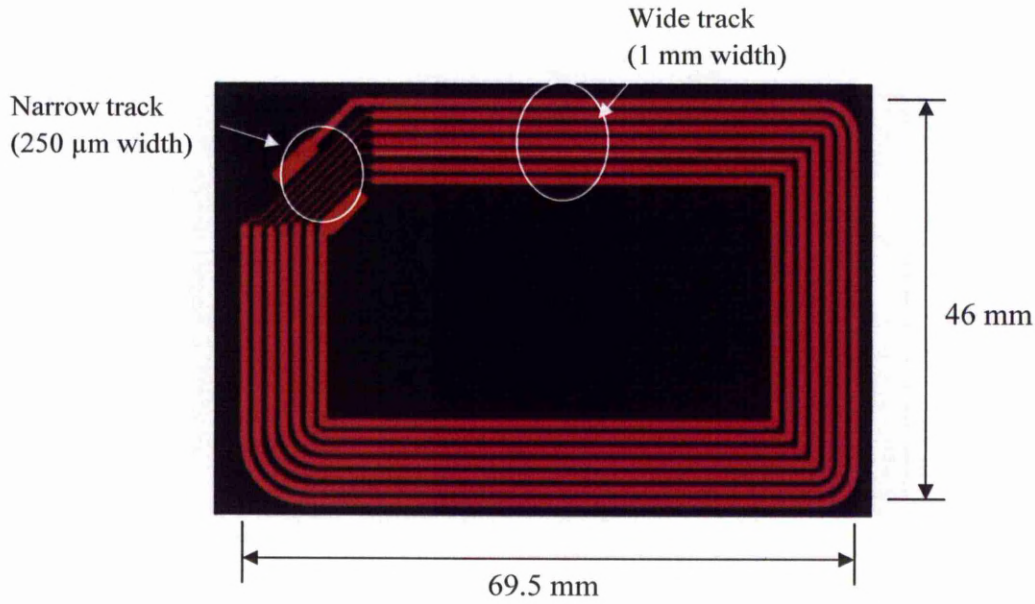

Figure 4.2: Silver ink RFID antenna

Table 4.1: Key dimensions of the silver ink RFID tag design

Width (mm)	Length (mm)	Thickness (mm)	Wide Track width (mm)	Narrow Track width (mm)
46.000	69.500	0.020	1.000	0.025

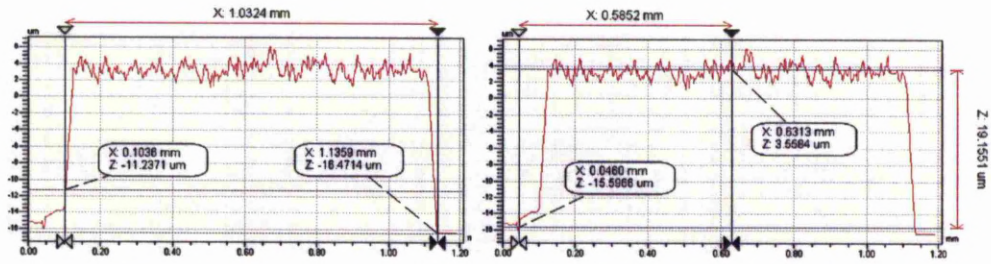

(a) (b)

Figure 4.3: Cross-section profile of etched copper (a) line width (b) height

4.3.2 Experimental Apparatus

The main apparatus used to deposit the tag geometries was the syringe based DW system, shown in Figure 4.4. The deposition process was based on a pressurized air driven ink deposition syringe, with the geometrical paths controlled by the CAM software integrated with the robotic system. The range of line widths available was from 100 μm upwards. A detailed explanation of the main components of the syringe based DW technique was discussed in the earlier Chapter 3 (Section 3.3).

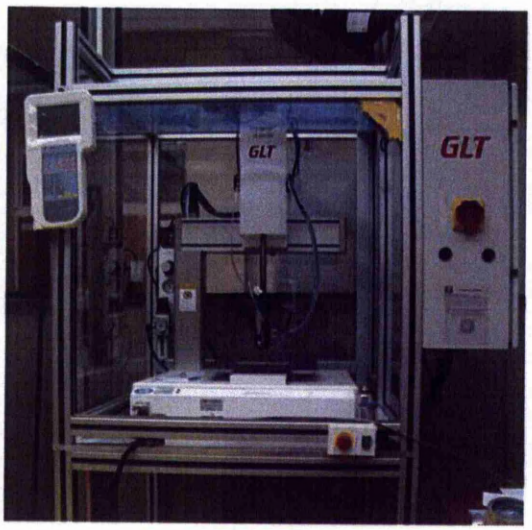

Figure 4.4: Syringe-based DW apparatus

The syringe based DW technique used conductive inks which comprises of resin (vehicle), binder and metallic particles, hence it require a heating process which in this case could be achieved either by using an oven or by laser curing. For this experiment, a laser curing process was applied to cure the ink once it was laid out on the substrate.

For performance measurement, the optical profiling system via Wyko NT1100 white light surface interferometer was used. Samples generated have been scanned before and after curing to assess densification of the sample as a result of the curing process. The illustration of this equipment was previously

been shown in Figure 3.11 in the earlier chapter. The NT1100 utilized the white light interferometry for high resolution 3D surface measurements from sub-nanometer toughness to millimetre high steps. The optical system is placed on the pressure leveller which ensures the Wyko is in balance position to give more accurate. The Wyko NT1100 allows seeing any height difference under the optical system.

A constant-pressure four-point probe system has been designed and built to accurately measure resistances for resistivity calculations. For temperature-resistance data this has been integrated with a K-series thermocouple and data logger. This method is usually employed in the electrical assessment of films. A direct contact approach will be implemented where all probes are brought directly into contact with the track to measure its resistance at four locations. The measurement method includes a forced current i through the outer probe 1 and 4 and a measurement of voltage drop over probe 2 and 3, using a very high Ohmic measurement device, so that the current flowing through pin 2 and 3 is nearly zero (Figure 4.5) [32]. In that case the individual, additional contact resistance does not play a role as it cancels out of the equation. All measured resistance are converted into resistivity according to the following formula:

$$R = \rho \frac{l}{A} \tag{4.1}$$

where R is the electrical resistance of a uniform specimen of the material (measured in ohms, Ω), l is the length of the structure (measured in meters, m), A is the cross-sectional area (width x height) of the specimen (measured squared meters, m^2) and ρ is the specific resistivity in Ωm or the practical unit is μΩcm. The four point probe used is shown in Figure 4.6.

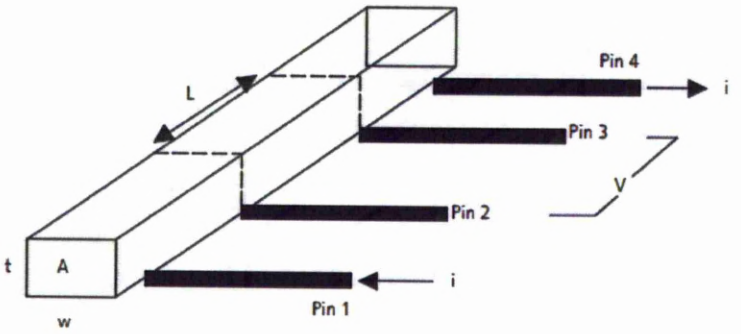

Figure 4.5: Schematic illustration of the contact points arrangement of four point probes for measurement purposes (Source : Marinov, 2007)

Figure 4.6: Integrated four-point probe and data logger

4.3.3 Material, Substrate and Methods

The conductive inks used were based on silver inks in three different types of composition denoted as Laser Curable D5, Hybrid D6 and Graphite D5. A silver based polymer ink was used due to it being both inexpensive compared to copper and printable in affordable way on thin substrates [60]. It is the preferred choice since copper would have to be slowly electrodeposited

and wastefully etched afterwards. Copper also suffers from oxidation, making interconnects troublesome. High temperatures are needed to anneal copper precursor inks but still the resulting conductivity not close enough to bulk copper. Yet silver is printed in a huge number of products today from UHF antennas in approaching billions of RFID tags yearly, membrane keyboards, battery testers on batteries and other printed electronics and electrics [63]. The characteristics of the inks used are presented in Table 4.2.

Table 4.2: Characteristics of silver inks

Material	Composition	Solid Content at 700°C (%)	Curing conditions (°C, min)	Viscosity at 25°C (Pa-s)	Resistivity at 25 μm (mΩ)
Laser Curable D5	Urea Resin (1-10%) 2-Butoxyethanol (1-10%)	77.55	160, 30	3-17	34.30
Hybrid D6	DI (Ethylene Glycol) Methyl Ether (1-10%)	61.60	180, 60	3-34	9.88
Graphite D5	DI (Ethylene Glycol) Methyl Ether (1-10%)	61.09	N/A	4-25	9.72

The substrate material used was Polyethylene teraphthalate, commonly abbreviated as PET, PETE or the obsolete PETP or PET-P. The substrate had a thickness of 0.35 mm and was in its biaxially oriented condition. The experimental design was carried out by comparing the resistance between both copper etched and silver ink tags. In addition, the performance of both tags were also characterized and compared. Several steps processes were taken to meet the aim of this experiment which are:

1) Measure the input resistances of both tags
2) Measure and compare the performance of impedance matched for both tags
3) Measure and compare the insertion loss using 'black-box' method that relies solely on the measured S-parameter data for both tags

4.4 Experimental Procedures

The construction of the silver tag antenna was started by importing the drawing file into the CAD/CAM system. Next, the process of assigning the tool path and selecting the appropriate dispensing parameters especially dispensing speed were done accordingly. Once finished, sending the dispensing command to the robot was done consequently. The details of the process are explained below.

4.4.1 CAD Profiles Organisation

Since the design of the RFID tag antenna in this experiment is considered intricate, the development of the design needs to be done properly in the established CAD applications such as AutoCAD. By doing this it helps to reduce a lot of time in the development of product design without the need to manually teach every points of the pattern design. Furthermore, Visual Path Builder works like a 3D CAD application and adapted well with DXF, DWG, IGES, STL, OBJ, Gerber RS274D and Gerber RS274X vector and bitmap graphics. It has the ability to create instant working robot programs with import and export features. The completed CAD designs or models of the pattern are then imported into Visual Path Builder for generation of tool paths. Generation of tool paths and waypoints were determined using overlay features (Figure 4.7). The order and direction of tool paths can be freely specified in which important for the determination of dispensing lead time. Once completed; the task objects were then save and sent to JRC dispensing for automatically

translated into robotic language and preparation of dispensing parameters prior to deposition process.

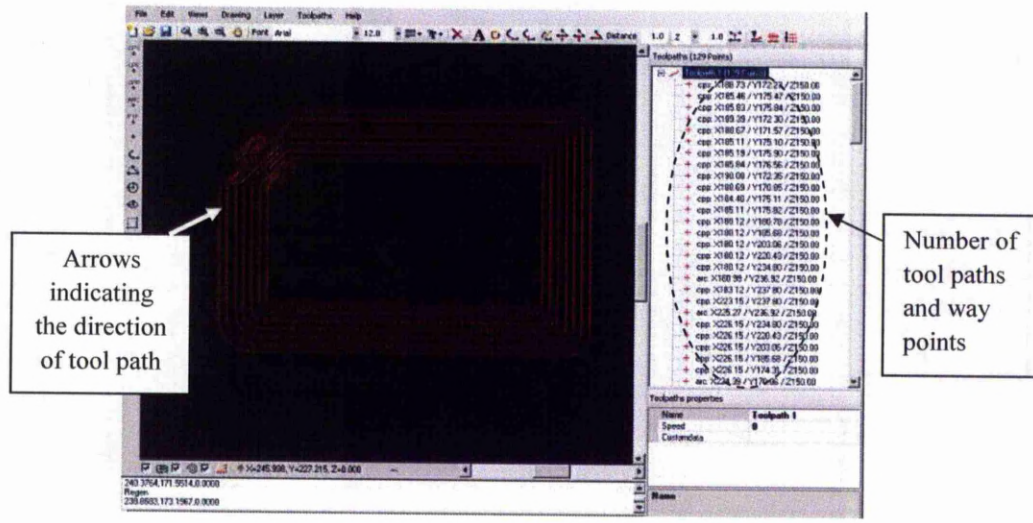

Figure 4.7: Assigning tool path to the profiles

Alignments and offset values are calculated fully automatically by using one or two reference points. By specifying one or two reference points the system will compute offset-values and deviation angle in order to adjust the CAD coordinates with the machine coordinates. The specified tasks are translated into a robot program automatically without user interaction. The integrated simulation features in this software allows users to test the programs without having a robot connected. With this feature, on-line modification can be done which helps reducing the product development time massively. The robot control program is sent to the machine via serial connection and the detail coordinates and tool path including the dispensing speed are displayed as illustrated in Figure 4.8 below.

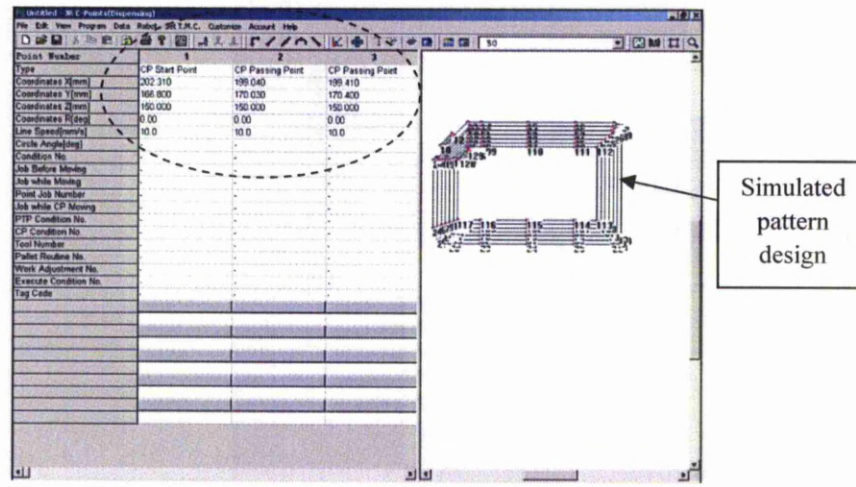

Figure 4.8: X, Y and Z coordinates with dispensing speed parameters in JRC dispensing environment as indicated by dotted circle line.

4.4.2 Ink Deposition

A series of experiments were undertaken to investigate control of both the deposited line width and height profile of the tracks in order to prevent spreading of the ink. The antenna conductor tracks were printed using the syringe-based DW technique (Figure 4.9). As before, biaxially-oriented PET substrates were cleaned and affixed to the CNC worktable with tape. The samples were pressed down using a heavy item to maximize flatness for 30 seconds.

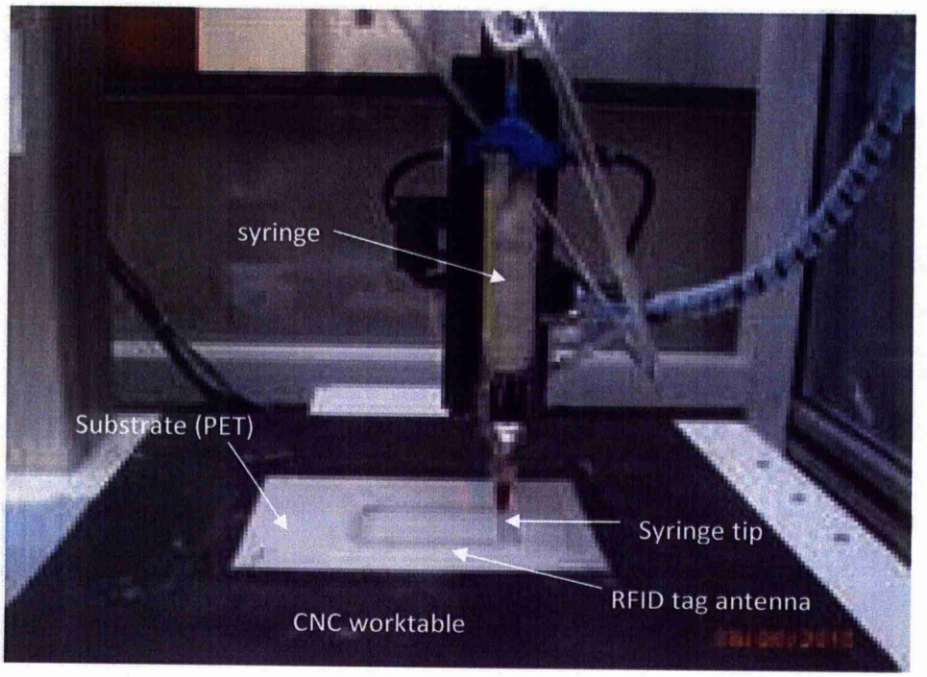

Figure 4.9: Syringe-based DW technique with substrate properly placed on and secured with tape to the CNC worktable.

The RFID tag geometry was subsequently produced by depositing in a vector pattern with a syringe standoff distance of 50 microns and by drawing the tip needle along the substrate. The details of how this process was carried out were already mentioned earlier in Chapter 3 (section 3.3.1).

The deposition parameters used were varied and optimized accordingly in order to get the required dimension for the track. Differences in wettability and hence cross-sectional geometry of the inks on PET after deposition and laser curing meant that a degree of calculation was required to produce samples of the required geometry. Account had to be taken of the spreading of the track profiles after deposition. The targeted dimension was 1 mm width for a wide track and 0.25 mm width for a narrow track as indicated in Figure 4.2.

There were four major deposition parameters that are needed to be considered consisting of printing speed, the applied pressure, the tip size and the stand-off distance. The geometrical characteristics of the track were also

affected by the surface wettability of the substrate used and the rheology of the conductive material used. The selection of the deposition parameters used was tabulated in Table 4.3 below.

Table 4.3: Specification of deposition parameters

Track Profile		RFID tag antenna		
Material		Graphite D5	Hybrid D5	Laser Curable D5
Syringe air pressure		25-45 psi	30-70 psi	50-100 psi
Tip size		250 μm		
Stand-off distance		50 μm		
Printing speed		Wide track : 3 mm/s, Narrow track : 8 mm/s		
Curing Technique	Laser Type	Nd: YAG (Green)		
	Wavelength	532 nm		
	Current	14.1, 14.2, 14.7, 15.1 A		
	Scanning speed	500, 2500 mm/min		
	No. of passes	1, 2, 3, 4		
Substrate		Plastic (PET)		

4.4.3 Laser Curing

Generally, the antenna tracks could be cured either by using pre-heated oven or laser curing technique. Laser curing technique is the preferred choice as opposed to traditional oven curing due to the speeds possible and its lack of effect on nearby heat sensitive components.

Here new curing strategy was employed that of raster-scanning the deposited ink. The laser scanning path followed a direction indicated by the red arrow in Figure 4.10 (a). Raster-scanning was a method that became available due to the limited interaction noted between the 532 nm wavelength and the PET substrate which meant that over scanning non-deposited areas did not result in damage to the PET substrate. This strategy could also be applied to both sides of the substrate to enable the ink track to be properly cured.

Parameters for laser curing using raster scanning were then derived empirically. In this case, which there were four significant factors that affected the results of curing that needed to be taken into account : current; time period between ink deposition; curing speed of the laser beam intersection; and method of curing.

Topographical changes to the deposited track as a result of laser curing were mapped and consideration given to the deposition geometry achieved in an iterative manner to compensate for the geometry of the antenna after laser curing

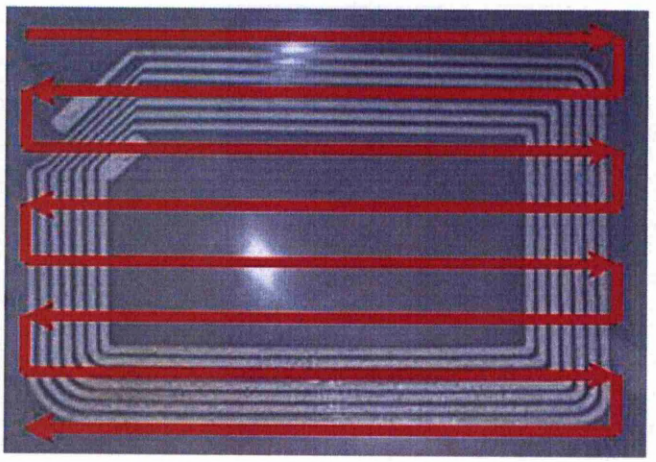

(a)

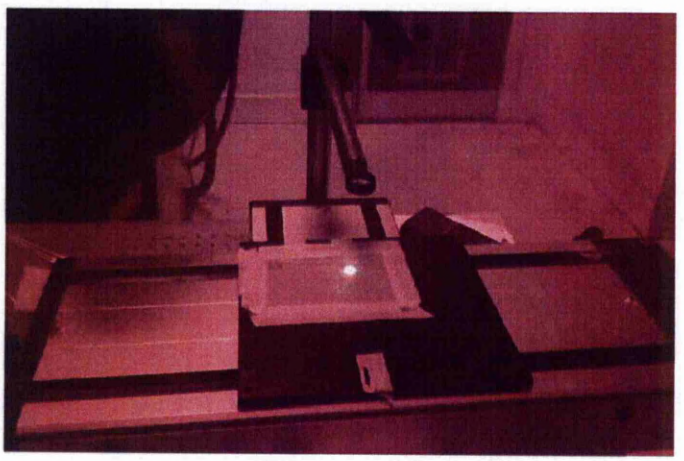

(b)

Figure 4.10: (a) Laser curing path in z direction (b) Multiple passes in a raster scan method in action where the laser scans over a defined area rather than line following

4.5 Results and Discussion

4.5.1 Morphology of the Track

The fabricated antenna sample is shown in Figure 4.11. In term of the track physical characteristics before curing, the tracks were consistent, uniform and straight as illustrates in Figure 4.12 (a) – (d). There were no sign of variation of tracks width as the velocity changes especially at corners and the spacing between lines are within requirement where they were not touching

each other. All the tracks for all inks were observed to have profiles approximating a squashed elliptical arc as depicted in Figure 4.13 (a) – (c). The cross sectional contour of the tracks looks well defined in geometry with sharp edges and the top surface is considered smooth as a very little variation of roughness in the region of 10 μm as observed in Figure 4.13 (a) – (c).

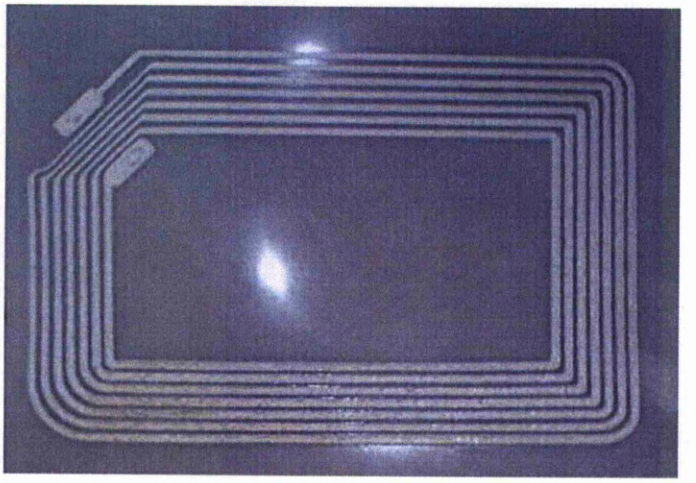

Figure 4.11: Sample of 13.56 MHz RFID antenna made by syringe deposition system

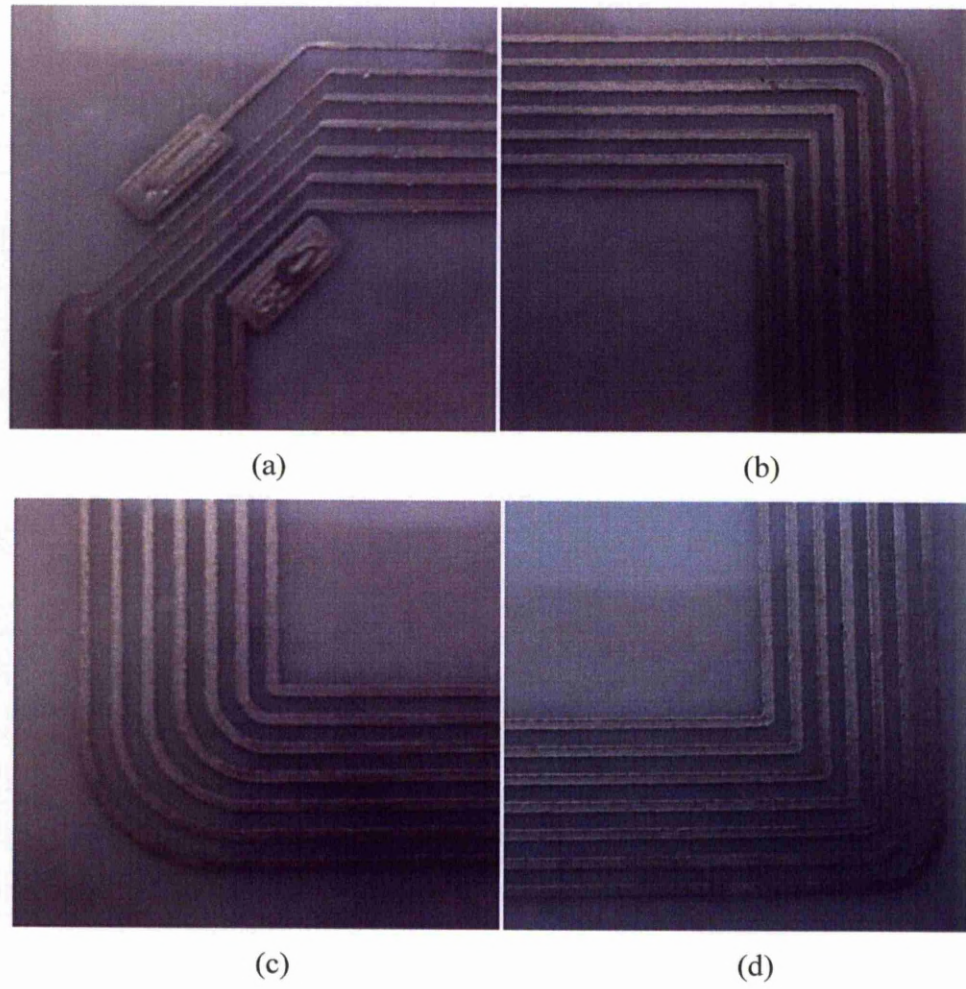

Figure 4.12: Images of the tracks at each corner of the RFID tag geometry.

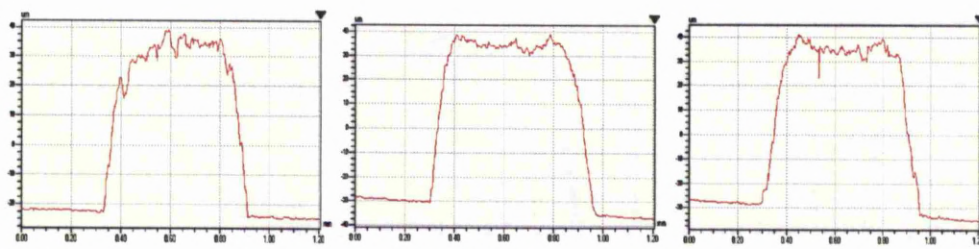

Figure 4.13: Cross-section profile of silver track (a) Laser Curable D5 (b) Graphite D5 (c) Hybrid D6

4.5.2 Pressure and Traverse Speed Variation

It was a challenge to dispense a consistent line width as the antenna profiles consists of two different widths of track; 1 mm and 250 μm as depicted in Figure 4.2. To print the required dimension, appropriate range of dispensing parameters were successfully determined and optimized. The easiest method found to control the required line width was by utilizing two different sizes of needle tip for each line width, although it would take a longer process cycle to fabricate the whole antenna. Hence, to shorten the printing time and reducing the process cycle, a single tip of 250 μm was used, but at the same time the line width was controlled by optimizing the dispensing parameters accordingly.

Varying the delivery pressure to the syringe was investigated as one of the possible methods for controlling deposition geometry. A range of pressures were applied to evaluate their effect on the track morphology. According to Figure 4.14 - 4.16, increasing the pressure increased both the line width and height for all inks as expected, since the pressure applied was proportional to the resultant line width according to the dispensing model described earlier in Chapter 3 (Section 3.5).

Unfortunately the resultant line widths and heights showed a non-linear variation with a lag-response evident at the deposition face. Hence pressure of ink transport through the syringe has been chosen for consistent line width of the thickest line required, associated with consistent ink transport at any higher traverse speeds required. It can be seen that there is a choking effect at the syringe tip for Hybrid D6 ink at high pressures, which caused variation in deposition rates.

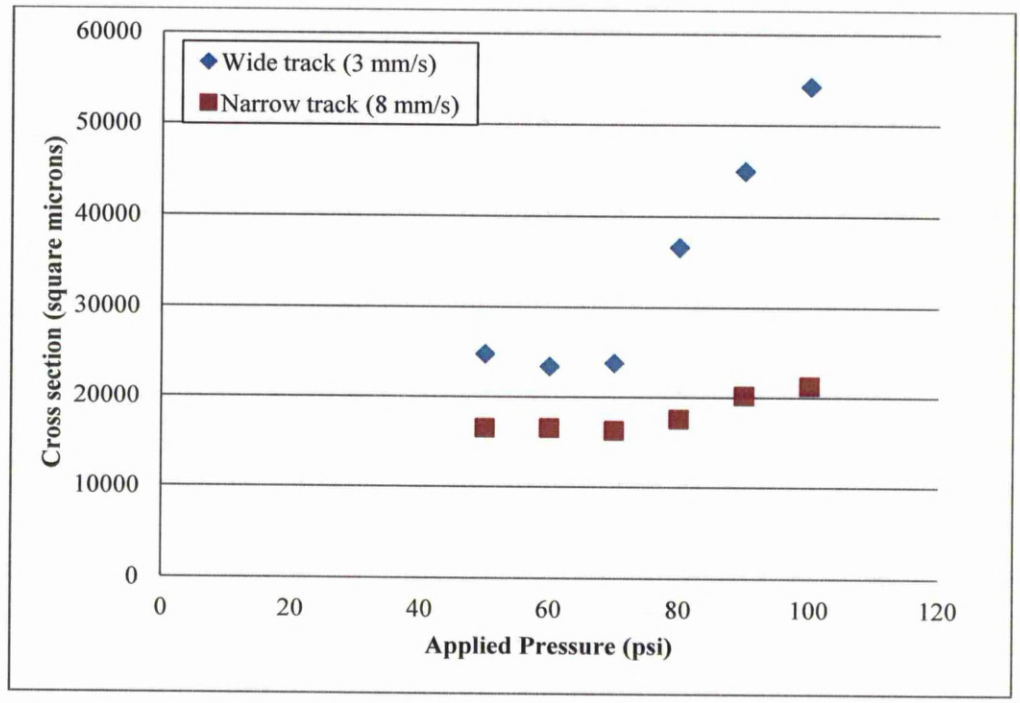

Figure 4.14: Pressure against cross-section for Laser Curable D5 ink.

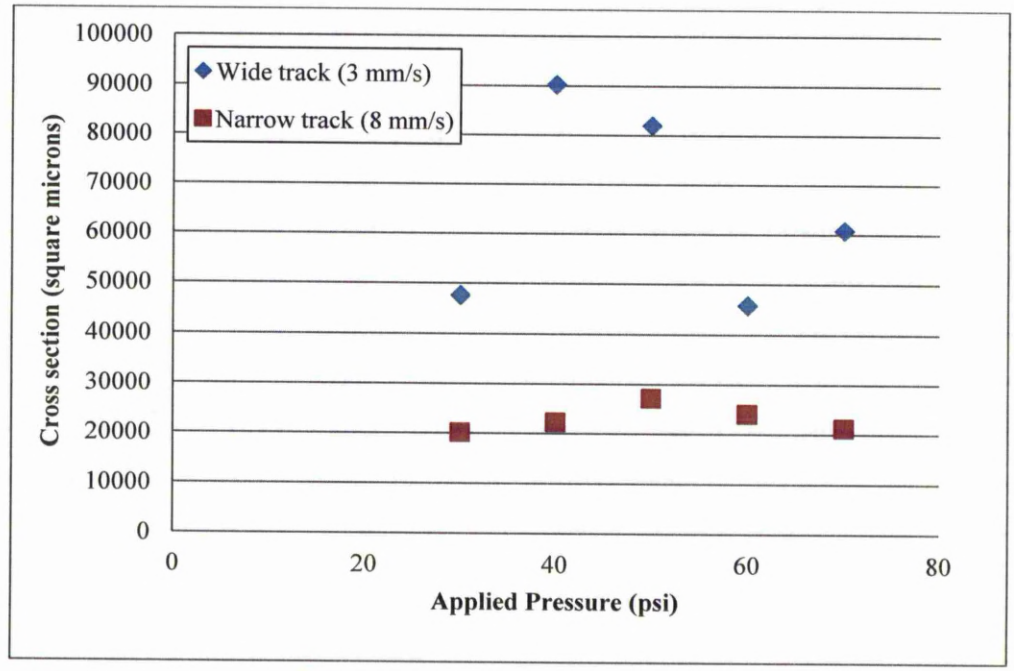

Figure 4.15: Pressure against cross-section for Hybrid D6 ink.

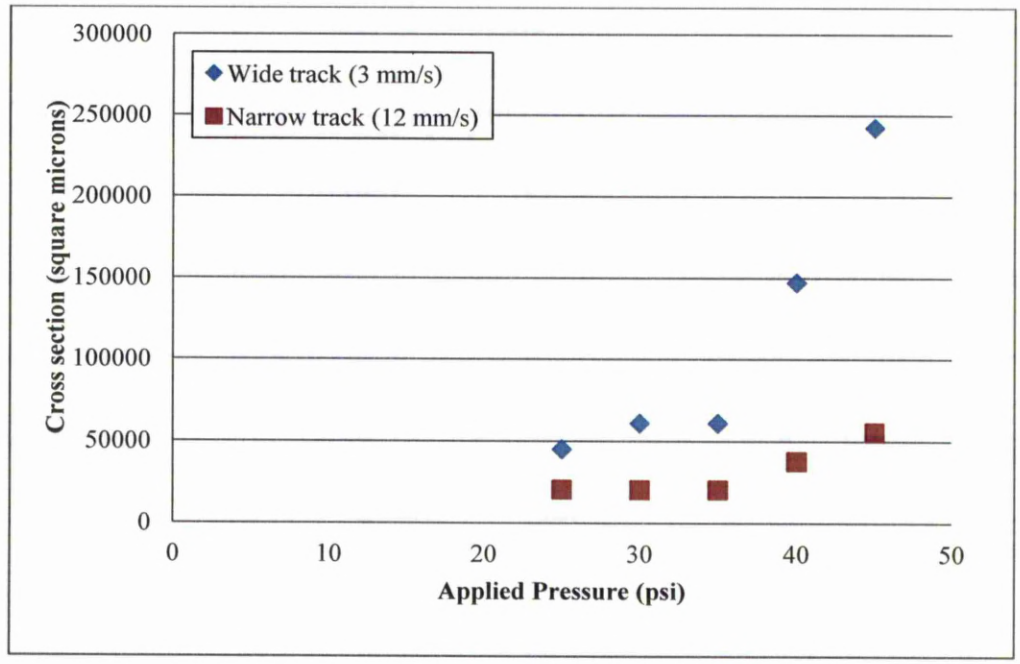

Figure 4.16: Pressure against cross-section for Graphite D6 ink.

A more promising method of control of the system has proved to be by controlling line width by traverse speed control for all type of inks used as shown in Figure 4.17 and 4.18. The method was proven capable of meeting the required dimensions in which two different types of printing speed were used; 3 and 8 mm/s in one single process. This allows a range of line widths to be produced for a single deposition tip, including those thinner than the tip diameter itself. This method of control, while still non-linear, is consistent and repeatable, allowing the generation of initial antenna samples.

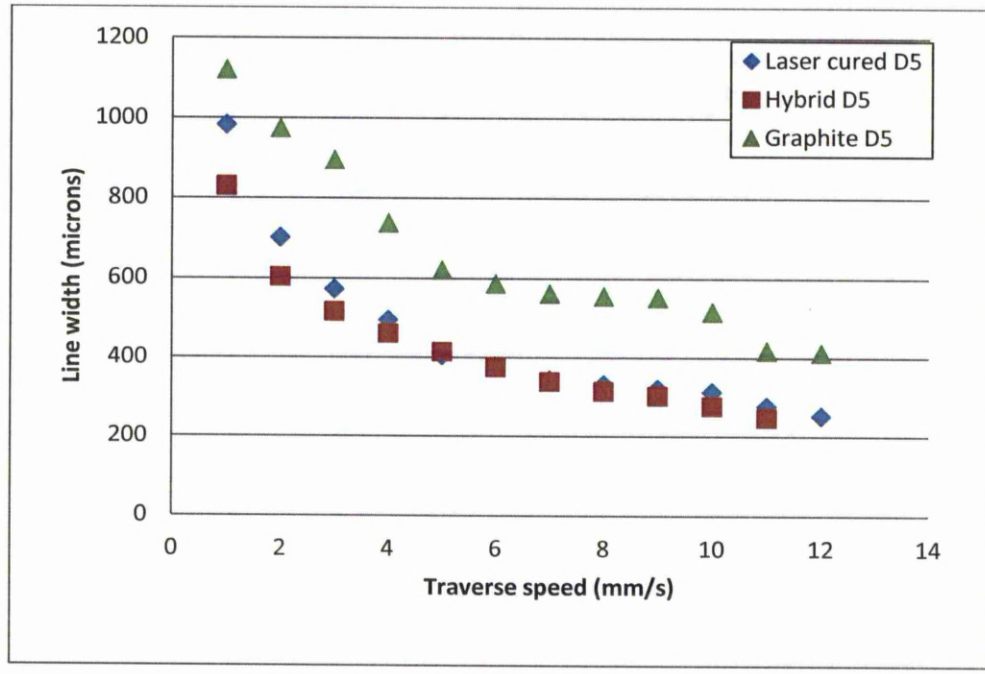

Figure 4.17: Line width of deposited inks as a function of traverse speed.

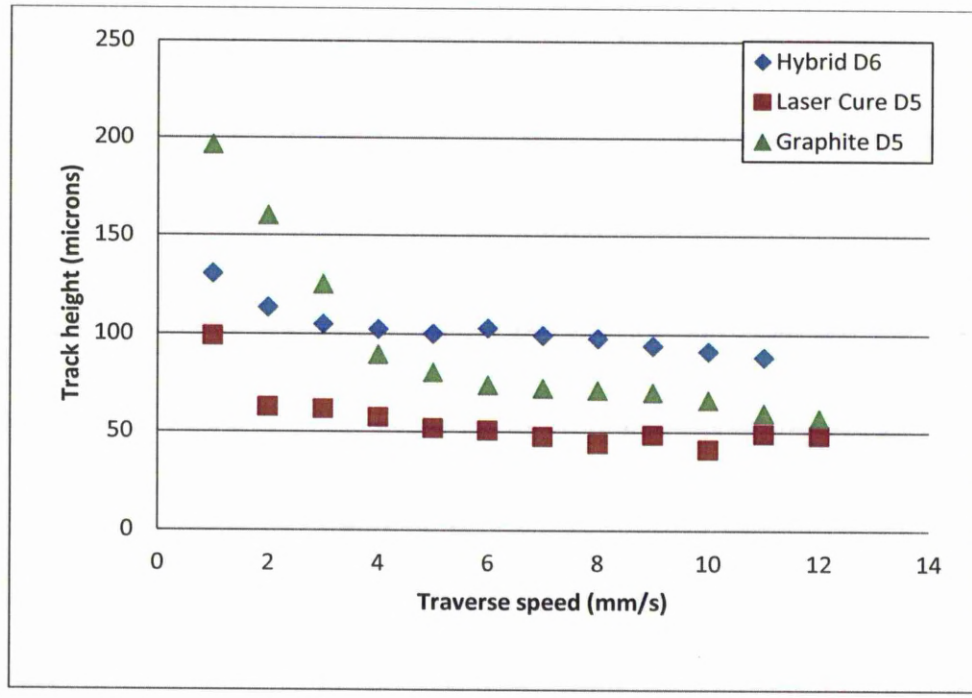

Figure 4.18: Tracks height of deposited inks as a function of traverse speed.

4.5.3 Effect of Laser Curing by Raster Scanning

Between the three inks, there were obvious differences in track morphology after curing especially for Laser Curable D5 and Graphite D5 inks where there were sign of some materials left on the substrates possibly resin represented by these two small peaks at both edges of the tracks cross-sections. This is not happening to Hybrid D6 ink where sharp edges were observed from its cross-section of tracks (Figure 4.19 - 4.21). Further investigation is needed to investigate this condition. All the inks profiles were in 'U' shape which is might not be the most ideal cross-sectional profile but it should not effect in this certain application as the surface roughness and profile shape were not the major factors affecting the resistance of the antenna.

Most of the tracks width were increased when it was cured by Nd:YAG laser and the lowest resistance achieved was around 6.4 Ω which is considered quite low. On average, the laser cured samples increase in line width by 50-60% for the wider tracks and between 70-80% for the narrow tracks. Roughness measurements of cured tracks show little change from the uncured sample. These samples after curing by raster scanning are quite soft in comparison to earlier samples created by line following. Laser cure D5 shows increased widening as a result of curing compared to the graphite doped and the hybrid. In addition there is evidence of thermally-induced substrate damage not visible on the other samples.

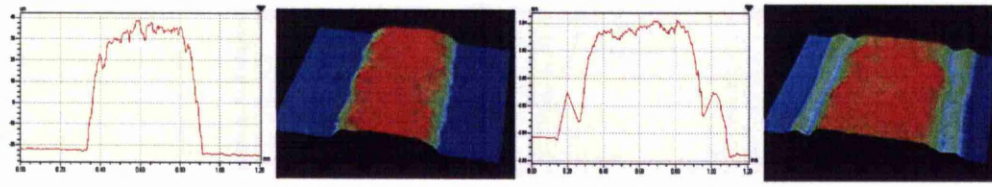

(a) (b)

Figure 4.19: 2D and 3D surface profile of laser Curable D5 (a) before curing (b) after curing

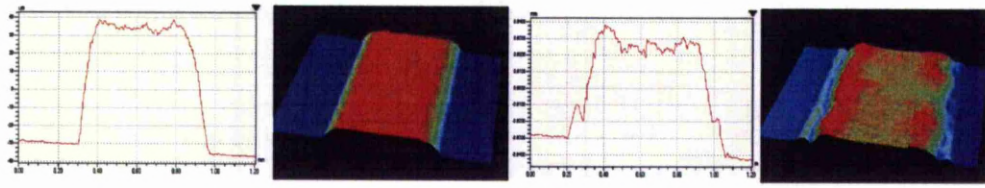

(a) (b)

Figure 4.20: 2D and 3D surface profile of Graphite D5 (a) before curing (b) after curing

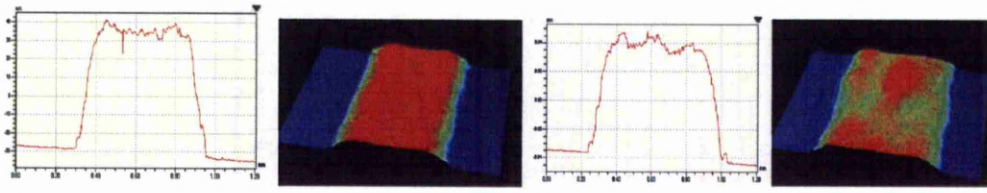

(a) (b)

Figure 4.21: 2D and 3D surface profile of Hybrid D6 (a) before curing (b) after curing

4.5.4 Electrical Properties

The antenna properties were investigated by resistance measurement before the samples were despatched to an outside company for further analysis of their frequency response and read range. The aim was to obtain as low as possible resistance or at least comparable to the etched copper antenna (reference) which the resistance was 2.2 Ω. The first few antenna samples had a relatively high value of resistance. Thus, a method was needed to be explored to reduce the resistance by half and widen the lines to 1 mm, since most of the antenna tracks were not quite 1 mm in width.

Reducing the resistance could be achieved by increasing the cross-sectional area according to the formula $R = \rho. \, l \, / \, A$. To realize this, two approaches were taken which were: (i) widening the tracks by adjusting the

syringe deposition parameters; and (ii) depositing thicker lines and curing from both sides. Two antenna samples were made with different cross-sectional area on the same substrate and cured using the same laser parameters; 18 A of laser input current with 2150 mm/min of laser scanning speed and two passes. It was found that the sample with bigger cross-sectional area result in lower resistance value (Figure 4.22). Around 4.6 Ω resistance was measured and considered quite low compared with samples that had smaller cross-sectional area; 7.3 Ω. It was evident that cross-sectional area had significant effect on resistance, as expected.

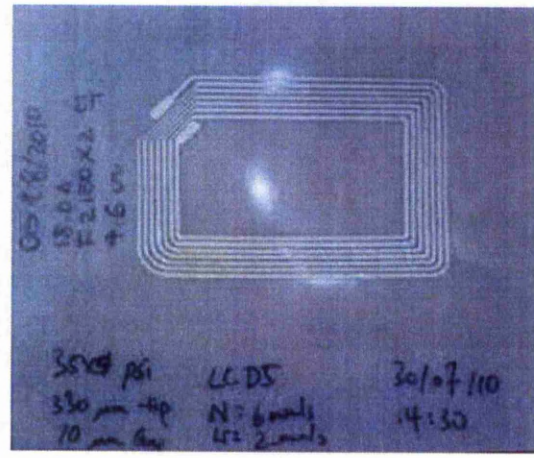

Figure 4.22: Antenna G

With the results provided, it would enable to calculate the resistivity of the tags samples. As the antenna had two different cross-sectional areas, therefore the formula of resistivity can be simultaneously applied. The following equation enables the cross-sectional area to be given in ratio with the length of wider line and narrow lines.

$$A_a = \frac{L_W}{L_{total}}(A_\Delta) + A_n \tag{4.2}$$

where A_a is the average cross-sectional area by ratio, L_w is the wider line length, L_{total} is the total length of the antenna, A_Δ is the differences in cross-sectional area between the wider line and narrow line and A_n is the cross-sectional area of the narrow line.

4.5.2 Antenna Performance Testing

The antenna design supplied by an external company was successfully manufactured on PET, using three inks identified as having high conductivity. The samples were manufactured using syringe-based DW deposition robot. The requirement for reduction in overall resistance measurement of the samples to be halved and the line widths increased has been met.

Nine antenna samples were successfully delivered to an external company for performance testing. HP8722D vector network analyser (VNA) was used to extract the scattering matrix of the line, and from these data the insertion loss was determined by a 'black-box' method that relies solely on the measured S-parameter data.

The method to thicken the tracks to reduce the resistance was successful which the achievable resistance is about 4.6 Ω but the resonant frequency was still too high. This might be due to the antenna shape design.

Only four samples were analysed due to some issues which is fragility of the bonding between the track pads and the substrate. Table 4.5 presented the tested results from the company where the row highlighted in red was the reference performance of the commercial copper etched antenna which its resistance is about 2.2 Ω.

Table 4.5: Measured antenna parameters (electrical)

Sample	Resonance Frequency (MHz)	Quality Factor, Q	Response at Resonance Frequency (dB)	Read Range (cm)
D	15.5	20	-5	23
F	15.57	22	-8	25
G	15.6	31	-5	24
I	15.5	30	-5	23
Ref.	13.5	55	-11	55

The reduced read distance was considered to be due to the resonance being 2 MHz high and the track design was calculated to have correct inductance to give resonance at 13.56 MHz. The calculation method has previously proved reasonably accurate for copper tracks on FR4. Adding an extra capacitor to the samples brought the resonance frequency into line and the performance of the new antenna was as good as a commercial antenna and this was tested on Antenna G. Table 4.6 shown the new tested result of Antenna G with extra capacitor.

Table 4.6: Average measured values of antenna parameters

Sample	SRF (MHz)	Quality Factor, Q	Response at SRF (dB)	Read Range (cm)
G	13.2	25	-5	55
Ref.	13.5	55	-11	55

4.6 Chapter Summary

The experiments discussed in this chapter have indicated that a range of silver particulate inks are laser curable using a 532 nm wavelength laser, and give resistivity values comparable or better than those available using the CO_2 laser. The 532 nm wavelength laser also improves upon the earlier work in the increased speed of cure possible and in the poor coupling of 532 nm into PET, allowing a single raster scanning method to be used independently of circuitry pattern. This method of laser cure has proved to have significant advantages in terms of successful cure of the silver inks to better effect than the CO_2 laser and at much faster rates while avoiding damage to the PET substrate.

The use of Graphite D5 for producing samples using the syringe-based DW technique is indicated by its controllability of deposition and its achievable conductivity. Laser cure D5 appears to have wet ability issues when producing thin lines and high heat input into the PET substrate which is not shared by the other two inks and Hybrid D6 has issues in controllability of deposition geometry.

The track design shape is not causing the reduced read range since it was calculated to have a correct inductance to give resonance at 13.56 MHz and it was also proven to give accurate result for copper track (etching) on FR4 substrate previously. The reduced read range might due to the cross-sectional shape of the silver track since the ink deposited by syringe deposition system normally will produce track approximating a squashed elliptical arc (plano-convex) as illustrated in Figure 4.14 whereas most commercial copper tracks are in rectangular (step) cross-sectional shape and the thickness is quite thin around 19 to 20 μm.

To investigate the effect of cross-sectional shape of the track, a simple dipole antenna will be made as depicted in Figure 5.1 in the next Chapter 5. The antenna is designed to be operated at 900 MHz frequency and several characteristics of the antenna are needed to be measured in order to characterize its performance such as resonance frequency, band width and return loss. In addition the following characteristic measurements would also

be desirable if possible; radiation efficiency, input impedance and radiation pattern.

Chapter 5

Effects of Conductor Cross-sectional Shape on Antenna Characteristics

5.1 Introduction

Traditionally, most electronics components including antennas have been fabricated from a thin metallic layer of copper or aluminium adhered to a thin insulator substrate. The metal is then etched using a photolithography process which is subtractive in that the metal is selectively removed to form the antenna circuit [45]. Such a manufacturing approach is considered wasteful since it involves the use of chemicals and production of waste material that is hazardous to the environment, even if it is recyclable. New low cost manufacturing tools must therefore be developed and introduced to fabricate these antennas which points here towards a Direct Write (DW) technique being developed.

DW is becoming popular nowadays among researchers worldwide and it is an emerging technique to fabricate electronics by engaging traditional printing medium with very low cost such as inkjet [42, 53, 72, 102, 69]. By

definition, DW is an additive technology to fabricate two or three dimensional functional structures by directly depositing material onto flat or conformal surfaces [2]. DW allows electrical conductors and components to be directly printed on almost surfaces. It mainly involves two steps: first where the material (usually in the form of an ink, slurry or paste) is dispensed or printed on a substrate; and then secondly curing of the ink (mainly by heating) to drive off solvent to leave a conductive track of compacted metallic particles. With the ability of DW that can write in any surfaces, it allows for further miniaturisation for electronic devices whereby it provides feature sizes down to less than 20 microns with a wide range of materials possibilities [3]. It is a fast process and since it was an additive process, all materials used are fully utilised. It is a cheap technique where there is no mask involves and it provides a wide variety of materials choices.

DW was firstly adopted in 1980 when metal conductors were printed for solar cells using ink jet printing technique [42, 53, 69, 72, 102]. Since then numerous applications have been seen adopting DW using diverse DW technologies such as in electronics especially flexible electronics [1], telecommunications particularly RFID tag antenna which inkjet has been used to print RFID antennas for high frequency applications [76], displays [84], optics [103], aerospace [21] and many others. On the other hand, some attempted to employ roll to roll printing technology, which is envisaged to then be suitable for mass production of printed electronics in the future.

In printed electronics, the cross-sectional shape of the antennas tracks fabricated using photolithography technique generally exhibited rectangular cross-sectional shape. Antennas with other than rectangular cross-sectional shape have not yet been systematically reported. It is significant to investigate further on the influence factor of cross-sectional shape other than traditional rectangular shape since recent works done at University of Liverpool have proven that after some improvements made on the plano-convex cross-sectional shape fabricated from syringe-based DW technique provided better read range than their conductivity and Q factor. The previously reduced read range might due to the cross-sectional shape of the ink track since the ink

deposited by syringe deposition system produces track with plano-convex shape whereas most commercial copper tracks are in rectangular (step) cross-sectional shape and the thickness is quite thin around 19-20 μm. The height of the track were increased to improve the conductivity since the basic laws of conductivity for homogeneous media states that the ohmic losses decreases as conductor cross-section increases. Thus, similar behaviour can be applied to printed ink traces even though it is not homogeneous.

5.2 Objective

This chapter aims to investigate further the influence of deposited track geometry on its resulting performance as an antenna. The plano-convex cross-sectional shape produced by syringe-based DW technique and several key process variables that resulted in variety of plano-convex cross-sectional of the track shape will be investigated. The antenna performance will be characterized and compared using simulation and direct measurement

5.3 Experimental Arrangement

5.3.1 Antenna Design

Ideally the antenna should be designed as a resonant dipole to achieve its good performance as a RF transmitter/receiver device and this requires the dipole physical length to be slightly shorter than a free space half a wavelength long. According to Zingg [104], it is about 0.47 times the wavelength. Thus, the length of the resonant dipole is calculated using equation 1 below,

$$Dipole\ length = 0.47\ x\ \lambda\ = 0.47\ x\ \frac{v}{f} \qquad (5.1)$$

where v is the actual propagation speed on the dipole length. This speed depends on the effective dielectric constant of the medium surrounding the

dipole and the speed with which electromagnetic waves propagate through a dielectric medium is always less than the velocity with which they propagate through a vacuum. Thus the actual propagation speed, v could be calculated using equation 5.2 below,

$$v = \frac{c}{\sqrt{\varepsilon_{eff}}} \tag{5.2}$$

where c is the speed of light in vacuum and ε_{eff} is the effective dielectric constant of the surrounding medium. Since the effective dielectric constant for a dipole printed on a substrate depends on the geometry and the dielectric constant of the substrate, the effective dielectric constant is calculated using equation 5.3 [104] below,

$$\varepsilon_{eff} = \left(\frac{\varepsilon_r+1}{2} + \frac{\varepsilon_r-1}{2}\right) x \left[\left(1 + \frac{12xh}{w}\right)^{-\frac{1}{2}} + 0.04\, x \left(1 - \frac{w}{h}\right)^2\right] \tag{5.3}$$

where ε_r the relative dielectric constant of the substrate used, h is the thickness of the substrate and w the width of the track.

A half-wave dipole antenna is selected as a benchmark due to its simplicity and this was designed for a nominal resonant frequency of 900 MHz. The appropriate dipole length was calculated using equations mentioned before and the geometry which describes the dimensions of the antenna is shown in Figure 5.1.

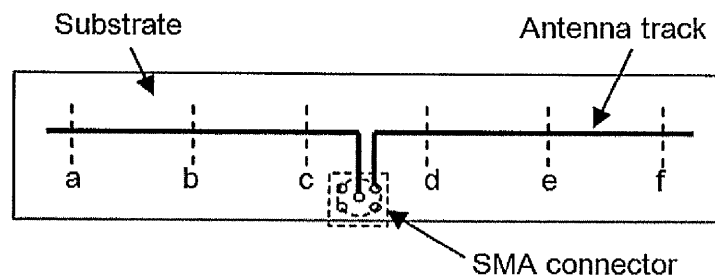

Figure 5.1: Geometry of a half-wave dipole antenna. Symbols a, b, c, d, e, f represented the six points where the track profiles were measured

5.3.2 Simulation

A number of simulations were performed to optimize the dipole length using the commercially available software tool; Ansoft HFSS (High Frequency Structure Simulator). This is an interactive software package for calculating the electromagnetic behaviour of a structure and uses the Finite Element Method (FEM) to compute solutions. It allows for the computation of the basic electromagnetic field quantities, S-parameters, and resonance of a structure. The reflection coefficient/return loss (S_{11}) of the antenna was measured for normally incident plane-wave excitation. The antennas were modelled as a plano-convex cross-sectional shape to determine their appropriate dipole length to achieve a resonance dipole. At the same time, the antenna performance was also characterized.

5.3.3 Fabrication of Antenna

Several samples, comprising of traditional rectangular cross-sectional shapes to replicate the etching process and plano-convex shapes from the syringe-based DW technique, were developed and fabricated to validate the results from simulations. The traditional rectangular shapes samples were fabricated using a doctor blade technique in which the inks were carefully laid out on a piece of steel plate with thickness approximately 30 μm. The steel plate had been previously cut into a designated pattern to develop the track pattern as shown in Figure 5.2. At first, substrates were cleaned using 2-butoxyethanol with a lint free cloth and then subsequently air dried. The interface between the deposited ink and the substrate must be free of foreign bodies so that any thermal transition is consistent along the length of the deposited line and no localised absorption occurs. Once dried, a modelling tape was applied to the surface. The modelling tape was specifically chosen for its adhesive properties, in that it was specially formulated to have low tack and not leave a residue upon the surface when removed. A metallic stencil was then placed over the tape with an internal portion, with various designated

dimensions ranges. A central portion of the tape was removed using scalpel, exposing the substrate below. A polymeric silver paste was then applied to the substrate through the tape stencil using a spatula producing a thin film track of a depth determined by the tape thickness, in this case about 60 microns [21]. This method provided a technique for consistently producing tracks of a certain volume with repeatable results. This was considered crucial to the reliability of the results obtained. The films were then processed by curing in a pre-heated oven.

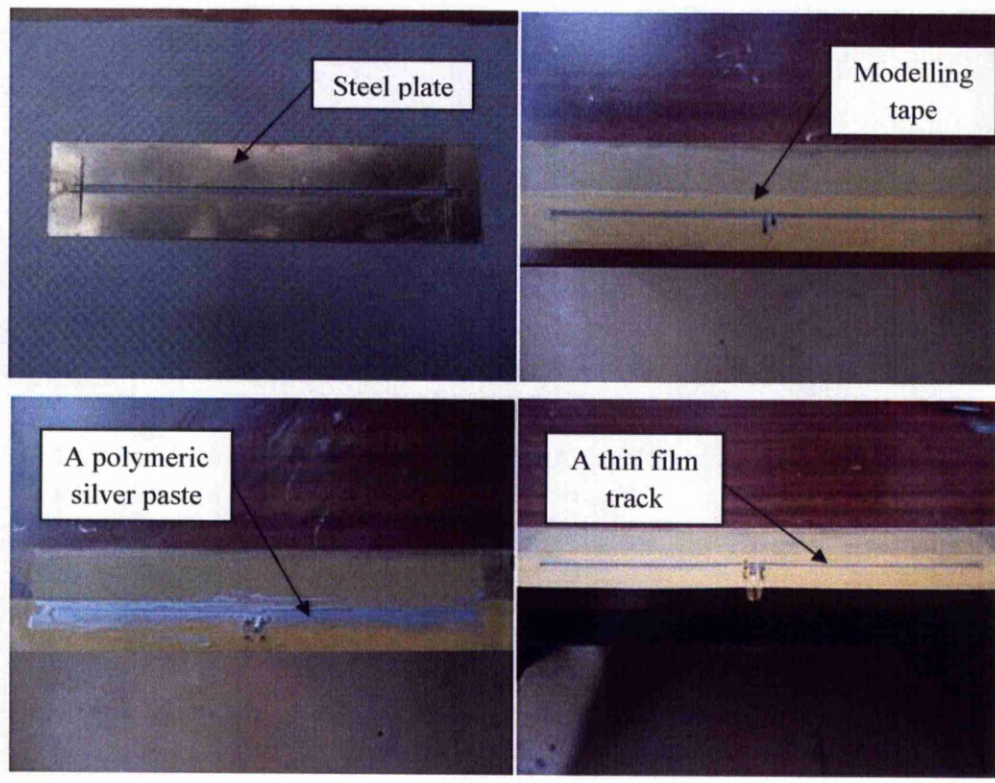

Figure 5.2: Doctor blade technique

In the mean time, plano-convex cross-sectional shaped samples, were fabricated using the syringe-based DW deposition system. There are numerous existing DW technologies such as screen printing [33, 105], ink jet [42, 53, 69, 72, 102], gravure printing [93-95], flexography and offset printing that can be employed for antenna manufacturing. Since the plano-convex shape can only

be realized using syringe-based DW technique thus this chapter will only focus on syringe-based DW deposition technique. The fabrication process started by cleaning the substrates using 2-butoxyethanol with a lint free cloth and then subsequently air dried. Once dried, SMA connecter was inserted by drilling four holes so that its legs were properly placed at its appropriate area. The substrates then were placed on the CNC worktable to prepare for the deposition process as depicted in Figure 5.3. The deposition process was then started according to the program set. The description of syringe-based DW deposition technique used has been described previously in Chapter 3. The films were then processed by curing in a pre-heated oven.

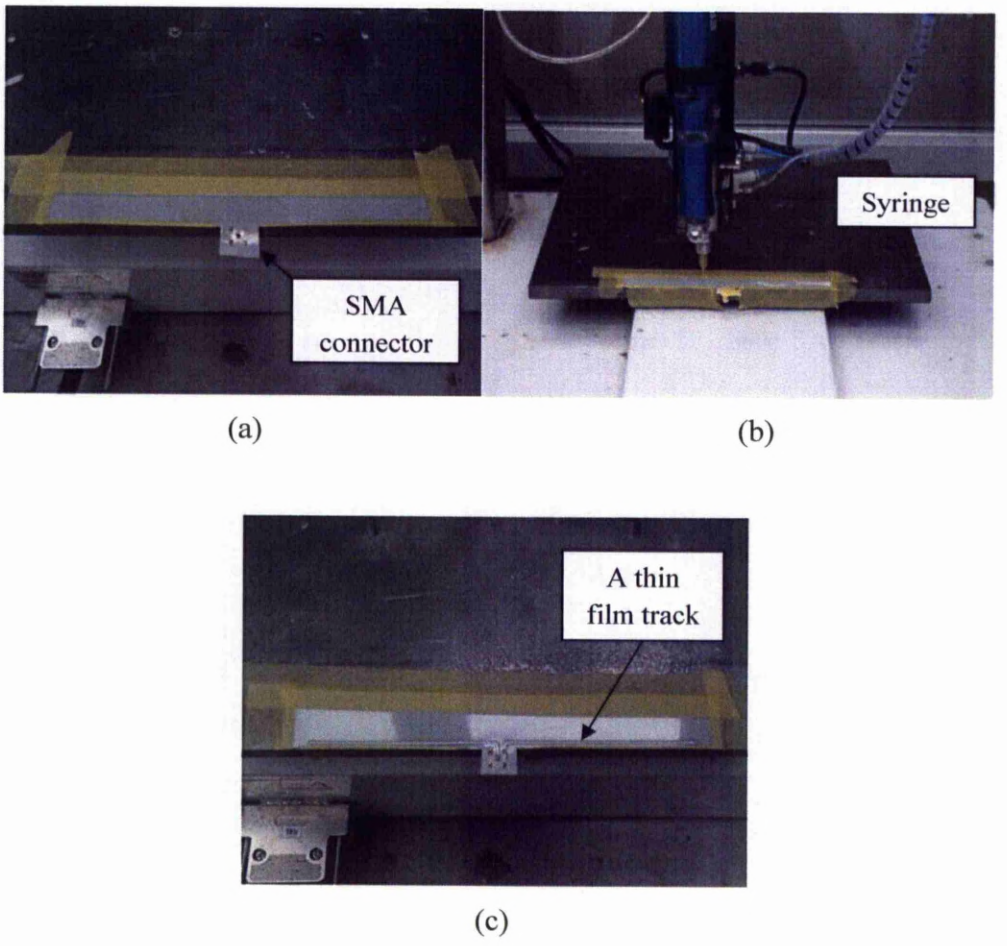

(a) (b)

(c)

Figure 5.3: Antenna samples fabricated by the syringe-DW deposition process (a) substrate placed on the CNC worktable ready for deposition process (b) deposition process in action (c) finished antenna sample

5.3.4 Material, Substrate and Methods

Silver based ink was used, due to this being inexpensive compared to copper and printable in an affordable way on thin substrates. It is also the preferred choice since copper fabrication requires slow electrodeposition followed by wasteful etching. Copper ink also suffers from oxidation, making interconnects troublesome. High temperatures are needed to anneal copper precursor inks, which their toxicity and resulting conductivity are much less than bulk. Silver is used in a vast number of printed products today ranging from UHF antennas (approaching billions of RFID tags yearly) membrane keyboards, battery testers on batteries and other printed electronics and electrics.

The silver inks used here consisted of 20 μm silver flakes particles dispersed in benzyl alcohol (Gwent Electronics Materials Ltd.). Polyethylene terephthalate (PET) film of 0.35 μm thickness was used as the substrate for the direct-write deposition process. After printing the silver inks, all antennas were thermally-treated in a pre-heated oven at 135°C for 30 minutes. The main characteristics of the inks used are tabulated in Table 5.1.

Table 5.1: Characteristics of the silver ink

Solid Content (%)	Viscosity (Pa-s)	Sheet Resistivity at 25 μm (mΩ/square)
64.55-65.5	22-27	25 - 35

The experimental design was carried out by comparing both cross-sectional shapes; rectangular and plano-convex, in terms of their performance characteristics. Several process steps were taken to meet the aim of this research, which were:

1) Determine an appropriate dipole length, such that the antenna would resonate at a designated frequency for both cross-sectional shapes
2) Simulate the performance of both antenna cross-sectional shapes using the appropriate simulation package
3) Measure the input resistances of various plano-convex dipole samples with a network analyzer and compare them with rectangular cross-sectional dipole samples
4) Measure and compare the performance of impedance matched plano-convex dipoles samples with rectangular dipoles samples.

5.4 Antenna Performance Testing

5.4.1 Return Loss, S_{11}

The reflection coefficient/return loss was measured using a Vector Network Analyzer (VNA); the front control panel of which is shown in Figure 5.4. The VNA measures both the magnitude and phase angles of the reflection and transmission coefficients. The ratio of the magnitudes and phase angles of the response and excitation signals with respect to a reference plane is accurately measured and displayed. The antenna under test (AUT) was connected to the analyzer by a coaxial cable (Port 1) of the S-parameter test set and was placed in front of the analyzer in a distance about 1 meter length as depicted in Figure 5.5. All of the antenna samples were positioned in the same way during the measurement process. The detected signal was processed and fed to the display unit for output. The measured S_{11} data in the VNA is acquired and stored in ASCII format in the interface computer.

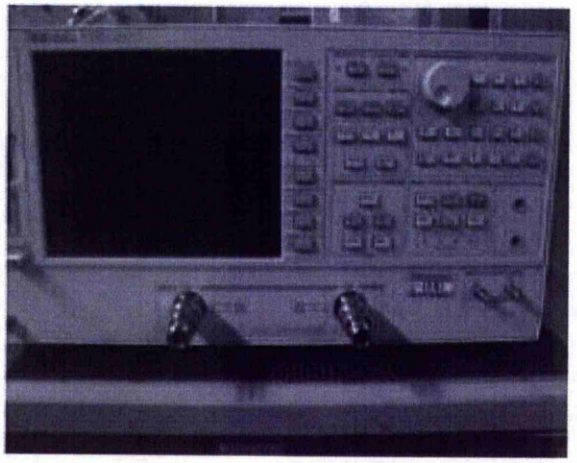

Figure 5.4: Vector Network Analyzer (Hewlett Packard Model: 8753E 30 MHz – 3 GHz)

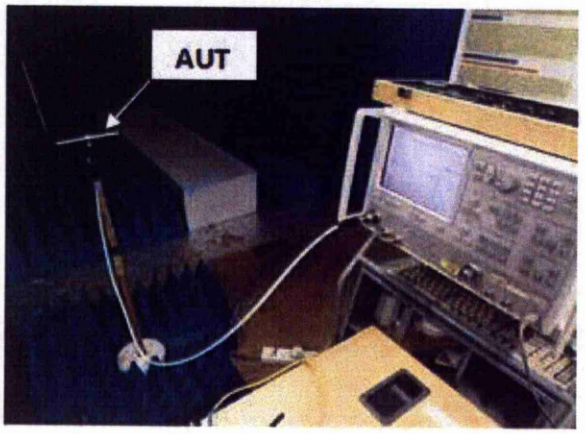

Figure 5.5: Photograph showing position of the AUT in front of the analyzer during return loss tests

5.4 Results and Discussion

5.4.1 Effect of deposition parameters

There were two key parameters to be considered when dispensing the ink using the syringe-based DW technique; that being the width and height

variations of the ink track. The cross-sectional area of the track is changed due to these variations, resulting in the deviations of antenna performances such as gain, radiation efficiency and read range. The feature size of the track depends on various factors such as printing speed, applied pressure, tip size, stand-off distance, substrate material, rheology and etc. There were fourteen samples fabricated using syringe-based DW in which the inks were dispensed at a constant pressure of 80 psi with a 330 diameter μm tip and a 50 μm stand-off distance. The printing speed was varied from 3 to 8 mm/s.

The results of varying width and height of the ink track produced are illustrated in Table 5.2. It can be observed that as the printing speed increased, the width of the tracks decreased in a linear fashion, as illustrated in Figure 5.6. This is because, when higher speeds were used the inks did not have time to spread resulting in less material being dispensed and a reduced volume of ink deposited. The inks were stretched as the printing speed increased causing the tracks to decrease in their width and height. Only slight changes in height were observed. It was also noticed that the resulting reduction in track width was more significant compared with the height. This result was thought to be due to the fact that the gap between the tip and the substrate was set quite close (50 μm) and the ink dispensed was spread away more to the side rather than sticking on its deposited position. More ink was distributed to the side when the speed was low (e.g at 3 mm/s) and this reduced as the speed increased to 7 mm/s. At some point between 7 and 9 mm/s, there were very little changes in track width and so presumably there would be no further change in track width if higher speeds had been used.

5.4.4 Antenna Performances

5.4.4.1 Effect of width and height variation

Several samples from Table 5.2 were grouped together according to their width and height variation in order to investigate the effect of different width and height of antenna track to antenna performance (Table 5.3 and 5.4). The result of S_{11} parameters plot for both investigations was depicted in Figure 5.16 and 5.17. It was found that increasing the width will result in a better return loss which fewer signals are reflected back to the analyzer thus could improve the antenna performance. A similar result was obtained for different height variations; whereby increasing the height resulted in better return loss. From this, it could be seen that increasing both the width and thickness could improve the antenna performance, with reduced reflection of signal back to the analyzer.

Table 5.3: Characteristics of the measured samples (width variation)

Sample	Length (mm)	Width (mm)	Height (mm)	Conductivity (S/m)
S2	71.4	1.018	0.158	714805.3
S3	71.4	1.314	0.155	415768.0
S4	71.4	1.419	0.158	285124.7

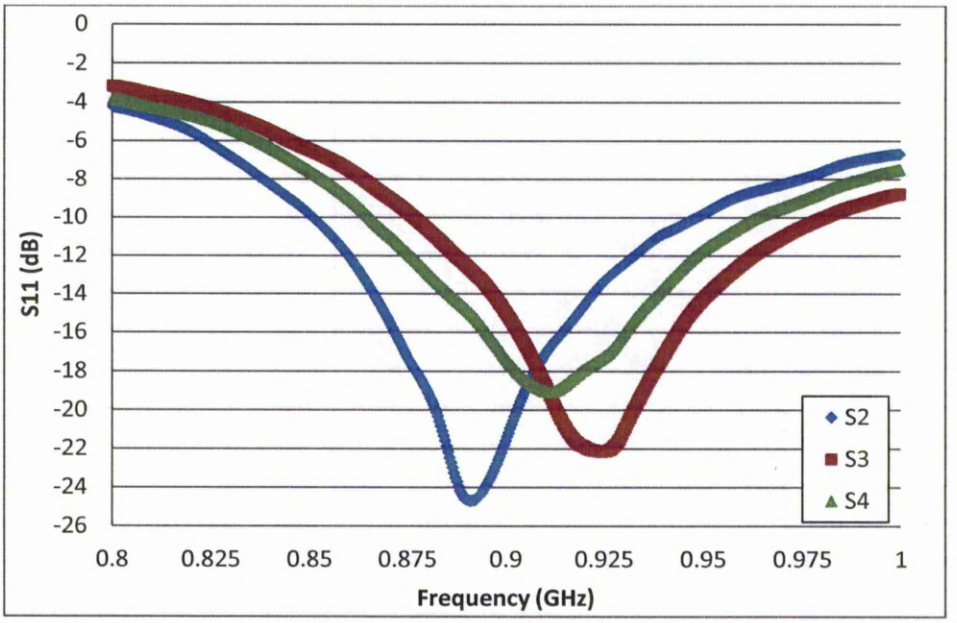

Figure 5.16: S_{11} parameters plot for measured samples (width variation)

Table 5.4: Characteristics of the measured samples (height variation)

Sample	Length (mm)	Width (mm)	Height (mm)	Conductivity (S/m)
S6	71.4	1.552	0.148	480681.5
S7	71.4	1.552	0.156	390951.6
S9	71.4	1.516	0.250	105771.4

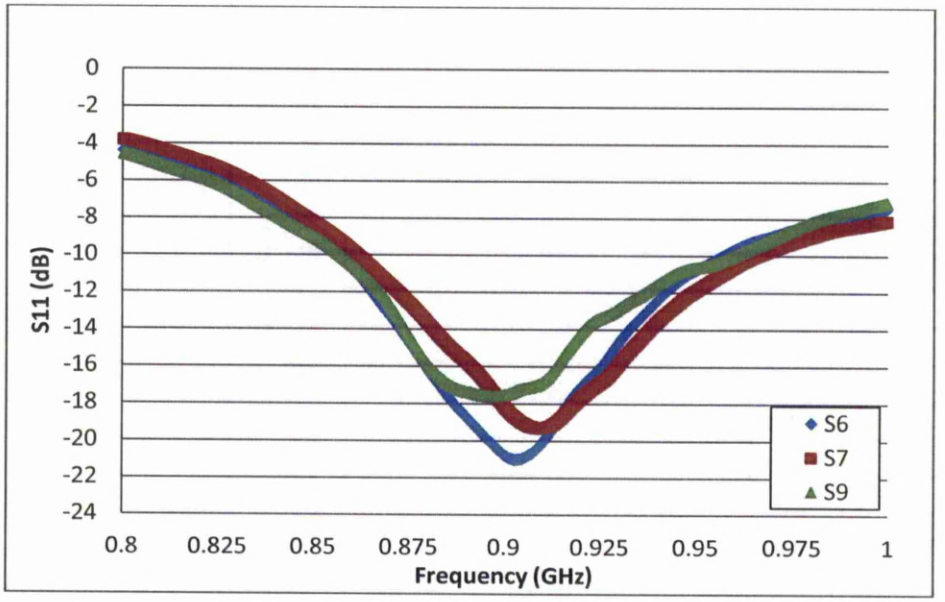

Figure 5.17: S_{11} parameters plot for measured samples (height variation)

However these results were not taking into account the slight difference in conductivity for samples compared. The slight difference in conductivity is due to the fact that the curing parameters used were constant for all samples but the volume for each sample is different from one another. The energy to fully cure each sample would therefore be different depending on the volume of the material needed to be cured off, provided that all other curing parameters remained constant.

To validate the effect of width and height variation, several simulations were performed where the conductivity value now were set to be constant through the whole simulation process (Table 5.5 and 5.6). The variation of widths and heights were also set according to the aim targeted in which for the evaluation of width variation, the heights were set to be constant and vice versa. The results are illustrated in Figure 5.18 and 5.19. From the Figure 5.18, it was observed that using conductor track height more than one penetration depth yields significant improvement to the electrical performance of the tag. In addition, the height of the conducting track also affects the input impedance of the tag antenna which indicated by the shift in resonant

frequency as the height of the track was thicker. Hence, this must be considered in tag antenna design in order to tune the antenna to the right frequency and to achieve sufficient performance. Besides, increasing the width of the track could also improve the antenna performance as retun loss was smaller (less signal were reflected back to the analyzer) according to the result shown in Figure 5.19.

Table 5.5: Characteristics of the simulated tracks (height variation)

Sample	Length (mm)	Width (mm)	Height (mm)	Conductivity (S/m)
S1	71.4	1.552	0.160	481000
S2	71.4	1.552	0.170	481000
S3	71.4	1.552	0.190	481000
S4	71.4	1.552	0.210	481000

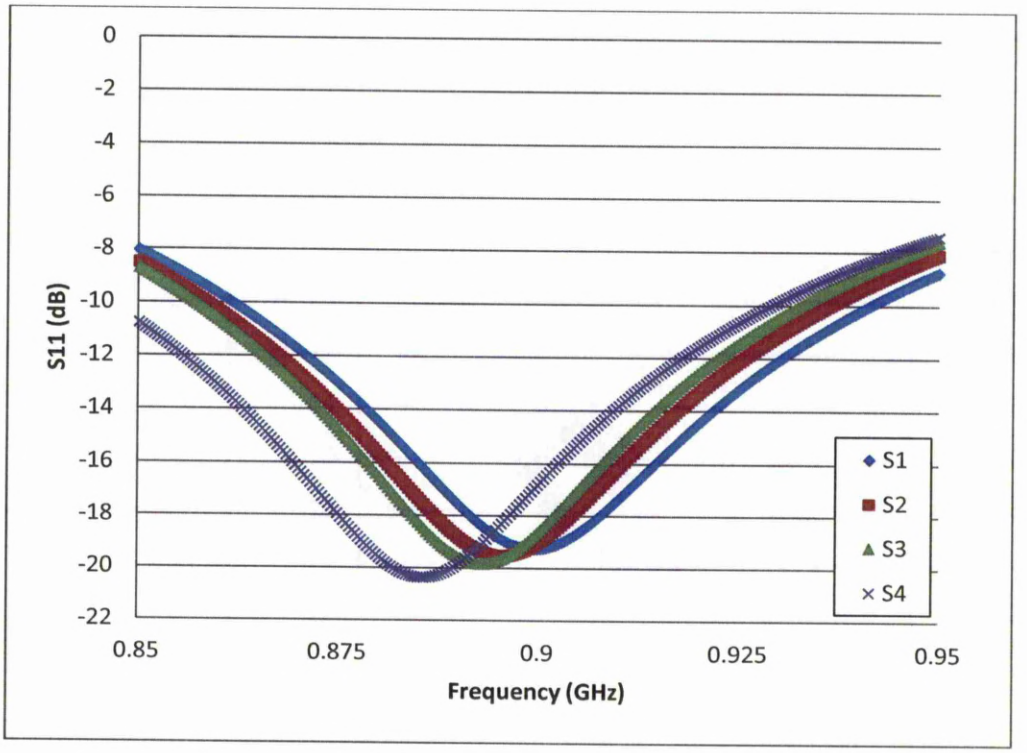

Figure 5.18: Simulated S_{11} parameters plot for height variation

Table 5.6: Characteristics of the simulated tracks (width variation)

Sample	Length (mm)	Width (mm)	Height (mm)	Conductivity (S/m)
S1	71.4	1.552	0.160	481000
S2	71.4	1.552	0.170	481000
S3	71.4	1.552	0.190	481000
S4	71.4	1.552	0.210	481000

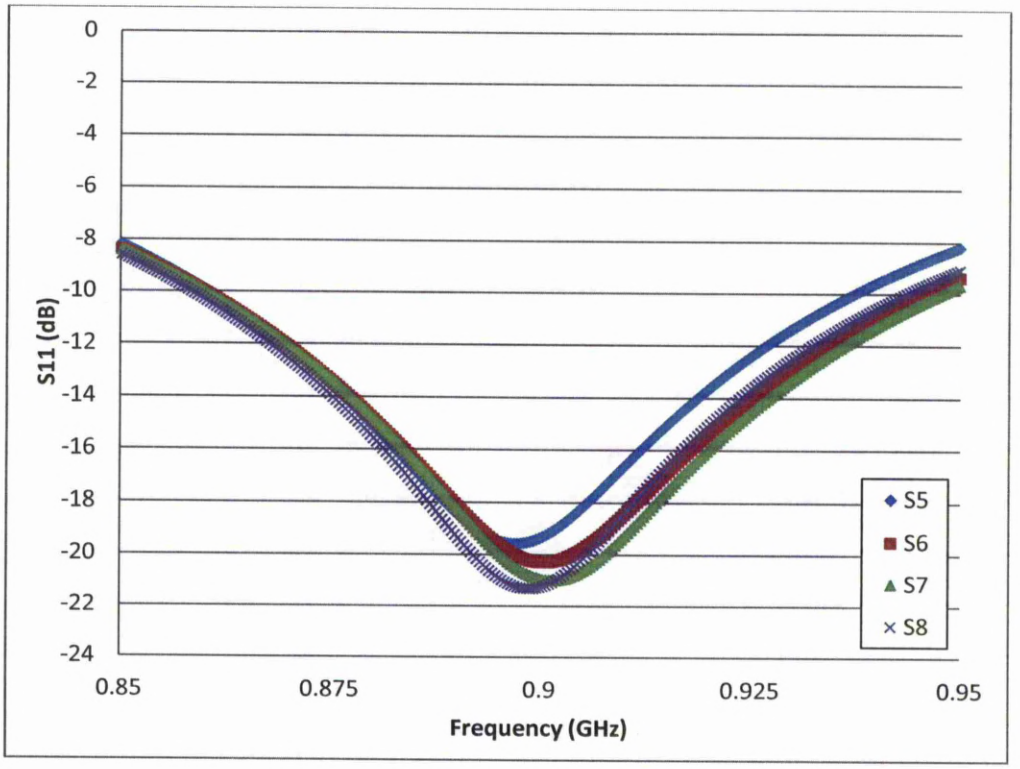

Figure 5.19: Simulated S_{11} parameters plot for width variation

5.4.4.2 Effect of cross-sectional shape

Since the results showed before had validated the effects of height and width variation to the antenna electrical performance, comparison between

several samples were made to assess the effect of the cross-sectional shape to the characteristics of the antenna electrical performance. The characteristics of samples that are being compared is tabulated in Table 5.7 and the schematic illustration of the antenna cross-sectional shape compared is depicted in Figure 5.20. From the comparison of the electrical performance, it was found that the difference in cross-sectional shape of these antenna samples changed the characteristics of the electrical antenna performance. As both the height and width of the track getting thicker and wider (Figure 5.21), it will result in smaller return loss which could improve the antenna electrical performance as higher power being absorbed by the antenna and fewer signals is reflected back to the analyzer. It was also noticed that the conductivity differences play a significant role in changing the antenna electrical characteristics.

Table 5.7: Characteristics of the compared samples taken from Table 5.2

Sample	Dipole Length		Measurement						Dispensing Parameters	
			Average							
	Calculation (mm)	Simulation (mm)	Width (mm)	Height (mm)	Dipole Length (mm)	Area (mm^2)	Volume (mm^3)	Conductivity (S/m)	Speed (mm/s)	Pressure (psi)
S14	114.8	71.4	0.990	0.135	71.4	0.105	7.489	1038864.689	4	40
S1	121.3	71.4	0.939	0.143	71.4	0.106	7.545	906304.7599	9	80
S12	98.8	71.4	1.330	0.081	71.4	0.085	6.044	170928.3667	4	60
S10	89.7	71.4	1.516	0.250	71.4	0.298	21.285	105771.4587	4	80

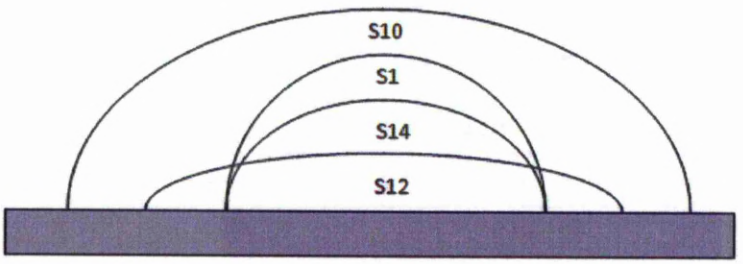

Figure 5.20: Schematic illustration of the antenna samples compared

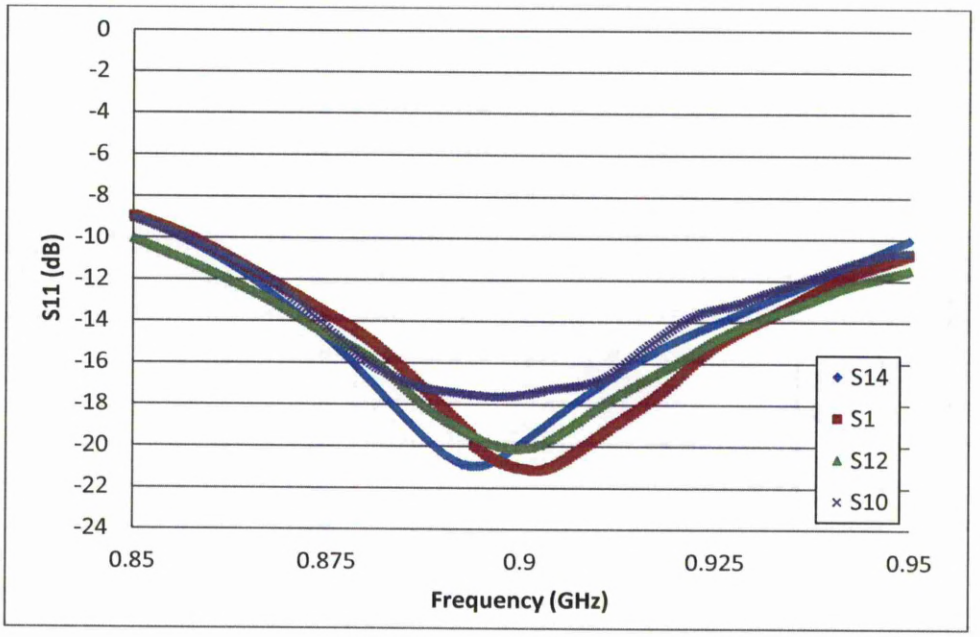

Figure 5.21: S_{11} parameters plot for measured samples (effect of the cross-sectional shape)

Since dispensing using syringe-based DW technology always resulting in variation of these two key parameters; width and height variations, controlling those two parameters are significant in modifying the electrical performance of antenna design.

In addition, sample 5 and 11 from Table 5.2 were selected and compared with its rectangular counterpart in order to investigate the influence of the plano-convex cross-sectional shape to the traditional rectangular cross-sectional shape. Their geometrical characteristic could be found in Table 5.2. They were compared by its rectangular counterpart from simulation since it was proven before that the rectangular cross-sectional shape from simulation can be used to imitate the measured ones. The reason why the comparison were made using the simulation not the measurement because of it was realised during development at the experiments that a number of highly uniform square could not be fabricated in practice for comparing to their model equivalent. Only a few of uniform square samples were successfully made by the proposed technique mentioned earlier. However, the true plano-convex shape could both

fabricated and modelled. Thus, a rectangular shape from simulation was used as a reference. The antenna performances were characterized accordingly by measuring their S_{11} parameters against the operating frequency and the results were shown in Figure 5.22 and 5.23.

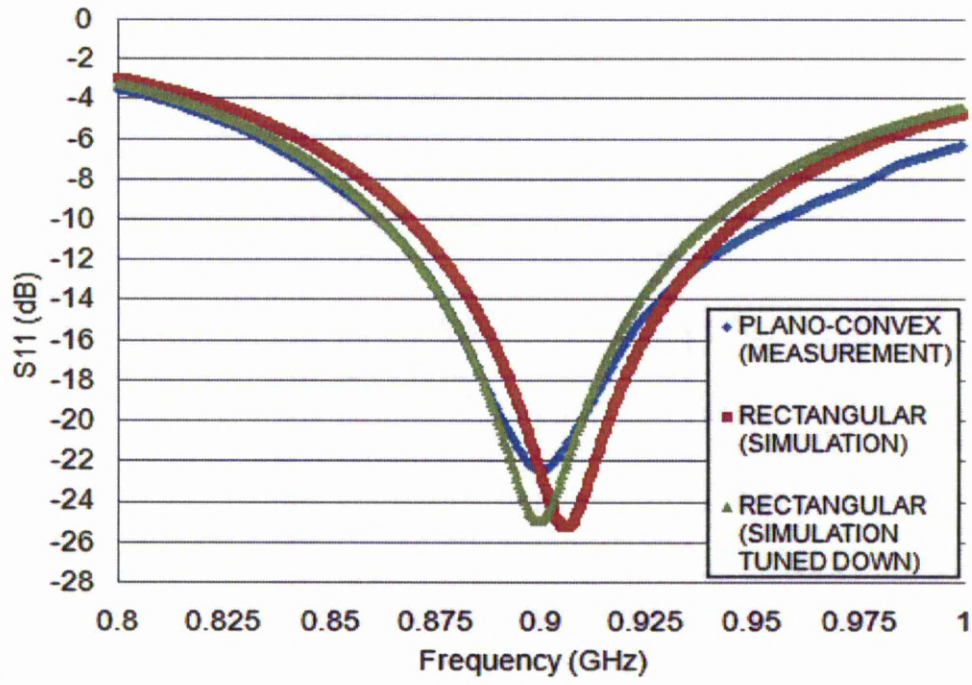

Figure 5.22: Comparison of return loss between measurement and simulation for sample 5

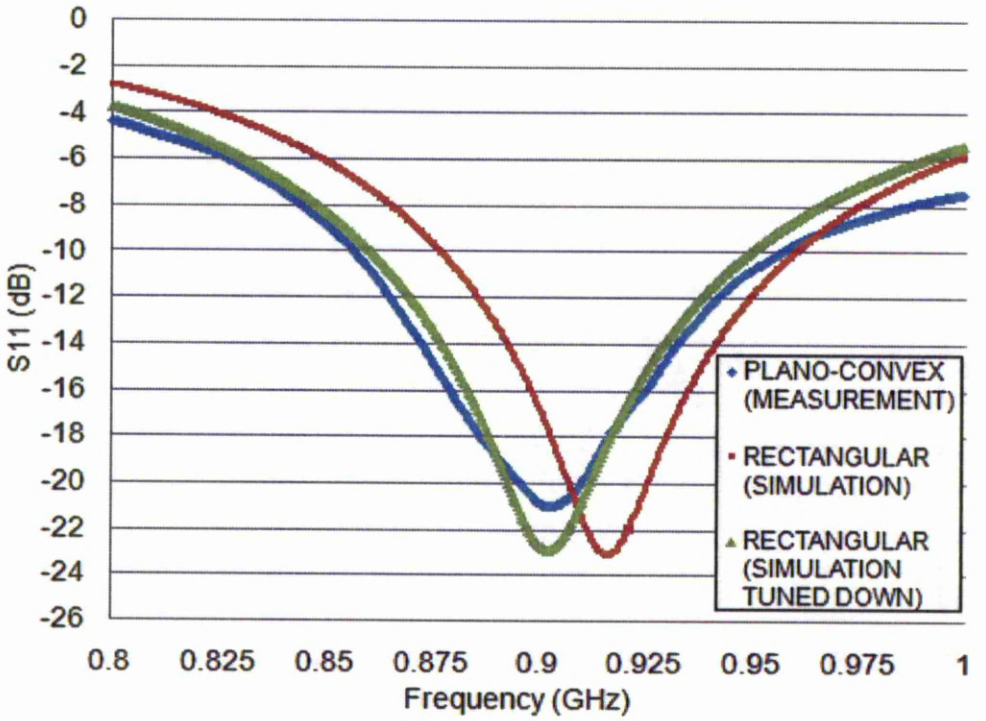

Figure 5.23: Comparison of return loss between measurement and simulation for sample 11

Referring to Figure 5.20 and 5.21, it was found that the resonant frequencies (the position of the inverted peak) were slightly shifted to the right (higher frequency) which is approximately at 906 MHz (sample 5) and 918 MHz (sample 11) as expected since the reference samples (rectangular shape) had a higher volume. In order to properly compare the performance, the reference samples needed to be tuned down in order to resonate at 900 MHz as depicted in Figure 5.20 and 5.21. This led to additional length of dipoles from previously 71.4 mm to approximately 72.1 mm for both cases. It means that in order for plano-convex shape to get the equal performance (resonant) with the rectangular cross-sectional track shape, its dipoles length needs to be shorten resulting in a less material being used. It is very beneficial to the antenna manufacturing industry since it will dramatically reduce the cost where the cost is always a major concern and at the same time increase the throughput. The

difference between the resultant reflections coefficient/return loss were not very significant as little as 1-2% signal power being transmitted back.

In addition, the bandwidth can be directly obtained from the S_{11} data by noting the range of frequencies (Δf_r) over which the reflection coefficient is less than equal to -10 dB. The resultant bandwidths for both samples (samples 5 and 11) were slightly wider than the reference samples within the range of 16-17 MHz. This is another advantageous where wider bandwith of antenna gives a wider reception hence more information could be gathered from the antenna respectively.

5.5 Chapter Summary

This chapter has described work carried out to investigate the influence of the cross-sectional shape of antenna track on antenna performance. From the investigation, it was found that increasing the width and height of the cross-sectional track could improve the antenna electrical performance by reducing the retun loss exhibited when driving the antenna from a signal source.

In addition, in order for plano-convex shape to get the equal performance (resonant) with the rectangular cross-sectional track shape, its dipoles length needs to be shorten resulting in a less material being used. This finding is very favourable to the antenna manufacturing industry as it will drastically reduce the consumption of material thus reduce the production cost where the cost is always a major distress and at the same time increase the throughput. In addition, the resultants bandwidth of the plano-convex cross-sectional shape is wider than the rectangular shape which is desirable and gives a huge potential for the generation of wider band of antenna.

This chapter also aimed to determine if the antennas could be successfully manufactured using the direct-write process. The antenna performance was tested and results showed the predicted performance for simulated antenna did not markedly differ from silver antennas fabricated by

direct-write. In some instances especially the band width, the performance of syringe based DW printed antennas is better than the simulated one.

The results provide evidence that it is possible to direct-write functional antennas. These printed antennas show comparable performance to simulated one. It follows that these direct-write techniques represent a rapid prototyping route to RFID antenna designs that is simple, straightforward, timely, and cost-effective.

Chapter 6

Conclusions and Recommendations

6.1 Summary of Findings of the Investigation

The electronics industry is experiencing a transformation in which new manufacturing and their process materials are more important than ever before. It is imperative to reduce the cost of the entire electronics system and to use environmental friendly production methods to manufacture electronics. Syringe-based DW technology is an interesting method for manufacturing future electronic devices with a wide range of material and substrates.

In this research, silver flakes polymer inks and flexible substrate were explored and the requirements of their use in syringe deposition process were discussed. Functional materials can be implemented in syringe-based DW technology if their limitations are thoroughly understood in the syringe deposition process. In this thesis, the application specific electrical requirements, the properties of functional inks, the structure of the designed

electronic components, and the process variants were defined which likely to affect syringe-based DW technology in general.

The conductive material (inks) plays a very major role in achieving adequate antenna performance. The conductivity of the printed tracks affects the impedance of the antenna, the ohmic losses and the impedance matching. The ink composition is a critical factor in the electrical conductivity of the conductive polymer silver inks.

The morphology of the printed films is another factor altering the antenna performance. Using conductor track height more than one penetration depth yields significant improvement to the electrical performance of the antenna, but reducing the track height with little effect on ohmic losses (skin effect) can be favourable trade-off to improve cost effectiveness through savings in materials. However, the height of the conducting track also affects the input impedance of the tag antenna and this must be considered in tag antenna design in order to tune the antenna to the right frequency and to achieve sufficient performance.

Some of the tracks printed were irregular and in addition to the ink composition, both substrate material and the deposition process influence the track morphology. Height variation occurred even if the substrate material is smooth, thus increase ohmic losses. For very thin conductor track layers, possible non-uniform distribution of the conducting material also detunes the antenna significantly when the irregularities occur in a high current density region. Print quality, therefore needs special attention when RFID tags antenna are printed using very thin conducting layers.

Curing conditions also have an effect on the antenna performance significantly as optimum curing parameters are essential depending on the volume of the track deposited. Determination of fully cured condition is critical to exhibit very low ohmic losses in order to achieve desired conductivity hence improving the electrical performance of the antenna.

6.2 Contribution to New Knowledge

The main original contributions delivered by this research are listed as follows:

1. Materials in DW and to be used with syringe-based DW technology are still in their development phase and need to be further developed. Manufacture by hybrid manufacturing technique helps to overcome many current obstacles in materials, electrical performance, production speed and reliability and offers significant cost reductions in high-volume production. In this thesis, syringe-based DW technology was used together with laser and oven curing process to enable hybrid electronic manufacturing technique. The advantages of syringe-based DW technology are plentiful including elimination of photolithography and etching steps, vacuum processing, masks, and material waste during manufacturing process, overall reduction of process and product costs and provided adequate throughput especially for small batch production.

2. New and exciting opportunities were provided by the use of syringe-based DW technology and novel materials for antenna manufacturing. Controlling the deposition parameters which resulting a variety of cross-sectional shape of the conductor track affecting the electrical antenna performance characteristics hence open up new prospects especially for application in higher frequency range e. g. GHz and low-cost antenna manufacturing. Printing on challenging surfaces (curve and doubly-curve) could also be realized hence promoting the development of new ways of integrating antenna into other structures such as packaging and on curvy products.

3. Through careful design and the use of electrically conductive polymer silver inks, it is possible to achieve levels of performance that are comparable with traditional etched copper circuit implementations. The use of direct write process and conductive polymer silver inks is also an alternative for use in RFID tag antenna fabrication.

6.3 Recommendations for Further Investigation

Further work is required to improve the RFID tag using the silver conductive polymer inks and also to evolve other novel applications especially in higher frequency applications. Research should seek to fabricate passive circuit elements, e.g. inductors, capacitors and resistors on a large area and mechanically flexible substrates. The application should also be tested in real situations.

Future work on this topic should consider also the role of the application enablers in the technology management cycle and their potential for transferring knowledge to the electronic industry. They are considered the main adopters of syringe-based DW technology and promoters of commercialization, because they provide the actual functional end products.

Technologically, syringe-based DW technology devices should also meet the requirements of conventional electronic manufacturing environment, if they are to be used as complimentary tools in electronic production.

Furthermore, smaller needle tips should be used for the deposition of finer structures with better uniformity, and syringe-based DW technology deposition parameters should be carefully adjusted for high quality starts and ends of circles and dots.

Besides, printing on non-planar surfaces (curve and doubly-curve) could also be accomplished to encourage the progress of alternative ways of incorporating antenna into packaging and products.

Some considerable improvements in terms of track resolution are required in the future since the system (syringe-based DW technology) has the drawbacks of low throughput and limited resolution in below micro-scale for high-end applications.

References

[1] Peng, W., Hurskainen, V., Hashizume, K., Dunford, S., Quander, S., Vatanparast, R., 2005, Flexible Circuit Creation with Nano Metal Particles, Proceedings of 55th. Electronic Components and Technology Conference, 1 : 77-82

[2] Pique, A., Chrisey B. D., 2002, Direct-Write Technologies for Rapid Prototyping Applications, Sensors, Electronics, and Integrated Power Sources, Academic Press

[3] nScrypt, Inc., www.nscryptinc.com, 2006

[4] Wang, Y., Bokor, J., Lee, A., 2004, Maskless Lithography Using Drop-On-Demand Inkjet Printing Method, Edited by R. Scott Mackay, Proceedings of SPIE - The International Society for Optical Engineering (Emerging Lithographic Technologies VIII), 5374 : 628-636

[5] Li, B., Church, K. H., Clark, P. A., 2007, Robust direct-write dispensing tool and solutions for micro/meso-scale manufacturing and packaging, Proceedings of the 2007 International Manufacturing Science And Engineering Conference, 715-721

[6] Li, B., Church, K. H., Clark, P. A., Roy, T. D., Smith, C. M., 2007, A Robust true direct print technology for tissue engineering, Proceedings

of the 2007 International Manufacturing Science And Engineering Conference, 103-108

[7] Li, X., Li, H., Chen, Y., Zeng, X., 2004, Silver conductor fabrication by laser direct writing on Al2O3 substrate, Applied Physics A, 79 : 1861–1864

[8] Teng, K., Vest, R., 1987, Characterization of inks and ink application for ink-jet printing: model and simulation, IEEE Transactions On Components Hybrids And Manufacturing Technology

[9] Lewis, J. A., Gratson, G. M., 2004, Direct writing in three dimensions, Journal of Materials Today, 7/ 7 : 32-39.

[10] Pique, A., Chrisey, D. B., Fitz-Gerald, J. M., Mc Gill, R. A., Auyeung, R. C. Y., Wu, H. D., Lakeou, S., Nguyen, V., Chung, R., Duignan, M., 2000, Direct Writing of electronic ans sensor materials using a laser transfer technique, Journal of Material Research, Vol. 15, No. 9

[11] Li, B., Church, K. H., Clark, P. A., 2007, Robust direct-write dispensing tool and solutions for micro/meso-scale manufacturing and packaging, Proceedings of the 2007 International Manufacturing Science And Engineering Conference, 715-721

[12] Shah, V. G., Hayes D. J., 2002, Trimming and Printing of Embedded Resistors Using Demand-Mode-Ink-Jet Technology and Conductive Polymer, microFab Technologies, Inc./IPC Printed Circuit Expo, 1-5

[13] Wartena, R., Curtright, A., E., Arnold, C., B., Pique, A., Swider-Lyons, K., E., 2004, Li-ion microbatteries generated by a laser direct-write method, Journal of Power Sources, 123 : 193-202

[14] Noy, A., Miller, A., E., Klare, J., E., Weeks, B., L., 2002, Fabrication of Luminescent Nanostructures and Polymer Nanowires Using Dip-Pen Nanolithography, American Chemical Society, 2(2) : 109-112.

[15] Choi, T., Y., Poulikakos, D., 2004, Fountain-pen based laser microstructuring with gold nanoparticle ink, Amercian Institutes of Physics, 85 (1) : 13-15

[16] Lewis, J. A., Smay, J. E., Stuecker, J., Cesarano III, J., 2006, Direct ink writing of three-dimensional ceramic structures, Journal of the American Ceramic Society, 89/12 : 3599-3609.

[17] Whites, K. W., Amert, T., Woessner, S. M. Kim, N., Decker, S., Kellar, J., 2007, Direct-write printing of multilayered appliqué antennas on high impedance surfaces, Antennas and Propagation International Symposium, IEEE, 9-15 June : 2765-2768

[18] Kirschenmann, K., Whites, K. W., Woessner, S. M., 2007, Inkjet printed microwave frequency multilayer antennas, Antennas and Propagation International Symposium, IEEE, 9-15 June : 924-927.

[19] Montoya, T. P., Kirschenmann, K. J., 2007, Antennas with discrete resistive loading built by direct-write fabrication, Antennas and Propagation International Symposium, IEEE, 9-15 June :4080-4083

[20] Cao, Y., Zhou, L., Wang, X., Li, X., Zeng, X., 2009, Micropen Direct-write Deposition of Polymide, Microelectronic Engineering, 86, 1989-1993

[21] Sato, T., Fearon, E., Curran, C., Watkins, K., G., Dearden, G., Eckford, D., 2009, Laser-assited Direct Write for aerospace applications, Proceeding of IMechE/Part g/Aerospace Engineering, 223 : 1-8

[22] Chung, J., Ko, S., Bieri, N., R., Grigoropoulos, C., P., 2004, Conductor microstructures by laser curing of printed gold nanoparticle ink, Applied Physics Letters, 84 50) : 801-803

[23] Chung, J., Ko, S., Grigoropoulos, C. P., 2004, Microconductors on polymer by nanoink printing and pulsed laser curing, Proceedings of the ASME Heat Transfer/Fluids Engineering Summer Conference, 4 : 597-605

[24] Chung, J., Ko, S., Bieri, N., Dockendorf, C., Poulikakos, D., 2005, Damage-Free Low Temperature Pulsed Laser Printing of Gold Nanoinks On Polymers, ASME, 127 : 724-732

[25] Bieri, N., R., Chung, J., Haferi, S., E., Poulikakos, D., Grigoropoulos, C., P., 2003, Microstructuring by printing and laser curing of nanoparticle solutions, Applied Physics Letters, 82(20) : 3529-3531

[26] Bieri, N. R., Chung, J., Poulikakosa, D., Grigoropoulos, C. P., 2004, Manufacturing of nanoscale thickness gold lines by laser curing of a discretely deposited nanoparticle suspension, Superlattices and Microstructures, 35 : 437–444.

[27] Bieri, N., R., Chung, J., Poulikakos, D., Grigoropoulos, C., P., 2005, An experimental investigation of microresistor laser printing with gold nanoparticle-laden inks, Applied Physics A/Material Science & Processing, 80 ; 1485-1495

[28] Atanasov, Y., Vaselaar, D., Khan, A., Marinov, V., 2006, Enhanced Direct-Write Deposition for High-Frequency Applications on Low Temperature Substrates, IEEE Transactions on Electronics Packaging Manufacturing, 1-11

[29] Cai, Z., Li, X., Hu, Q., Zeng, X., 2009, Laser sintering of thick-film PTC thermistor paste deposited by micro-pen direct write technology, Microelectronic Engineering, 86 : 10-15

[30] Marinov, V., Atanasov, Y., 2006, Improved Direct Write Technology for High Frequency Interconnects on Flexible Substrates, Proceedings of the 39th IMAPS International Symposium

[31] Marinov, V. R., Atanasov, Y. A., Khan, A., Vaselaar, D., Halvorsen, A., Schulz, D. L., Chrisey, D. B., 2007, Direct-Write Vapor Sensors on FR4 Plastic Substrates, IEEE Sensors Journal, 7/6 : 937-944

[32] Marinov, V. R., 2007, Electrical Resistance of Laser Sintered Direct-Write Deposited Materials for Microelectronic Applications, 1-8

[33] Kim, J. S., Lee, J-H., Park, J-H., Han, Y-H., 1999, A study on the Laser Curing of Arrylic Resin for the Application in Screen Printing, Journal of Applied Polymer Sciene, 73 : 515-520

[34] Kim, D., Jeong, S., Park, B. K., Moon, J., 2006, Direct writing of silver conductive patterns: Improvement of film morphology and conductance by controlling solvent compositions, Applied Physics Letters, 89 : 264101-3.

[35] Kim, D., Jeong, S., Lee, S., Park, B. K., Moon, J., 2007, Organic thin film transistor using silver electrodes by the ink-jet printing technology, Journal of Thin Solid Films, Elsevier, 515 : 7692-7696

[36] Khan, A., Rasmussen, AN., Marinov, V., Swenson, O., F., Laser sintering of direct write silver nano-ink conductors for microelectronic applications, Proc. of SPIE, 6879, 687910-1 -687911

[37] Albert, A. D., Becker, M. F., Keto, J. W., Kovar, D., 2008, Low Temperature, Pressure-assisted Sintering of nanoparticulate Silver Films, Acta Materialia, Elsevier Ltd., 56, 1820-1829

[38] Dockendorf, C. P. R., Choi, T., Poulikakos, D., Grigoropoulos, C. P., 2006, Multilayer Direct-writing of Electrical Conductors With Gold Nanoinks Using The Fountain–pen Principle, Proceedings of the ASME/Pacific Rim Technical Conference and Exhibition on Integration and Packaging of MEMS, NEMS, and Electronic Systems: Advances in Electronic Packaging, 1959-1961

[39] Fuller, S. B., Wilhelm, E. J., Jacobson, J. M., 2002, Ink-jet printed nanoparticle microelectromechanical systems, Journal of Microelectromechanical Systems, 11/1 : 54-60

[40] Szczech, J. B., Megaridis, C. M., Gamota, D. R., 2002, Fine-Line Conductor Manufacturing Using Drop-On-Demand PZT Printing Technology, IEEE Transactions on electronics packaging manufacturing, 25/1 : 26-33

[41] Smith, P. J., Shin, D. Y., Stringer, J. E., Derby, B., 2006, Direct ink-jet printing and low temperature conversion of conductive silver patterns, Journal of Material Science, 41 : 4153–4158

[42] Bidoki, S. M., Lewis, D. M., Clark, M., Vakorov, A., Millner, P. A., McGorman, D., 2007, Ink-jet fabrication of electronic Components, Journal of Micromechanics and Microengineering, 17 : 967–97410

[43] Goghari, A. A., Chandra, S., 2007, Producing droplets smaller than the nozzle diameter by using a pneumatic drop-on-demand droplet generator, Journal of Experiment in Fluids, Springer, 44/1 : 105-114.

[44] Morissette, S. L., Lewis, J. A., Clem, P. G., Cesarano, J., Dimos, D. B., 2001, Direct-write Fabrication of Pb (nb, Zr, Ti) O3 Devices : Influence of Paste Rheology on Print Morphology and Component Properties, Journal of the American Ceramic Society, 84/11 : 2462–2468

[45] Park, B. K., Kim, D., Jeong, S., Moon, J., Kim, J. S., 2007, Direct writing of copper conductive patterns by ink-jet printing, Thin Solid Films, 515 : 7706–7711

[46] Periard , D., Malone, E., Lipson, H., 2007, Printing Embedded Circuit, Proceedings of the 18th Solid Freeform Fabrication Symposium, Austin, Texas

[47] Yu, H., Gruntzig, A., Zhao, Y., Sharon, A., Li, B., Zhang, X., 2004, Direct Writing, of 3D Microstructures Using A Scanning Laser System, Mat. Res. Soc. Symposium Proceeding, Vol. 782.

[48] Liu, Q., Orme, M., 2001, High Precision Solder Droplet Printing Technology and The State-of-the-Art, Journal of Materials Processing Technology (Elsevier Ltd.), 115 : 271-283.

[49] Orme, M., Liu, Q., Smith, R., 2000, Molten Aluminum Micro-Droplet Formation and Deposition for Advanced Manufacturing Applications, Journal of Aluminum Transaction.

[50] Kawase, T., Sirringhaus, H., Friend, R. H., Shimoda, T., 2000, All-Polymer Thin Film Transistors Fabricated by High-Resolution Ink-jet Printing, IEEE International Electron Devices Meeting

[51] Cuk, T., Troian, S. M., Hong, C. M., Wagner, S., 2000, Using Convective Flow Splitting for the direct printing of fine copper lines, Applied Physics Letters, 77/13 : 2063-2065

[52] Sears, J., Colvin, J., Carter, M., 2007, Fabricating devices using nano-particulates with direct write technology, Materials Science Forum, 534-536 : 1385-1388

[53] Calvert, P., 2001, Inkjet Printing for Materials and Device, Chemical Material, American Chemical Society, Tucson, 13 : 3299-3305

[54] Scott, J. G. V., 2005, Digital printing for printed circuit boards, Circuit World, Emerald Group Publishing Limited, 31/4 : 34–41

[55] Leung, S., Y., Y., Tiu, P., K., Lam, D., C., C., 2006, Printed polymer base RFID antenna on curvilinear surface, IEEE Transcript

[56] Leung, S., Y., Y., Lam, D., C., C., 2007, Performance of Printed Polymer-Based RFID Antenna on Curvilinear Surface, IEEE Transac./Electronics Packaging Manufacturing, 30(3) :200-205

[57] Leung, S., Y., Y., Lam, D., C., C., 2007, Geometric and Compaction Dependence of Printed Polymer-Based RFID Tag Antenna Performance, IEEE Transcript/ Electronics Packaging Manufacturing

[58] Chen, Y., He, W., Zhou, G., He, X., Zhou, H., Mo, Y., He, B., 2010, Compaction Uniformity and Environmental Adaptability of Printed RFID Antenna, IEEE, 277-280

[59] Merilampi, S. L., Bjorninen, T., Vuorimaki, A., Ukkonen, L., 2010, The Effect of Conductive Ink Layer Thickness on the Functioning of Printed UHF RFID Antennas, Proceedings of IEEE, 98(9) : 1610-1619

[60] Bjorninen, T., Merilampi, S., Ukknonen, L., Ruuskanen, P., Sydanheimo, L., 2010, Performance comparison of silver ink and copper conductors for microwave applications, IET Microwaves, Antennas & Propagation, 4(9) : 1224-1231

[61] Shin, D. Y., Lee, Y., Kim, C. H., 2009, Performance characterization of screen printed radio frequency identification antennas with silver nanopaste, Thin Solid Films, 517 : 6112-6118

[62] Merilampi, S., Laine-Ma, T., Ruuskanen, P., 2009, The characterization of electrically conductive silver ink patterns, Microelectronics Reliability, 49 : 782-790

[63] Rida, A., Yang, L., Tentzeris, M., M., 2007, Design and Characterzation of Novel Paper-based Inkjet-Printed UHF Antennas for RFID and Sensing Applications, IEEE, 2749-2752

[64] Tentzeris, M.,M., Yang, L., Rida, A., Vyas, R., Traille, A., Kruessi, C., 2008, Conductive Inkjet-Printed Wireless Sensor Nodes on Flexible Low-Cost Paper-Based Substrates, 297-305

[65] Virtanen, J., Bjorninen, T., Ukkonen, L., Kaija, K., Joutsenoja, T., Sydanheimo, L., Elsherbeni, A., Z., The Effect of Conductor Thickness in Passive Inkjet Printed RFID Tags

[66] Virtanen, J., Passive UHF Inkjet-Printed Narrow-Line RFID Tags, 2010, IEEE Antennas and Wireless Propagation Letters, 9 : 440-443

[67] Molesa, S., Redinger, D., R., Huang, D., C., Subramanian, V., 2003, High-quality inkjet-printed multilevel interconnects and inductive components on plastic for ultra-low-cost RFID applications, Material

[68] Yang, L., 2007, RFID Tag and RF Structures on a Paper Substrate Using-Inkjet-Printing Technology, IEEE Transaction/Microwave Theory and Techniques, 55(12) : 2894-2899

[69] Redinger., D., 2004, An Ink-Jet Deposited Passive Component Process for RFID, IEEE Transactions/Electron Devices, 51(12) : 1978-1983 Research Symposium Proceeding, 769

[70] Siden, J., Nilsson, H. E., 2007, Line Width Limitations of Flexographics-Screen and Inkjet printed RFID Antennas, IEEE, 1745-1748

[71] Kang, B., J., Oh, J., H., 2009, Geometical characterization of inkjet-printed conductive lines of nanosilver suspensions on a polymer substrate. Thin Solid Films, 1-7

[72] Jung, H. C., Cho, S. H., Joung, J. W., 2007, Studies on Inkjet –Printed Conducting Lines for Electronic Devices, Journal of Electronic Materials, 36(9) : 1211-1218

[73] Jeong, S., Song, H. C., Lee, W. W., Choi, Y., Ryu, B. H., 2010, Preparation of aqueous Ag Ink with long-term dispersion stability and its inkjet printing for fabricating conductive tracks on a polyimide film, Journal of Applied Physics, 108 : 102805-1 – 102805-5

[74] Perelaer, J., Hendriks, C., H., Laat, A., W., M., Schubert, U., S., 2009, One-step inkjet printing of conductive silver tracks on polymer substrates, IOP Publishing/Nanotechnology, 20 : 1-5

[75] Nur, H. M., Song, J. H., Evans, J. R. G., Edirisinghe, M. J., 2002, Ink-jet printing of gold conductive tracks, Journal of Material Science/Materials in Electronics, 13 ; 213-219

[76] Mantsyalo, M., Mansikkamaki, P., 2009, An inkjet deposited antenna for 2.4GHz applications, Int. J. Electron. Commun, 63 : 31-35

[77] Alemohammad, H., Aminfar, O., Toyserkani, E., 2008, Morphology and microstructure analysis of nano-silver thin films deposited by laser-assisted maskless microdeposition, Journal of Micromechanics and Microengineering, 18 : 1-12

[78] Auyeung, R. C. Y., Nurnberger, M. W., Pique, A., Arnold, C. B., Abbot, A. R., Schuette, L. C., 2004, Laser fabrication of GPS conformal antennas, SPIE's LASE', 1-6

[79] Zeng, X., Cai, Z., Li, X., 2009, An additive method to fabricate conductive lines and electronic components directly by laser microcladding electronic materials, Proc. IMechE/Part C/J. Mechanical Engineering Science, 224 : 1087-1098

[80] Pique, A., Lyons, K. E. S., Weir, D. W., Love, C. T., Modi, R., 2001, Laser Direct Writing of Microbatteries for Integrated Power Electronics, SPIE's LASE'2001, Proceedings, 4279-39

[81] Serra, P., Pradas, J. M. F., Collina, M., Duocastella, M., Dominguez, J., Morenza, J. L., 2006, Laser-induced forward Transfer: A Direct-writing Technique for Biosensor Preparation, Journal of Laser Micro/Nanoengineering, Vol. 1, No. 3

[82] Chen, Q., Tong, T., Longtin, J., P., Tankiewicz, S., Sampath, S., Gambino, R., J., , 2004, Novel Sensor FabricationUsing Direct-Write Thermal Spray and Precision Laser Micromachinig, ASME, 126 : 830-836

[83] Auyeung, R. C. Y., Kim, H., Mathews, S. A., Pique, A., 2007, Laser Direct-Write of Metallic Nanoparticles Inks, Journal of Laser Micro/ Nanoengineering, 2(1) : 21-25

[84] Henry, M., Harrison, P. M., Wendland, J., 2007, Laser Direct Write of Active Thin-Films on Glass for Industrial Flat Panel Display Manufacture, Journal of Laser Micro/ Nanoengineering, 2(1 : 49-56)

[85] Li, X., Li, H., Chen, Y., Zeng, X., 2004, Silver conductor fabrication by laser direct writing on Al2O3 substrate, Applied Physics A, 79 : 1861–1864.

[86] Li, X., Li, H., Liu, J., Qi, X., Zeng, X., 2004, Conductive line preparation on resin surfaces by laser micro-cladding conductive pastes, Applied Surface Science, 233 : 51–57.

[87] Li, X., Zeng, X., Li, H., Qi, X., 2005, Laser direct fabrication of silver conductors on glass boards, Thin Solid Films, 483 : 270 – 275

[88] Sangoi, R., Smith, C. G., Seymour, M. D., Venkataraman, J. N., Clark, D. M., Kleper, M. L., Kahn, B. E., 2004, Printing Radio Frequency Identifiifcation (RFID) Tag Antennas Using Inks Containing Silver Dispersions, Journal odf Dispersion Science and Technology, 25(4) : 513-521

[89] Ng, J. H. G., Desmulliex, M. P. Y., Lamponi, M., Moffat, B. G., 2009, a Direct-writing approach to micro patterning of copper onto polymide, Circuit World, 35/2 : 3-17

[90] Felmet, K., Loo, Y. L., 2004, Patterning conductive copper by nanotransffer printing, Applied Physics Letter, 85(15) : 3316-3318

[91] Lee, D. Y., Hwang, E. S., Yu, T. U., Kim, Y. J., Hwang, J., 2006, Structuring of micro line conductor using electro-hydrodynamic printing of a silver nanoparticle suspension, Applied Physics A/ Material science & Processing, 82 ; 671-674

[92] King, B. H., Dimos, D., Yang, P., Morissette, S. L., 1999, Direct-Write Fabrication of Integratesd, Multilayer Ceramic Components, Journal of Electroceramic, 32 : 173-178.

[93] Pudas, M., Hagberg, J., Leppavuoris, S., 2004, Gravure offset printing of polymer inks for conductors, Progress in Organic Coatings, 49 : 324-335

[94] Pudas, M., Hagberg., J., Leppavuori, S., 2004, Printing paramaters and ink components affecting ultra-fine-line gravure-offset printing for electronics applications, Journal of European Ceramic Society, 24 : 2943-2950

[95] Pudas, M., Halonen, N., Granat, P., Vahakangas, J., 2005, Gravure printing of conductive polymer inks on flexible sbstrates, Progress in Organic Coatings, 54 :310-316

[96] Choi, B., Kim., S. M., Kim, D. S., 2009, Manufacturing ultra-high-frequency radio frequency identification tag antennas by multilayer printings, Proceedings of IMechE/Journal of Mechanical and Engineering Science, 224 :149-156

[97] Hoey, J. M., Reich, M. T., Halvorsen, A., Vaselaar, D., Braateen, K., Maassel, M., Akhatov, I. S., Ghandour, O., Drzaic, P., Schulz, D. L ., 2009, Rapid Prototyping RFID Antennas Using Direct Write, IEEE Transactions on Advanced Packaging, Vol. 32, No. 4

[98] Merilampi, S. L., Bjorninen, T., Ukkonen, L., Ruuskanen, P., Sydanheim, L., 2011, Characterization of UHF RFID tags fabricated directly on convex surfaces by pad printing, Inernational Journal of Advanced Manufacturing Technology, 53:577-591

[99] Zeng, X., Siden, J., Wang, G., Nilsson, H., 2007, Siver Ink Patch Antenna for Passive RFID, Proceedings of ISAP : 612-615.

[100] Cao, Y., Zhou, L., Wang, X., Li, X., Zeng, X., 2009, Micropen Direct-write Deposition of Polymide, Microelectronic Engineering, 86, 1989-1993

[101] Vozzi, G., Previti, A., De Rossi, D., Ahluwalia, A., 2002, Microsyringe-Based Deposition of Two-Dimensional and Three-Dimensional Polymer Scaffolds with a Well-DefinedGeometry for Application to Tissue Engineering, Tissue Engineering, 8/6 : 1089-1098

[102] Moscicki, A. , Felba, J., Dudzinski, W., 2006, Conductive Microstructures and Connections for Microelectronics Made by Ink-Jet Technology, 1 : 511-517

[103] Hon, K. K. B., Li, L., Hutchings, I., 2008, Direct Writing Technology-Advances and Developments, Annals of the CIRP, Vol. 52/2/2008

[104] Zingg., R., 2009, University of Colorado at Boulder

[105] Shin, D. Y., Lee, Y., Kim, C. H., 2009, Performance characterization of screen printed radio frequency identification antennas with silver nanopaste, Thin Solid Films, 517 : 6112-6118

Bibliography

[1] Bhattacharya, S., Marinov, V., 2009, Simple, Inexpensive, and Reliable, High Density Interconnect Technology for Flexible Electronics Applications, IEEE

[2] Bahl, I. J., Trivedi, D. K., 1977, A Designer's Guide to Microstrip Line, Microwaves, 174-182

[3] Bonadiman, R. Marques, M. Freitas, G. Reinikainen, T., 2008, Evaluation of printing parameters and substrate treatment over the quality of printed silver traces, 2nd. Electronics System-Integration Technology Conference, 1343-1348

[4] Calgar, U., Kaija, K., Mansikkamaki, P., 2008, Analysis of Mechanical Performance of Silver Inkjet-Printed Structures, IEEE International Nanoelectronics Conference, 851-856

[5] Chen, B., Cui, T., Liu, Y., Varahramyan, K., 2003, All-polymer RC filter circuits fabricated with inkjet printing technology, Solid-State Electronics, 47 : 841–847

[6] Chrisey, D. B., 2000, Materials processing : The power of direct writing, Journal of Science, Elsevier Inc., 289/5481: 879.

[7] Fearon, E., Sato, T., Wellburn, D., Watkins, K., G., Dearden, G., 2007, Thermal effects of substrate materials used in the laser curing of

particulate silver inks, Laser Assisted Net Shape Engineering 5/ Proceedings of the LANE, 379-390

[8] Hedges, M., Renn, M., Kardos, M., 2005, Mesoscale Deposition Technology for Electronics Applications, 5th International Conference on Polymers and Ashesives in Microelectronics and Photonics, 53-57

[9] Huang, Y., Boyle, K., 2008, Antenna from Theory and Practice, John Wiley & Sons Ltd., First Edition

[10] Hwang, K., Dinh, V. D., Lee, S. H., Kim, Y. J., Kim, H. M., 2007, Analysis of Line width with Nano Fountain Pen Using Active Membrane Pumping, Proceedings of the 2nd IEEE International Conference on Nano/Micro Engineered and Molecular Systems, 759-763

[11] King, B. H., Morissette, S. L., Denham, H., Cesarano III, J., Dimos, D., 1998, Influence of rheology on deposition behavior of ceramic pastes in direct fabrication systems, Solid freeform fabrication symposium, 391-398.

[12] Lee, H. H., Chou, K. S., Huang, K. C., 2005, Inkjet printing of nanosized silver colloids, Nanotechnology, 16 : 2436–2441

[13] Liu, Y., Cui, Varahramyan, 2003, All-polymer capacitor fabricated with inkjet printing technique, Solid-State Electronics, 47 : 1543-1548

[14] Liu, Z., Su, Y., Varahramyan, K., 2005, Inkjet-printed silver conductors using silver nitrate ink and theirelectrical contacts with conducting polymers, Thin Solid Films, 478 : 275– 279

[15] Luechinger, N. A., Athanassiou, E. K., Stark, W. J., 2008, Graphene-stabilized copper nanoparticles as an air-stable substitute for silver and gold in low-cost ink-jet printable electronics, Nanotechnology, 19, 445201 (6pp)

[16] Malone, E., Lipson, H., 2007, Fab@Home : The Personal Desktop Fabricator Kit, Rapi Prototyping Journal (Emerald Group Publishing Limited), 13/4 : 245-255.

[17] Mei, J., Lovell, M. R., Mickle, M. H.,2005, Formulation and Processing of Novel Conductive Solution Inks in Continuous Inkjet Printing of 3-D Electric Circuits, IEEE Transactions on Electronics Packaging Manufacturing, 28/3 : 265-273

[18] Moscicki, A., Felba, J., Gwiazdzinski, P., Puchalski, M., 2007, Conductivity improvement of microstructures made by nano-size-silver filled formulations, 6th International IEEE Conference on Polymers and Adhesives in Microelectronics and Photonics, Polytronic Proceedings, 305-310

[19] Moscicki, A., Felba, J., Sobierajskil, T., Kudzia, J., Arp, A., Meyer, W., 2005, Electricalty Conductive Formulations Filled Nano Size Silver Filler for Ink-Jet Technology, 5th Intemational Conference on Polymers and Adhesives in Microelectronics and Photonics, 40-44.

[20] Murata, K., Matsumoto, J., Tezuka, A., Matsuba, Y., Yokoyama, H., 2005, Super-fine ink-jet printing : toward the minimal manufacturing system, Microsyst Technology, 12 : 2-7.

[21] Natori, A. Y., Frasson, A. M. F., Ceschin, A. M., 2003, Organic Conducting Films Fabricated with Ink Jet Printing Technology and Possible Application in Electric-Field Probes, BMO/IEEE MTT-S International Microwave and Optoelectronics Conference Proceedings, 345-347

[22] Orme, M., Smith, R. F., 2000, Enhanced Aluminum Properties by Means of Precise Droplet Deposition, Journal of Manufacturing Science and Engineering, Transactions of the ASME, August, 122 : 484-493.

[23] Perelaer, H., Laat, A., W., M., S Hendriks, C., H., Schubert, U., S., 2008, Inkjet-printed silver tracks : low temperature curing and thermal stability investigation, Journal of Materials Chemistry,18 : 3209-3215

[24] Perelaer, J., Gans, B- J., Schubert, U., S., 2006, Ink-jet printing and Microwave Sintering of Conductive Silver Tracks, Advanced Materials, 18 : 2101-2104

[25] Pique, A., Lyons, K. E. S., Weir, D. W., Love, C. T., Modi, R., 2001, Laser Direct Writing of Microbatteries for Integrated Power Electronics, SPIE's LASE'2001, Proceedings, 4279-39

[26] Rida, A., Yang, L., Vyas, R., Bhattacharya, S., Tentzeris, M., M., 2007, Design and Integration of Inkjet-printed Paper-Based UHF Components for RFID and Ubiquitous Sensing Applications, Proceedings of 37th European Microwave Conference, 714-727

[27] Rivkin, T., Curtis, C., Miedaner, A., Perkins, J., Alleman, J., Ginley, D., 2002, direct write processing for photovoltaic cells, Photovoltaic Specialists Conference, Conference Record of the Twenty-Ninth IEEE, 1326- 1329

[28] Shao, B., Chen, Q., Amin, Y., hllstedt, J., Liu, R., Tenhunen, H., Zheng L-R., Process-Dependence of Inkjet Printed Foldede Dipole Antenna for 2.45 GHz RFID Tags,2336-2339

[29] Sirringhaus, H., Kawase, T., Friend, R. H., Shimoda, T., Inbasekaran, M., Wu, W., Woo, E. P.,2000, High-Resolution Inkjet Printing of All-Polymer Transistor Circuits, Science, 290 : 2123.

[30] Song, J. W., Kim, J., Yoon, Y. H., Choi, B. H., Kim, J. H., Han, C. S., 2008, Inkjet printing of single-walled carbon nanotubes and electrical characterization of the line pattern, Journal of Nanotechnology, 19/9 : 1-6

[31] Songping, W., Shuyuan, M., 2005, Preparation of ultrafine silver powder using ascorbic acid as reducing agent and its application in MLCI, Materials Chemistry and Physics, 89 : 423–427

[32] Tekin, E., Smith, P., J., Schubert, U., S., Inkjet printing as a deposition and patterning tool for polymers and inorganic particles, 2008, The Royal Society of Chemistry, Soft Matter, 4 : 703-713

[33] Wallace, D., Hayes, D. J., Thing, C., Shah, V., Radulescu, D., Cooley, P., Wachtler, K., Nallani, A., 2007, Ink-jet as a MEMS manufacturing tool, Proceedings of the International Conference on Integration and Commercialization of Micro and Nanosystems : 1161-1168.

[34] Wang, H. T., Nafday, O. A., Haaheim, J. R., Tevaarwerk,E., Amro, N. A, Sanedrin, R. G., Chang, C. Y., Ren, F., Pearton, S. J., 2008, Toward conductive traces: Dip Pen Nanolithography of silver nanoparticle-based inks, Applied Physics Letters, 93 : 143105

[35] Wu, S. P., Gao, R. Y., Xu, L. H., 2009, Preparation of micron-sized flake copper powder for base-metal-electrode multi-layer ceramic capacitor, Journal of Materials Processing Technology, 209 : 1129–1133

[36] Wu, S. P., Yung, K. C., Xu, L. H., Ding, X. H., 2008, Fabrication of Polymer Silver Conductor Using Inkjet Printing and Low Temperature Sintering Process, IEEE Transactions on Electronics Packaging Manufacturing, 31/4 : 291-296.

[37] Zeng, X., Cai, Z., Li, X, 2009, An additive method to fabricate conductive lines and electronic components directly by laser microcladding electronic materials, Proc. IMechE/Part C/J. Mechanical Engineering Science, 224 : 1087-1098

[38] Zeng, X., Li, X., Liu, J., Qi, X., 2006, Direct Fabrication of Electric Componentson Insulated Boards by Laser Microcladding Electronic Pastes, IEEE Transactions on Advanced Packaging, 29 : 2